University of Cyprus
Department of Mechanical and Manufacturing Engineering

IN VITRO INVESTIGATION OF THE ROLE OF RAS SUPPRESSOR-1 (RSU-1) AND INTEGRIN-LINKED KINASE (ILK) IN GLIOMA PROGRESSION AND INVASION

DOCTOR OF PHILOSOPHY DISSERTATION

MARIA LOUCA

2019

Πανεπιστήμιο Κύπρου
Τμήμα Μηχανικών Μηχανολογίας
και Κατασκευαστικής

IN VITRO ΔΙΕΡΕΥΝΗΣΗ ΤΟΥ ΡΟΛΟΥ ΤΩΝ ΠΡΩΤΕΙΝΩΝ RAS SUPPRESSOR-1 (RSU-1) ΚΑΙ INTEGRIN-LINKED KINASE (ILK) ΣΤΗΝ ΕΞΕΛΙΞΗ ΤΟΥ ΓΛΟΙΩΜΑΤΟΣ ΚΑΙ ΤΗ ΜΕΤΑΣΤΑΣΗ

ΔΙΔΑΚΤΟΡΙΚΗ ΔΙΑΤΡΙΒΗ

ΜΑΡΙΑ ΛΟΥΚΑ

ΔΙΑΤΡΙΒΗ Η ΟΠΟΙΑ ΥΠΟΒΛΗΘΗΚΕ ΠΡΟΣ ΑΠΟΚΤΗΣΗ ΔΙΔΑΚΤΟΡΙΚΟΥ ΤΙΤΛΟΥ ΣΠΟΥΔΩΝ ΣΤΟ ΠΑΝΕΠΙΣΤΗΜΙΟ ΚΥΠΡΟΥ

ΝΟΕΜΒΡΙΟΣ 2019

VALIDATION PAGE

Doctoral Candidate: MARIA LOUCA

Doctoral Thesis Title: *In vitro* investigation of the role of Ras Suppressor 1 (RSU-1) and Integrin-Linked kinase (ILK) in glioma progression and metastasis

This Doctoral Dissertation was submitted in partial fulfillment of the requirements for the degree of Doctor of Philosophy at the ***Department of Mechanical and Manufacturing Engineering*** *and approved on the …….. by the* ***Examination Committee***.

Examination Committee:

Research Advisor:

Dr.Triantafyllos Stylianopoulos ……..……..……

Other Members:

Dr.Andreas Scorilas ……...……...

Dr. Dimitrios Bogdanos……..……..

Dr. Theodora Krasia……..……..……

Dr. Vasileios Vavourakis……..…….....

DECLARATION OF DOCTORAL CANDIDATE

The present doctoral dissertation was submitted in partial fulfilment of the requirements for the degree of Doctor of Philosophy of the University of Cyprus. It is a product of original work of my own, unless otherwise mentioned through references, notes, or any other statements.

Name and Signature of the Doctoral Candidate:

……

……

Περίληψη

Το πολύμορφο γλοιοβλάστωμα (Glioblastoma multiforme-GBM) είναι ο πιο επιθετικός τύπος καρκίνου του εγκεφάλου λόγω της ικανότητας των κυττάρων του να διεισδύουν σε γειτονικούς ιστούς. Η μέση επιβίωση για τους ασθενείς είναι 15 μήνες καθιστώντας επιτακτική την ανακάλυψη νέων θεραπευτικών στόχων. Η πρωτεΐνη Ras Suppressor-1 (RSU-1) αλληλεπιδρά με την πρωτεΐνη Particularly interesting new cysteine-histidine rich (PINCH1) που με τη σειρά της είναι συνδεδεμένη με την Integrin Linked Kinase (ILK) και την α-parvin (PARVA) σχηματίζοντας ένα σταθερό σύμπλοκο στις εστιακές προσκολλήσεις, συνδέσεις μεταξύ κυττάρου και εξωκυττάριας μήτρας (Extracellular matrix-ECM). Πρόσφατα, η RSU-1 αποδείχτηκε ότι εκφράζεται σε υψηλά επίπεδα σε δείγματα μεταστατικού καρκίνου του μαστού ενώ βρέθηκε ότι προάγει τη διεισδυτική ικανότητα καρκινικών κυττάρων ρυθμίζοντας τις πρωτεΐνες που σχετίζονται με την αναδιοργάνωση του κυτταροσκελετού της ακτίνης. Ο αυξητικός παράγοντας διαφοροποίησης-15 (Growth Differentiation Factor 15-GDF15) είναι επίσης γνωστό ότι εμπλέκεται στην αναδιοργάνωση του κυτταροσκελετού ακτίνης και στη μετάσταση.

Ο στόχος της παρούσας έρευνας ήταν να διερευνηθεί ο ρόλος των πρωτεϊνών RSU-1 και ILK στην επιθετικότητα των κυττάρων του γλοιώματος. Αρχικά, τέσσερις κυτταρικές σειρές γλοιώματος χωρίστηκαν σε δύο ομάδες: στις περισσότερο επιθετικές (A172 και U87-MG) και στις λιγότερο επιθετικές (H4 και SW088). Η RSU-1 βρέθηκε σημαντικά αυξημένη στα πιο επιθετικά κύτταρα γλοιόματος. Επιπλέον, η αποσιώπηση της RSU-1 είχε αντίθετο αποτέλεσμα ως προς τη διήθηση των κυττάρων του γλοιόματος αναστέλλοντας τη διήθηση των επιθετικών κυττάρων και προάγοντας εκείνη των λιγότερο επιθετικών κυττάρων μέσω της ρύθμισης της έκφρασης των γονιδίων Signal Transducer and Activator of Transcription 6 (STAT6) και της μεταλλοπρωτεϊνάσης 13 (MMP13).

Στη συνέχεια, παρατηρήθηκε ότι στις υπό μελέτη κυτταρικές σειρές η αυξημένη διηθητική ικανότητα συσχετιζόταν με αυξημένα επίπεδα έκφρασης RSU-1 και μειωμένα επίπεδα έκφρασης GDF15. Έτσι, το επόμενο ερώτημα ήταν αν υπάρχει κάποιου είδους συσχέτιση μεταξύ της RSU-1 και της πρωτεΐνης GDF15 όσον αφορά τη διεισδυτικότητα των κυττάρων. Τα αποτελέσματά μας έδειξαν ότι η διαφορετική έκφραση των πρωτεϊνών RSU-1 και GDF15 οδηγεί σε αναστολή της κυτταρικής διεισδυτικότητας στα λιγότερο επιθετικά H4 κύτταρα και προαγωγή στα περισσότερο επιθετικά A172 μέσω αλλαγών στην έκφραση των PINCH1, RhoA και MMP13.

Η ILK έχει επίσης αποδειχθεί ότι προάγει τη διεισδυτικότητα στο GBM, ωστόσο, λίγα είναι γνωστά σχετικά με τον εμπλεκόμενο μοριακό μηχανισμό. Έτσι, ο στόχος μας ήταν να μελετήσουμε την επίδραση της αποσιώπησης του γονιδίου ILK στη διηθητική συμπεριφορά των κυττάρων γλοιοβλαστώματος και να διασαφηνίσουμε τον εμπλεκόμενο μοριακό μηχανισμό χρησιμοποιώντας την κυτταρική σειρά H4 και την κυτταρική σειρά A172 που εκφράζει επίσης την πρωτεΐνη ILK σε πολύ υψηλότερα επίπεδα. Τα αποτελέσματά μας έδειξαν ότι η αποσιώπηση του γονιδίου ILK αναστέλλει τη διήθηση των άκρως διεισδυτικών κυττάρων A172, ενώ δεν επηρεάζει την ικανότητα μετακίνησης των κυττάρων H4. Αυτά τα δεδομένα υποστηρίχθηκαν από αντίστοιχες μεταβολές στην έκφραση της σχετιζόμενης με Rho κινάσης -1 (ROCK-1), και των γονιδίων Fascin-1 καθώς και της μεταλλοπρωτεϊνάσης MMP13.

Η παρούσα διατριβή έδειξε ότι τα επίπεδα έκφρασης των RSU-1, GDF15 και ILK επηρεάζουν τη διηθητκή ικανότητα των κυττάρων των γλοιωμάτων, θέτοντας τις πρωτεΐνες αυτές ως στόχους για την ανάπτυξη καινοτόμων θεραπευτικών προσεγγίσεων και για την αντιμετώπιση ενός από τους πιο επιθετικούς τύπους όγκων του εγκεφάλου.

Abstract

Glioblastoma multiforme (GBM) is the most aggressive type of malignant brain tumours due to its highly invasive phenotype. The average survival for patients with GBM is 15 months, making the discovery of novel invasion biomarkers and therapeutic targets imperative. Ras Suppressor-1 (RSU-1) is a cell-Extracellular matrix (ECM) adhesion protein that interacts with Particularly interesting new cysteine-histidine rich protein (PINCH-1), which is being connected to Integrin Linked Kinase (ILK) and alpha-parvin (PARVA). Recently, RSU-1 was shown to be up-regulated in metastatic breast cancer samples and was found to promote the invasive capacity of cancer cells by regulating the actin cytoskeleton remodeling-related proteins. Growth differentiation factor-15 (GDF15) is also known to be involved in actin cytoskeleton reorganization and metastasis.

Taking into consideration the above, the aim of this thesis was to investigate the role of RSU-1 and ILK in glioma cell aggressiveness. For this purpose, firstly, four brain cell lines were divided into two distinct groups: highly invasive glioblastoma cell lines (A172 and U87-MG) and less invasive cells (H4 and SW088). Interestingly, we found that RSU-1 was significantly upregulated in more aggressive glioma cells compared to less aggressive. Moreover, *RSU-1* silencing had opposing effects on glioma cell invasion depending on their aggressiveness, inhibiting migration and invasion of aggressive cells and promoting those of less aggressive cells through regulation of Signal Transducer and Activator of Transcription6 (STAT6) phosphorylation and Matrix Metalloproteinase13 (MMP13) expression.

We also observed that the investigated cell lines (H4 and A172) had increasing *RSU-1* expression levels and invasive capacity and decreasing *GDF15* levels. Thus, the next question was whether there is any kind of interplay between RSU-1 and GDF15 with regard to glioblastoma cell invasion. Our results showed that the differential expression of *RSU-1*

and *GDF15* in H4 and A172 cells lead to inhibition of cell invasion in H4 cells and promotion in A172 through respective changes in *PINCH1*, *RhoA* and *MMP-13* expression.

Regarding ILK in GBM aggressiveness little is known. Thus, the aim of the present work was to study the effect of *ILK* silencing on the metastatic behavior of glioblastoma cells *in vitro* and elucidate the underlying molecular mechanism using the neuroglioma H4 cell line and the GBM A172 cells, which also express ILK in much higher levels. My results showed that siRNA-mediated silencing of *ILK* inhibits cell migration and invasion of the highly invasive A172 cells while it does not seem to affect the motility capacity of H4 cells. These data were also supported by respective changes in the expression of *Rho-associated kinase -1 (ROCK-1)*, *Fascin-1* and *MMP13*. Finally, findings were corroborated further by an analysis of The Cancer Genome Atlas Glioblastoma Multiforme (TCGA-GBM) dataset.

In the present work it was clearly shown that RSU-1, GDF15 and ILK expression affects the *in vitro* metastatic properties of glioma/glioblastoma cells, setting the grounds for examining these molecules as potential target-molecules in the development of novel anti-metastatic therapeutic approaches for dealing with one of the most aggressive types of malignant brain tumors.

Acknowledgments

I would like to offer my special thanks to Dr. Triantafyllos Stylianopoulos for his valuable assistance and motivation. It has been an honor to be one of his Ph.D. students. Moreover, I would like to thank Dr. Vasiliki Gkretsi for extraordinary support and her valuable pieces of advice and guidelines I needed in my research all these years. I am thankful to her for all her help, not only as a supervisor but also as a friend.

Also, I would like to thank Dr. Stylianou Andreas for his helpful discussions and ideas and for many pieces of advice.

I am also grateful to all the members of the Cancer Biophysics lab, Dr. Chrysovalantis Voutouri, Dr. Fotios Mpekris, Dr. Maria Kalli, Ms. Myrophora Panagi and our technician Mr. Kypros Stylianou. Their friendly attitude, support and encouragement throughout the years were critical also important for completing my dissertation.

Contents

1 Introduction

1.1 Classification of brain tumors

Cancer is a multifactorial disease with rapidly growing worldwide prevalence and is the second leading cause of death before age of 70 years in developed countries[1, 2]. Specifically, in 2018, 18.1 million new cancer cases and 9.6 million cancer deaths have been reported by International Agency for Research on Cancer (IACR)[3]. The most frequent cancer type worldwide for males is lung cancer and breast cancer for females [1]. Brain and Central Nervous System (CNS) cancers, although not so common, as they are responsible for approximately 1.64% new cases, they have an extremely poor prognosis because the life expectancy has maximum of five years.[1].

Brain and CNS tumors are classified in grades (grade I through grade IV) based on predicted clinical behavior[4, 5]. Grade I tumors consist of cancer cells with low proliferative potential and surgical resection alone is enough for their cure. Grade II tumors consist of cells with low proliferative capacity which also sometimes have infiltrative capacity and are mostly treated successfully by surgical resection and radiotherapy. Grade III tumors contain cells characterized with nuclear atypia, intense mitotic activity and easy infiltration throughout the brain and surgical resection is not enough to eradicate the tumor as patients normally undergo radiation and/or chemotherapy treatments [6, 7]. Patients with grade III tumors usually survive for 2-3 years in contrast to grade II patients who survive for more than 5 years. Grade IV tumors are considered to be malignant brain tumors with GBM being the most aggressive type. Their cells have increased proliferative potential and invasive capacity, while these tumors are associated with rapid pre- and postoperative disease progression and death. The median survival for glioblastoma patients is one and a half years[8, 9].

The brain consists of two cell types, neurons, and glial cells. Glial cells surround neurons and support them by supplying them with nutrients and oxygen. Also, they protect neurons and insulate one neuron from another[10]. Gliomas are tumors that arise from glial or precursor cells and include astrocytomas, oligodendrogliomas, ependymomas and oligoastrocytomas[4]. Gliomas can be found above (supratentorial) or below (infratentorial) of the brain membrane

called tentorium (**Figure 1-1**). The majority of gliomas occur in the supra-tentorium (frontal, temporal, parietal, and occipital lobes)[11]. Astrocytic tumors, including glioblastoma, account for 75.8% of all gliomas[11] . GBM is the most malignant type of brain cancer and is known as grade IV astrocytoma because its cells arise from astrocytes, the star-shaped cells which are anchored on the cerebral hemispheres but can be also present anywhere in the brain or spinal cord[12].

As in all cases of cancer, brain tumors have a strong genetic background, as mutations in oncogenes or tumor suppressor genes significantly contribute to the initiation and development of tumors. Thus, research into glioma biology led to the discovery of many mutations and molecular alterations which are distinctive of each glioma and predict clinical aggressiveness[8, 9, 13, 14].

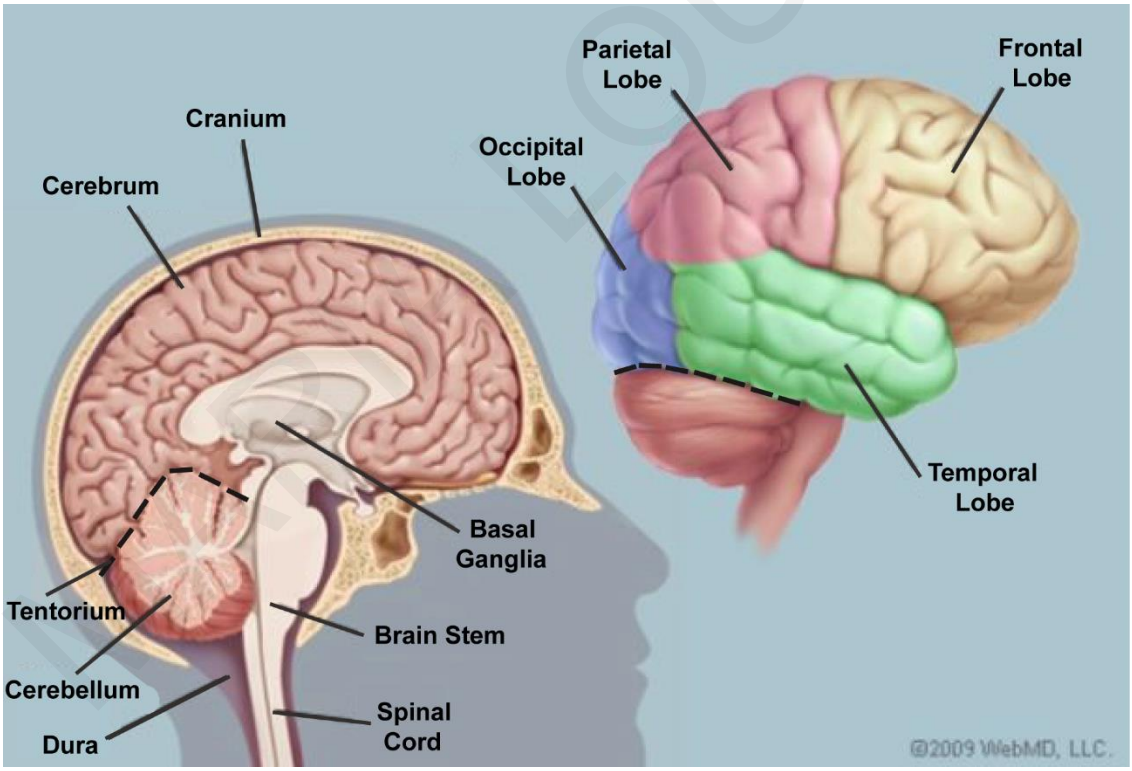

Figure 1-1. **Schematic representation of human brain.** Tentorium (dashed line) is a line which separates the supratentorial (cerebrum) of brain from the infratentorial (cerebellum).The majority of gliomas occur in the supra-tentorium (frontal, temporal, parietal, and occipital lobes. Source: https://www.webmd.com/brain/picture-of-the-brain#.

1.2 Metastasis of cancer cells

Although tumor formation is crucial and should be closely monitored and treated, most cancer patients do not die from the primary tumor but rather from the subsequent metastasis of cancer cells. Metastasis as shown in **Figure 1-2** is a multistage process during which cancer cells dissociate from cell-extracellular matrix (ECM) adhesions, lose contact with their neighboring cells and finally detach from the primary tumor. Then, they degrade surrounding ECM to invade adjacent tissues and are transported through the circulation or lymphatic system to other distant organs where they extravasate, adhere to the new environment and establish a new colony of malignant cells [15]. Notably, certain cancer cell types seem to show a preference with regard to their metastatic sites, a phenomenon known as metastatic tropism[16]**.** Breast cancer cells, for instance, tend to form metastases to the bones, the lung, the liver and the brain, while prostate cancer cells tend to metastasize preferentially towards the bone, and pancreatic cancer cells show a preference to the liver and the lung[17]. Glioblastoma tumors rarely metastasize outsize the CNS. However, following the same processes, all cancer cells in gliomas are able to invade and spread far from the initially site into normal parenchyma constituting a secondary tumor mass[18].

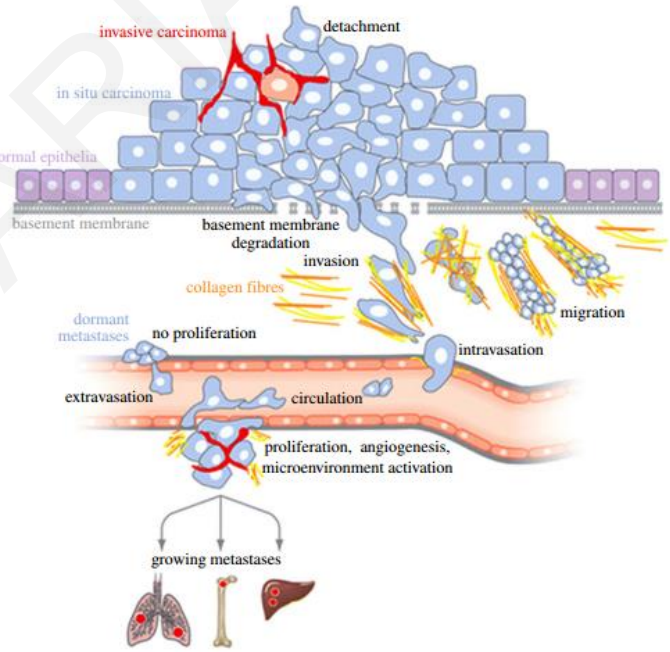

Figure 1-2. **A schematic model of metastasis.** This process begins with the loss of adhesion between the tumor cells and is followed by degradation of the ECM and invasion through surrounding stroma. The cancer cells at this point can intravasate into blood and lymph circulation. Finally, surviving cells extravasate to distant organs where they start proliferating and forming a metastatic tumor[19].

For the metastatic process to take place, integrins and integrin-related protein complexes formed at cell-ECM adhesion sites (also known as focal adhesion sites, FAs herein as shown **Figure 1-3**) are of fundamental importance [20, 21]. Thus, upon integrin activation, a signaling cascade is initiated resulting in important changes in terms of cell behavior that affect cell survival and apoptosis, cell differentiation, proliferation, and adhesion[22-24]. Moreover, due to the fact that most FA proteins maintain a tight connection either directly or indirectly to the actin cytoskeleton, integrin activation also affects processes such as cell migration and invasion of surrounding matrix, which are both intrinsically linked to metastasis [25, 26].

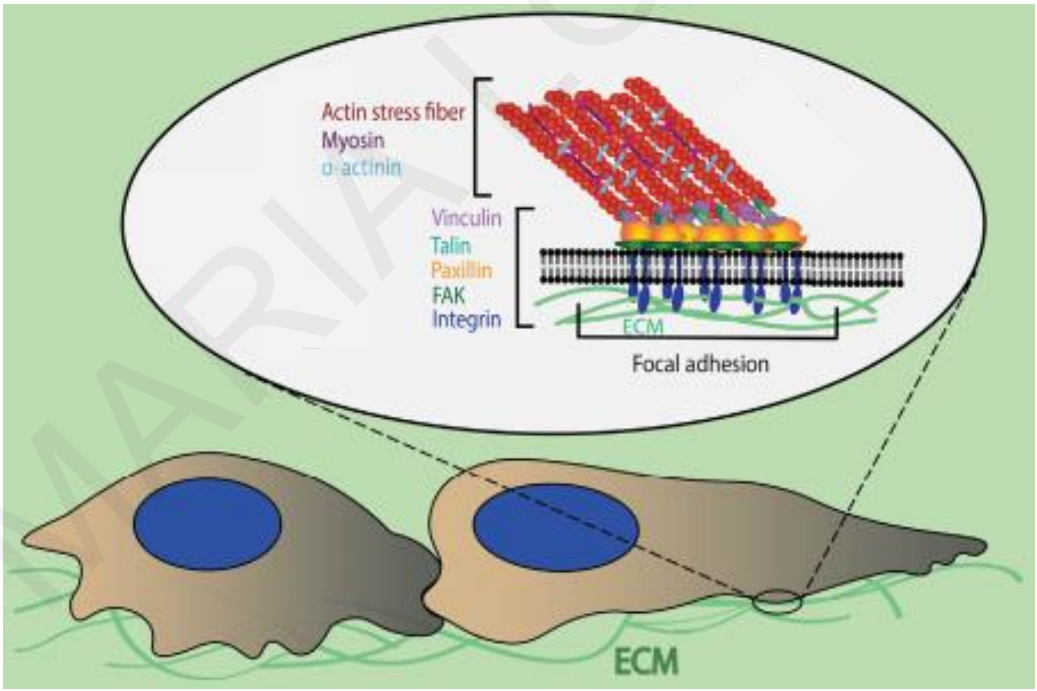

Figure 1-3. **Schematic representation of Focal Adhesion (FA) sites.** The binding of integrins to ECM, recruits signaling proteins and structural FA proteins such as talin, paxillin and vinculin, which are associated with actin cytoskeleton[27].

1.3 The Integrin-linked kinase, PINCH-1, parvin complex (IPP) at cell ECM adhesion sites

Integrin-linked kinase (ILK) is an important component of FAs [28]. It was initially described as an intracellular serine/threonine protein kinase that interacts with the integrin β1 cytoplasmic domain[29] to modulate various cellular functions. However, increasing data indicate that in most cases ILK acts as a pseudokinase as, in reality, it contains a domain with kinase homology that serves as mediator of several protein–protein interactions, rendering ILK a scaffold protein, with its main function being to target the IPP complex to FAs [30, 31]. ILK was found to play a vital role in promoting the aggressiveness of cancer cells by regulating the level and activation of several key molecular pathways downstream of integrins such as PKB/Akt, ERK and GSK3β [32-34]. Through its property to form protein-protein interactions ILK has been shown to form a stable ternary protein complex at FAs, namely IPP through its binding to PINCH-1 (Particularly Interesting new cysteine-histidine rich protein) and alpha-parvin as shown in **Figure 1-4** [35]. The IPP complex has been implicated in the regulation of several cell-ECM adhesion-mediated signaling pathways and many fundamental cellular functions such as cell survival, differentiation and adhesion to the ECM as shown in **Figure 1-5** [35-40].

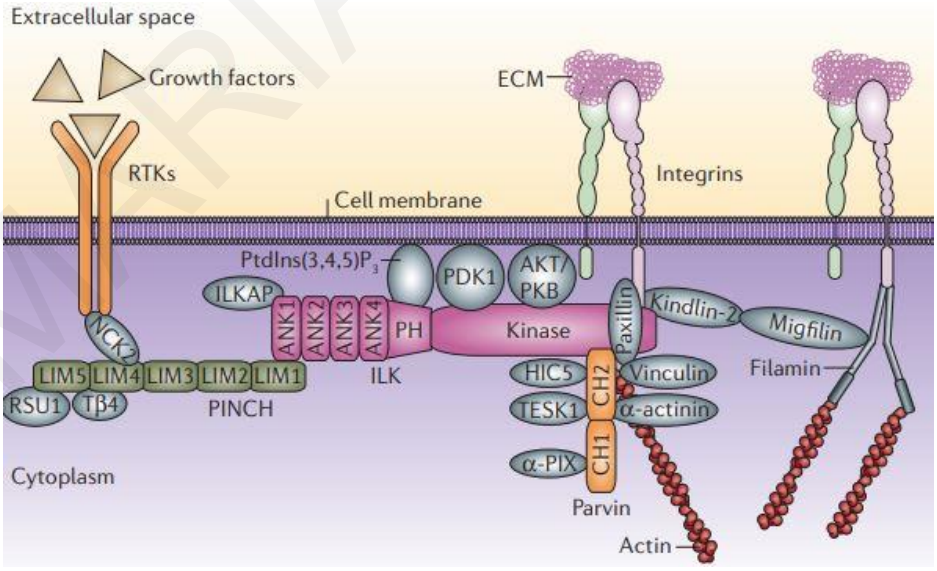

Figure 1-4. **A schematic model of IPP complex consisting of ILK, PINCH1 and Parvin proteins at FAs.** It is obvious that apart from its connection to integrins the complex is also connected to actin cytoskeleton[35].

Thus, identification of accessory proteins able to associate with the IPP complex and modulate tissue-specific processes is essential to enhance our understanding of the IPP involvement in health and how their deregulations leading to cancerous phenotype. For instance, parvins (alpha and beta , PARVA and PARVB, respectively) are important components of the IPP complex and have been shown to regulate cell attachment and spreading through activation of Ras-related C3 botulinum toxin substrate 1 (Rac1) **(Figure 1-5)** [41]. Furthermore, PINCH-1, which is the other component of IPP complex, has been also found to interact with another FA protein known as Ras Suppressor 1 (RSU-1) , and regulate cell survival, migration and spreading[40, 42].

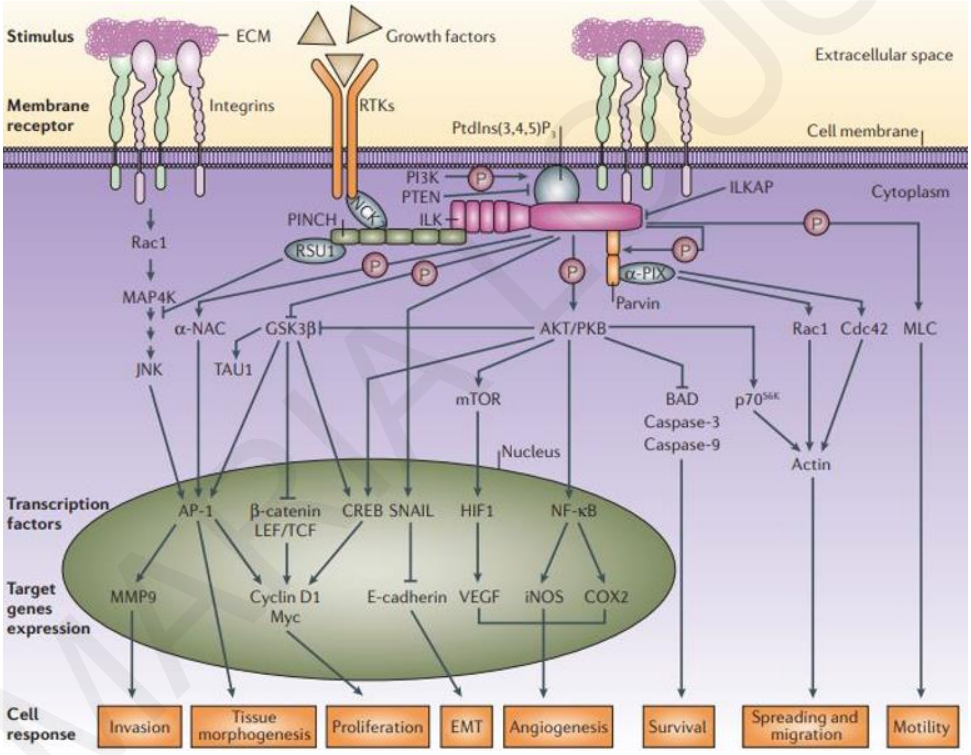

Figure 1-5. **Impliction of IPP complex in cell-ECM adhesion-mediated signaling pathways.** ILK protein of IPP complex upon ECM stimulus phosphorylates downstream proteins such as GSK3β and AKT/PKB and then other downstream proteins are regulated leading to alteration in gene expression and differential cell behavior such as invasion, migration and proliferation[35].

1.3.1 RSU-1 in normal tissue

RSU-1 is a 33kDa protein that is encoded by *RSU-1* gene located on human chromosome 10. RSU-1 was originally identified as a suppressor of Ras-dependent oncogenic transformation [43, 44] but it was later shown to localize to FAs where it interacts with PINCH-1 as shown in **Figure 1-4** [45].

Several research groups studied the role of RSU-1 in normal conditions **(Figure 1-6)**. When transiently overexpressed in NIH3T3 fibroblasts and PC12 pheochromocytoma cells, RSU-1 affected kinases downstream of *Ras* oncogene that are necessary for oncogenic transformation[46]. Specifically, *RSU-1* overexpression inhibited c-Jun N-terminal Kinase (JNK), and activated extracellular-signal-regulated kinase (ERK) in response to Epidermal Growth Factor (EGF) [46]. Moreover, PC12 cells overexpressing RSU-1 exhibited significant growth inhibition through elevation of p21 expression without being compromised in terms of their differentiation potential as seen by the fact that *RSU-1* overexpression resulted in Nerve Growth Factor (NGF)-induced differentiation through ERK activation [47].

Interestingly, the connection of RSU-1 with PINCH-1 seems to be crucial for its function, as depletion of *PINCH-1* reduces *RSU-1* expression leading to increased JNK activity in primitive endoderm cells [48]. Similarly, RSU-1 and PINCH-1 have shown to regulate JNK signaling and contribute to epithelial sheet migration during dorsal closure in Drosophila melanogaster development [49]. In fact, it was later shown in Drosophila that RSU-1 compensates for the loss of function occurring when the binding of PINCH-1 to ILK is compromised, maintaining the organism's viability and stabilizing the IPP complex [50]. To add more to the connection of RSU-1 to PINCH-1, it was shown that in MCF10A mammary epithelial cells, RSU-1 regulates PINCH-1 levels and stabilizes it while they act synergistically to regulate cell spreading through activation of Rac1 [42]. Nevertheless, it should be noted that RSU-1 function is not entirely dependent upon PINCH-1 localization to FA sites, as the depletion of either *PINCH-1* or *RSU-1* resulted in decreased cells adhesion, migration and loss of actin stress fibers in MCF10A cells while the reconstitution of *RSU-1*-depleted cells with PINCH-1 binding-defective *RSU-1* mutant could not rescue the effect of depletion on FAs or migration but did not affect cell spreading and p38 activation [51]. This indicates that RSU-1 and PINCH-1 are necessary for regulating adhesion and migration through the IPP complex but RSU-1 is also connecting FAs and spreading with p38 signaling [51]. Furthermore, it was recently shown that RSU-1 inhibited Akt

phosphorylation and promoted the mRNA expression of tumor suppressor gene Phosphatase and Tensin homologue (PTEN) through p38 activation[52].

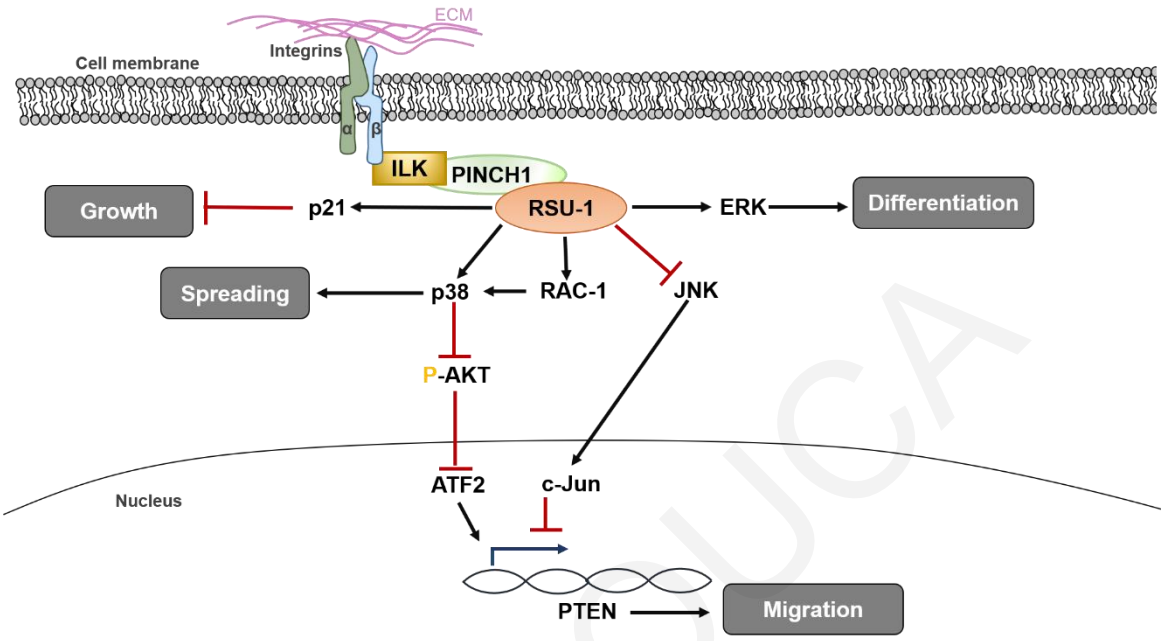

Figure 1-6. **Schematic representation of the role of RSU-1 in normal tissue.** Activation of RSU-1 regulates the spreading, migration, differentiation and proliferation of normal cells.

Finally, RSU-1 has been implicated in basic cellular functions of the CNS. More specifically, elimination of ILK in adult mammalian brain was found to enhance JNK activity and increase neural stem and progenitor cell proliferation via RSU-1 loss, suggesting that RSU-1 is critical in neurogenesis of the mammalian brain [53]. Furthermore, in another study, RSU-1 was shown to regulate synapse maturation through preventing spontaneous clustering of extrasynaptic acetylcholine receptors in Caenorhabditis elegans [54].

1.3.2 RSU-1 in cancer

RSU-1 has been identified to play a crucial role in many cellular processes and was initially identified as a suppressor of Ras-mediated oncogenic transformation, researchers have turned their interest in the involvement of RSU-1 in breast, liver and brain cancer progression through intracellular signaling transmission and actin remodeling as summarized in **Figure 1-7**[55, 56]. However, the exact role of *RSU-1* in cancer is still vague.

Initially, Vasaturo et al. in 2000 showed that overexpression of RSU-1 in MCF-7 breast cancer cells resulted in p21 activation and reduced cancer cell proliferation through inhibition of Cyclin-dependent kinase (CDK), proposing that RSU-1 acts as a tumor suppressor [57]. In a more recent study performed in 2015 using breast cancer cell lines, it was shown that *RSU-1* was upregulated in more aggressive MDA-MB-231 breast cancer cells compared to the non-aggressive MCF-7 breast cancer cells both at the mRNA and protein level and its silencing upregulated PINCH1 expression and induced cell proliferation through inhibition of p53 upregulated modulator of apoptosis (PUMA) [58]. Interestingly, these results were further validated in 32 human breast cancer samples with or without metastasis to the lymph nodes having normal adjacent tissues as controls. *RSU-1* was dramatically elevated in metastatic breast cancer samples and its expression was found to be negatively correlated with PINCH1 expression and positively with PUMA expression, indicating a possibly active pro-apoptotic mechanism.

Also, we recently employed a three-dimensional (3D) *in vitro* approach to grow breast cancer cells (3D culture) or form tumor spheroids and embed them in 3D collagen gels in an attempt to investigate cancer cell invasion in a more physiologically relevant manner that also takes account of the interactions with the ECM and the growth in 3D gels of different stiffness [59]. We found that RSU-1 was significantly upregulated in increased stiffness conditions while its depletion diminished the invasive capacity of tumor spheroids through inhibition of Urokinase Plasminogen Activator (uPA) and Matrix metalloproteinase 13 (MMP13)[59] . Interestingly and in support of our findings in the human breast cancer tissues, analysis of Kaplan-Meier survival plots revealed that high *RSU-1* expression is associated with poor prognosis for distant metastasis-free survival and remission-free survival in breast cancer patients [57, 59].

To shed more light upon the molecular mechanisms involved in the *RSU-1*-mediated promotion of cell invasion and metastatic behavior, *RSU-1* expression was transiently

silenced in breast cancer cells and we found that this silencing resulted in downregulation of Growth Differentiation Factor-15 (*GDF-15*)[60], a member of the Transforming Growth Factor-β family of proteins, known to be associated with actin cytoskeleton reorganization and metastasis [61-63]. *RSU-1* silencing also inhibited the expression of actin-modulating genes, namely *PARVA*, *RhoA*, Rho associated kinase-1 (*ROCK-1*), and *Fascin-1*. Notably, this inhibitory effect was completely reversed by GDF-15 treatment which also rescued the inhibitory effect of *RSU-1* silencing on cell migration and invasion [60].

It should be noted that apart from the originally-identified gene (*RSU-1*), an alternatively-spliced isoform, 29kDa protein, has been reported [64] to be expressed in human gliomas, which was also observed to be present in highly invasive MDA-MB-231 and MDA-MB-231LM2 breast cancer cells but not in the less invasive MCF-7 cells [65]. To decipher the exact involvement of *RSU-1* isoforms in cancer cell metastasis, we used shRNA-mediated silencing to generate breast cancer cell lines that permanently lacked *RSU-1*. Surprisingly, *RSU-1* depletion in the two cell lines had completely opposite effects on cell migration, invasion and tumor spheroid invasion. While *RSU-1* depletion from MCF-7 cells resulted in abrogation of migration, invasion and tumor spheroid invasion in 3D collagen gels, its depletion from MDA-MB-231-LM2 cells dramatically promoted all three pro-metastatic properties. At the same time short isoform of *RSU-1* was upregulated, perhaps as a compensatory mechanism for the loss of *RSU-1*. Interestingly, when the short isoform of *RSU-1* was also eliminated, RSU-1-depletion-induced migration and invasion were significantly inhibited along with reduction in uPA expression. Protein expression analysis data from 23 human breast cancer samples supported these findings showing *RSU-1* to be upregulated and the short isoform of *RSU-1* to be downregulated in metastatic samples.

All in all, it seems that both RSU-1 isoforms promote breast cancer cell invasion *in vitro* while the short isoform of *RSU-1* seems to act as a back-up for replacing the function of RSU-1 when the latter is lost. Hence, it is proposed that ideally both isoforms should be blocked to effectively eliminate metastasis.

Despite the fact that RSU-1 was studied more in breast cancer, some literatures about RSU-1 referred to liver cancer. Specifically, Donthamsetty et al., in 2013 [66] shown that elimination of PINCH1 in mice reduced *RSU-1* expression and liver cells proliferation. Moreover, has been shown that RSU-1 is frequent deleted in human liver cancer and its depletion in aggressive hepatocellular carcinoma cells (HepG2) reduced cell invasion[67]. Also, previously

was shown that Hepatitis C virus infection upregulates RSU-1 expression and liver cells growth abnormalities leading to cancerous phenotype [68].

Moreover, regarding the role of RSU-1 protein in brain cancer aggressiveness, was first made as early as in 1995[69]. Specifically, transient overexpression of *RSU-1* in U251 glioblastoma cells reduced the growth rate and aggressive cell behavior, indicating that *RSU-1* likely acts as a tumor-suppressor[69]. However, no information was available on the role of *RSU-1* in basic metastatic properties such as cell migration and invasion until recently.

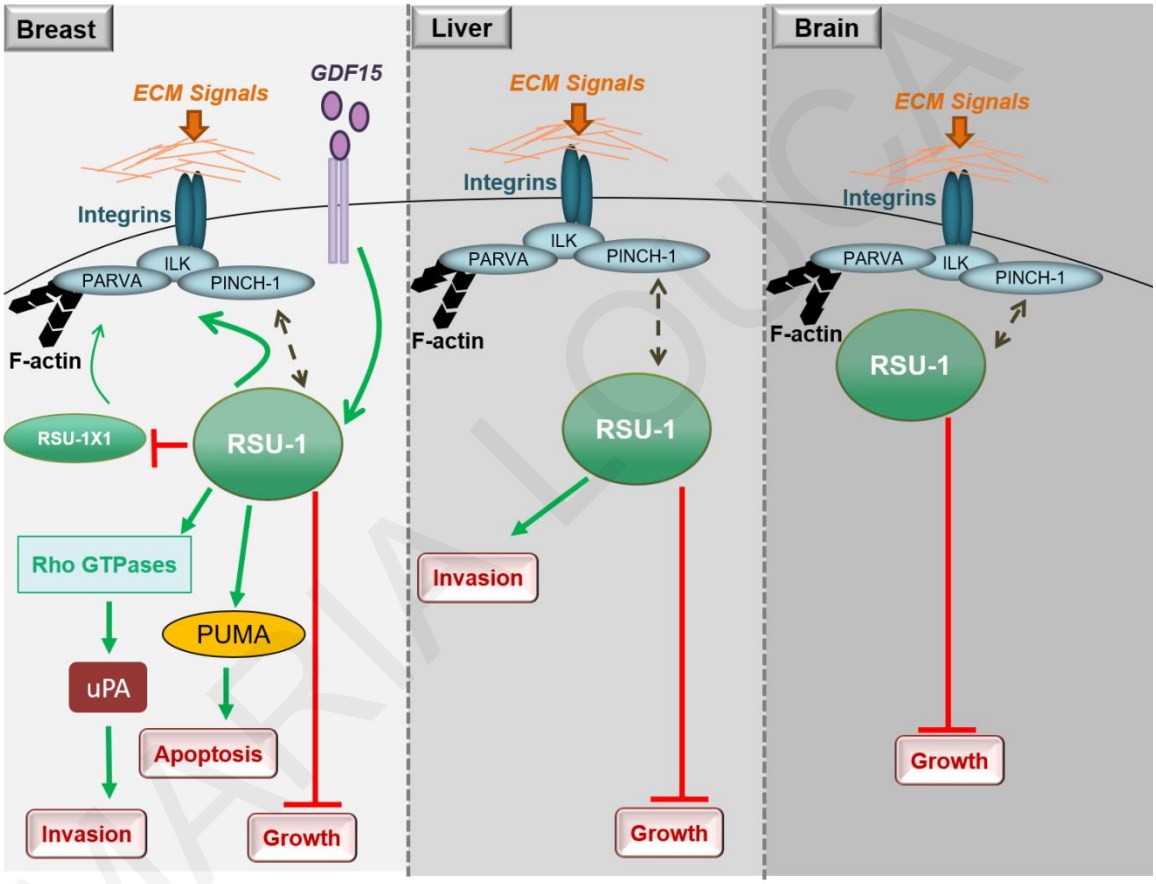

Figure 1-7. **Diagrammatic representation of RSU-1 role in behavior of breast, liver, and brain cancer cells** (Louca et al., submitted to Cancers, 2019).

1.4 Hypotheses and Objectives of this Ph.D thesis

Collectively, the above studies suggest that RSU-1 localization at FA sites is essential for many physiological cellular processes such as differentiation, adhesion, neurogenesis, migration and spreading in many different organisms (e.g. Drosophila, C. elegans) as well as in humans[42, 48-50]. However, deregulation of RSU-1 expression has been shown to correlate with certain cancer types [57, 58, 60, 65, 70].

Thus, taking into account that RSU-1 has a crucial role in basic cellular functions of the CNS[54], we hypothesized that alteration of RSU-1 expression levels may affect the glioma and more specifically glioblastoma progression. That was our motivation for this study because glioblastoma is the most aggressive type of brain cancer with a median survival of 1 year post-diagnosis[71] and no cure, so far.

Moreover, GDF15 which is responsible for actin cytoskeleton reorganization and regulates the invasion capacity in many types of cancer[72], was recently found to be involved in the regulation of RSU-1 protein expression levels and determines the behavior of breast cancer cells *in vitro*[60] . Therefore, we hypothesized that GDF15 may also regulate the expression of RSU-1 protein in glioma cells and affect their aggressiveness.

ILK protein is the main adaptor of the IPP complex which regulates the transmission of biochemical signals from the ECM into the cell[35]. Consequently, because RSU-1 is directly linked with IPP complex we hypothesized that ILK influences the motility and invasive behavior of glioma cells.

For these reasons, the objectives of this thesis are:

(i) Investigation of the role of RSU-1 in malignancy of human glioma cells and examination of the exact signaling pathway implicated in glioma cell invasion. *RSU-1* silencing approach through appropriate siRNA will be used.

(ii) Investigation of a possible connection between RSU-1 and GDF15 proteins and how their coordinated expression affects glioma cells' aggressiveness. For this purpose, three different approaches will be followed; human recombinant GDF15 (hrGDF15) treatment, *RSU-1* silencing and *GDF15* silencing with appropriate siRNA.

(iii) Investigation of ILK role in glioma cells aggressiveness and examination of the exact signaling pathway which is implicated in glioblastoma invasion. *ILK* silencing approach through appropriate siRNA will be used in vitro. Also, the Cancer Genome Atlas Glioblastoma Multiforme (TCGA-GBM) dataset will be used in order to corroborate our results with the protein expression of glioblastoma patients' tissues.

To accomplish the above goals a panel of four glioma cells with varying degree of aggressiveness will be used:

a) H4: Neuroglioma cell line, non-tumorigenic brain cells (Grade I),
b) SW1088: Astrocytoma cell line (Grade III),
c) A172: GBM cell line (Grade IV) and
d) U87-MG: GBM cell line (Grade IV)

2 Chapter 2: Ras suppressor-1 (RSU-1) promotes cell invasion in aggressive glioma cells and inhibits it in non-aggressive cells through STAT6 phospho-regulation

This research has been published in *Scientific Reports*: **Maria Louca**, Andreas Stylianou, Angeliki Minia, Vaia Pliaka, Leonidas G. Alexopoulos, Vasiliki Gkretsi and Triantafyllos Stylianopoulos. Ras suppressor-1 (RSU-1) promotes cell invasion in aggressive glioma cells and inhibits it in non-aggressive cells through STAT6 phospho-regulation. *Scientific Reports* volume 9, Article number: 7782 (2019) [doi: 10.1038/s41598-019-44200-8].

2.1 Introduction

As mentioned in the previous section, Glioblastoma multiforme (GBM), a type of astrocytoma arising from uncontrolled proliferation of astrocytes, is the most aggressive type of malignant brain tumors in the cerebral hemispheres [12, 73]. Its treatment, as with all gliomas, is multimodal consisting of surgical removal, radiotherapy and chemotherapy. However, although there are several therapeutic modalities, GBM still has poor prognosis due to the increased incidence of invasion of cancer cells into adjacent tissue forming metastases[74-76]. Indeed, invasion and migration of glioma cells away from the main tumor mass, is one of the most important issues in glioma therapy, being highly associated with decreased survival rates [77]. Genetic instability and deregulation of multiple focal adhesion (FA) proteins are known to be crucially involved in these processes[20, 78].

RSU-1 was first identified as a suppressor of *Ras* oncogene [46], exhibiting growth suppression effects [43, 57, 66, 69, 79] while it was later found to be localized to cell-ECM adhesion sites through its interaction with PINCH1 protein [45]. As mentioned in the previous section, beyond cancer cell proliferation, RSU-1 has been also documented to play a crucial role in

cancer cell migration and invasion [51, 65, 67, 80, 81] both of which are fundamental steps in the metastatic process. Little is known, however, regarding *RSU-1* expression and its role in tumors of the central nervous system[64]. It is hypothesized though that it should be involved in glioma pathogenesis as well, as it seems to play a critical role in regulating synapse maturation by preventing spontaneous clustering of extrasynaptic acetylocholine receptors [54] and enhances NGF-induced neuronal differentiation [47]. Also, lack of *RSU-1* activates JNK and neural stem and progenitor cell (NSPC) proliferation[53]. Hence, the main objective of this research work was the *in vitro* characterization of a panel of four commercially available glioma cell lines of varying degrees of invasiveness, namely H4, SW1088, A172 and U87-MG in terms of morphology, cytoskeleton organization, stiffness and aggressiveness as well as the determination of the involvement of RSU-1 in the metastatic properties of glioma cells.

2.2 **Methods**

Glioma cell lines. A panel of human glioma cell lines (H4, SW1088, A172 and U87-MG) was purchased from ATCC. Cells were grown in high-glucose DMEM medium supplemented with 10% fetal bovine serum and 1% antibiotic/antimycotic and were cultured in a humidified incubator supplied with 5% CO2 at 37°C.

Antibodies and reagents. Anti-RSU-1 rabbit polyclonal antibody for immunoblotting was kindly provided by Dr. Mary Lou Cutler, Professor at the Uniformed Services University of the Health Sciences, Bethesda USA. Anti-pSTAT6 and anti-STAT6 were obtained from Cell Signaling. Anti-MMP13 was purchased from Abcam. Phospho-STAT6 inhibitor, AS1517499, was obtained from Axon Medchem. *RSU-1* siRNA was

purchased from Santa Cruz Biotechnology. Rhodamine-Phalloidin was obtained from Biotium and 4',6-Diamidino-2-Phenylindole (DAPI) was obtained from Roche. Transwell inserts were purchased from Greiner Bio-One and Matrigel as well as Collagen I was obtained from Corning. QIAzol Lysis Reagent was purchased from QIAGEN.

Cell Elongation and Factor F measurement. Pictures of individual live cells were taken using a Nikon Eclipse TS100 inverted microscope equipped with a digital camera and a Nikon Ph1 DL 10x 0.25 phase microscope objective lens. ImageJ software was used to measure the factor E of the cells, which is calculated by dividing the longest axis by the shortest axis and subtracting one [82]. The elongation factor E describes the extent to which the equimomental ellipse is lengthened or stretched out [83]. Given the fact that factor E is zero (0) for a circle, and one (1) for an ellipsoid with an axis ratio 1:2, E values between 0–0.5 are considered to correspond to spherical cells, 0.5–1 to ellipsoids, and E values higher than 1 are considered to correspond to elongated cells [84].

Atomic Force Microscopy (AFM). Cells were cultured in 35 mm petri dishes overnight. Then the samples were directly mounded on AFM sample plates. The Young's modulus of cells was acquired by using a Molecular Imaging-Agilent PicoPlus AFM system with silicon nitride probes and a round, ball-shape tip (CP-PNPL-BSG-A-5, sQube, 5 μm diameter spheres, spring constant of 0.08 N/m). The Young's modulus which is in essence the stiffness of live cells was assessed by acquiring 8x8 points of force curves in an area of 5x5μm near the center of the cells [65]. For the acquisition of the force-displacement curves a set point of 1nN normal force at a 2 μm/s strain rate on each of the studied cells was used [85]. Subsequently, the AtomicJ software [86] and the Hertz model were employed for the calculation of the Young's modulus, while for the calculations the Poisson's ratio was assumed to be equal to 0.5.

Cytoskeleton assay staining and morphology identification. H4, SW1088, A172 and U87 cells were plated at a density of 10,000 cells per well on glass coverslips coated with 0.1% gelatin. Twenty-four (24) hours later, cells were fixed with 4% PFA for 20min and they were then permeabilized using a buffer containing 0.1% Triton X-100 and 2 mg/ml BSA in PBS. Cells were finally double stained with Rhodamine phalloidin and DAPI[87-89]. In order to characterize the actin cytoskeleton in terms of stress fiber formation and orientation, the freeware tool FilamentSensor was used. This tool is an open source software written in Java [http://filament-sensor.de/], for semi-automated detection of line segments in images. It is primarily designed for detection of actin fibers from microscopy images and it is based on the filament sensor (FS), a fast and robust processing sequence which detects and records location, orientation, length, and width for each single filament of an image[87]. In the analyzed figures the different fiber orientations of the F-actin stress fibers were represented with a different color[85, 87].

Transwell migration and invasion assays. Cell migration and invasion assays were performed using transwell chambers with 8 μm pore size membranes. The membranes of the inserts were either left uncoated and used for migration or were coated with diluted Matrigel (1:20) 24h before cell seeding and used for invasion, [90, 91]. In total, $3.5x10^4$ cells in 0.5ml of serum-free medium were added to the upper chamber, while the lower chamber was filled with 750μl of culture medium supplemented with 10% fetal bovine serum and 1% antibiotic/antimycotic. After a 24h incubation, the non-invading cells were removed from the upper surface of the membrane using a cotton swab. The cells that had passed through the membrane were fixed with 4% PFA for 20 min, and stained with 0.1% crystal violet in PBS for 20min[92-94]. All inserts were washed three times with ddH_2O and pictures were taken from nine (9) randomly selected microscopic fields that covered the

entire surface of the insert membrane using a Nikon Eclipse optical microscope equipped with a digital camera. Cells that migrated/invaded through the membrane were counted and the sum was taken for all nine optical fields. Three independent experiments were performed.

Tumor spheroids formation in collagen gels. The "hanging drop" technique was used to generate tumor spheroids, as described previously [65]. A suspension of $2.5x10^4$ glioma cells (H4, SW1088, A172 and U87-MG) was prepared and several drops of 20µl each containing 500 cells were placed on the cover of a culture dish. Spheroids were allowed to grow for 24 hours [95-97]. Individual spheroids were then embedded in wells of a 96-well plate containing 1.0 mg/ml collagen I [59]. Pictures were taken at time zero and at several time points. Spheroid's size was determined using the ImageJ software, and taking the mean length of the major and minor axis of the spheroid at a given time point compared to the initial size at time zero.

Phospho-STAT6 inhibitor treatment. Cells were treated with 100, 200 or 300 nM of phospho-STAT6 inhibitor, AS1517499, for at least 48h in high-glucose DMEM medium supplemented with 10% fetal bovine serum and 1% antibiotic/antimycotic according to previous studies[98, 99]. Inhibition of STAT-6 phosphorylation was verified by immunoblotting following standard procedures.

Transfection with siRNA. All cells were transfected with 100 nM siRNA against RSU-1 or a non-specific control siRNA, using the HiPerfect reagent (Qiagen) according to the manufacturer's guidelines. Cells were harvested 48h post-transfection.

Soft agar growth assay. Cells were trypsinized, suspended at a concentration of approximately $5x10^3$ cells/ml in 0.3% soft agar and placed on a layer of 0.6% soft agar in a

six-well plate. After a 30day incubation in a humidified atmosphere in the presence of 5% CO2 at 37°C, colonies were formed and were subsequently fixed with 4% PFA and stained with 0.01% crystal violet in PBS for 1h [100, 101]. Colonies were examined using an inverted microscope. Five randomly selected microscopic fields per well were used for quantification, and the number of total colonies per well were counted. Also, ImageJ software was used to measure the size of the colonies (area). The experiment was performed in triplicate for each cell line.

Sample preparation and phosphoproteins 'measurements. A custom 21-plex assay was built aiming to investigate cell invasion through the regulation of influential phosphoproteins. The Multiplex assay was designed following literature search to detect the most influential phosphoproteins and discover if these signaling molecules play an important role in glioma cell invasion upon RSU-1 silencing. Cells were lysed using cell lysis buffer (LysisPlex, ProtATonce, Cat Nr: LPA01) 48h post-transfection with appropriate siRNA (NSC or RSU-1 siRNA) and protein concentration was adjusted to 200μg/ml with lysis buffer. Cell lysates were used for the phosphoprotein measurements. Twenty-one (21) capture antibodies coupled to Luminex magnetic beads and 21 biotinylated detection antibodies were multiplexed to create the bead mix and the detection mix, respectively. The coupled beads (50μl of the bead mix) were incubated with the samples on a flat bottom 96-well plate on a shaker at 900rpm for 90 minutes at room temperature. Then, detection mix was added, and the samples were incubated further on a shaker at 900rpm for 60 minutes at room tempserature. The final step was the addition of freshly prepared SAPE solution (Streptavidin, R-Phycoerythrin conjugate, Cat Nr: S866, Invitrogen) for the detection of the signal. Following a 15minute incubation time with SAPE, samples were measured with the Luminex FlexMAP 3D instrument.

The following phospho-proteins were assessed: Transcription factor p65 (NF-Kb/TF-65, Cat Nr: P-NFKB-A01), Mitogen-activated protein kinase 12 (p38, Cat Nr: P-MK12-A01), RAC-alpha serine/threonine-protein kinase (AKT1, Cat Nr: P-AKT1-01), Serine/threonine-protein kinase WNK1 (WNK1, Cat Nr: P-WNK1-A01), Tyrosine-protein phosphatase non-receptor type 11 (PTN11, Cat Nr: P-PTN11-A01), Signal transducer and activator of transcription 3 (STAT3, Cat Nr: P-STAT3-A01), Heat shock protein beta-1 (HSP27/HSPB1, Cat Nr: P-HSPB1-A01), Transcription factor AP-1 (JUN, Cat Nr: P-JUN-A01), Signal transducer and activator of transcription 5A (STAT5, Cat Nr: -P-STAT5-A01), Glycogen synthase kinase-3 alpha/beta (GSK3A/B, Cat Nr: P-GSK3A/B-A01), 40S ribosomal protein S6 (RS6, Cat Nr: P-RS6-A01), Ribosomal protein S6 kinase beta-1 (p70S6K, Cat Nr: p-KS6B1-A01), Platelet-derived growth factor receptor beta (PGFRb, Cat Nr: P-PDGFRb-A01), Tyrosine-protein kinase Lck (LCK, Cat Nr: P-LCK-A01), Ribosomal pro/,tein S6 kinase alpha-1 (RSK1, Cat Nr: P-KS6A1-A01), Nuclear factor erythroid 2-related factor 2 (NRF2, Cat Nr: P-NRF2-A01), Cyclic AMP-responsive element-binding protein 1 (CREB1, Cat Nr: P-CREB1-A01), Signal transducer and activator of transcription 6 (STAT6, Cat Nr: P-STAT6-A01), Focal adhesion kinase 1 (FAK1, Cat Nr: P-FAK1-A01), Proto-oncogene tyrosine-protein kinase SRC (SRC, Cat Nr: P-SRC-A01), NF-kappa-B inhibitor alpha (Ik-Ba, Cat Nr: P-NFkB-A01), Proline-rich AKT1 substrate 1 (AKTS1, Cat Nr: P-AKTS1-A01).

RNA isolation and Real-Time Polymerase Chain Reaction (RT-PCR). Total RNA was extracted from cells using QIAzol Lysis Reagent as described previously [102]. The relative quantification of gene expression was assessed by RT-PCR in a CFX 96 Real Time-PCR machine (BioRad) and was analyzed by the ΔΔCt quantification method, using a relevant calibrator as specified in each figure legend. The sequences of the specific primers are described in **Table 1, in Appendices.**

Protein extraction and western blotting. Whole cell extracts were prepared using radio immunoprecipitation assay (RIPA) buffer containing a protease inhibitor cocktail tablet (Sigma) and 1% sodium dodecyl. Western blot analysis was performed using standard immunoblotting protocols as described previously [65, 102]. More specifically, equal amounts of total protein lysates were separated by 12% polyacrylamide gel electrophoresis. The proteins were transferred to a PVDF membrane using the Semi-dry transfer system (BioRad). Then, the membrane was blocked with 5% skim milk in tris-buffered saline-tween (TBS-T) buffer for 1 h and was incubated with appropriate antibodies overnight in 5% skim milk at 4 °C. The detection of the antibody was done with enhanced chemiluminescent system from Pierce and Kodak Biomax light films or using ChemiDoc XRS+ Imaging System (BioRad) and protein expression was quantified compared to the β-actin loading control using the ImageJ software. The mean intensity of respective protein bands from four different immunoblots was used for the quantification, as indicated.

Statistical Analysis. Results are represented as mean ± standard error (SE). Significant changes were determined by Student's t test using two-tail distribution. Differences with p values <0.05 were considered as statistically significant (indicated by an asterisk *).

2.3 Results

Glioma cell morphology is associated with their invasive behavior. We first set out to characterize the four human glioma cell lines (H4, SW1088, A172 and U87-MG) with regard to their morphology and assess the possible connection that morphology may have with cell aggressiveness. Optical microscopy imaging and elongation analysis demonstrated that A172 and U87-MG cells, which cause GBM, were more

elongated than H4 and SW1088, which are non-tumorigenic epithelial and fibroblast-like cells, respectively **(Figure 2-1A&1D)** [103-105]. As cytoskeletal remodeling is fundamental for metastasis-related processes, such as migration and invasion [106], cells were also stained with phalloidin, a widely-used fungal toxin known to bind filamentous actin, in order to detect possible changes in the organization of the cytoskeleton. **Figure 2-1B** shows that H4 and SW1088 cells exhibited abundant F-actin stress fibers in contrast to A172 and U87-MG cells where filamentous actin was not that prominent. Furthermore, we used the FilamentSensor tool software [87] in order to investigate the stress fiber orientation in each cell line. As shown in **Figure 2-1C**, stress fibers in H4 and SW1088 cells presented random orientation, while A172 and U87-MG exhibited well-organized actin fibers. Interestingly, A172 and U87-MG cells formed more lamellipodia, the thin sheet-like membrane protrusions found at the leading edge of migrating cells, as indicated by the arrow in **Figure 2-1B**, suggesting that these two cell lines are more prone to migration.

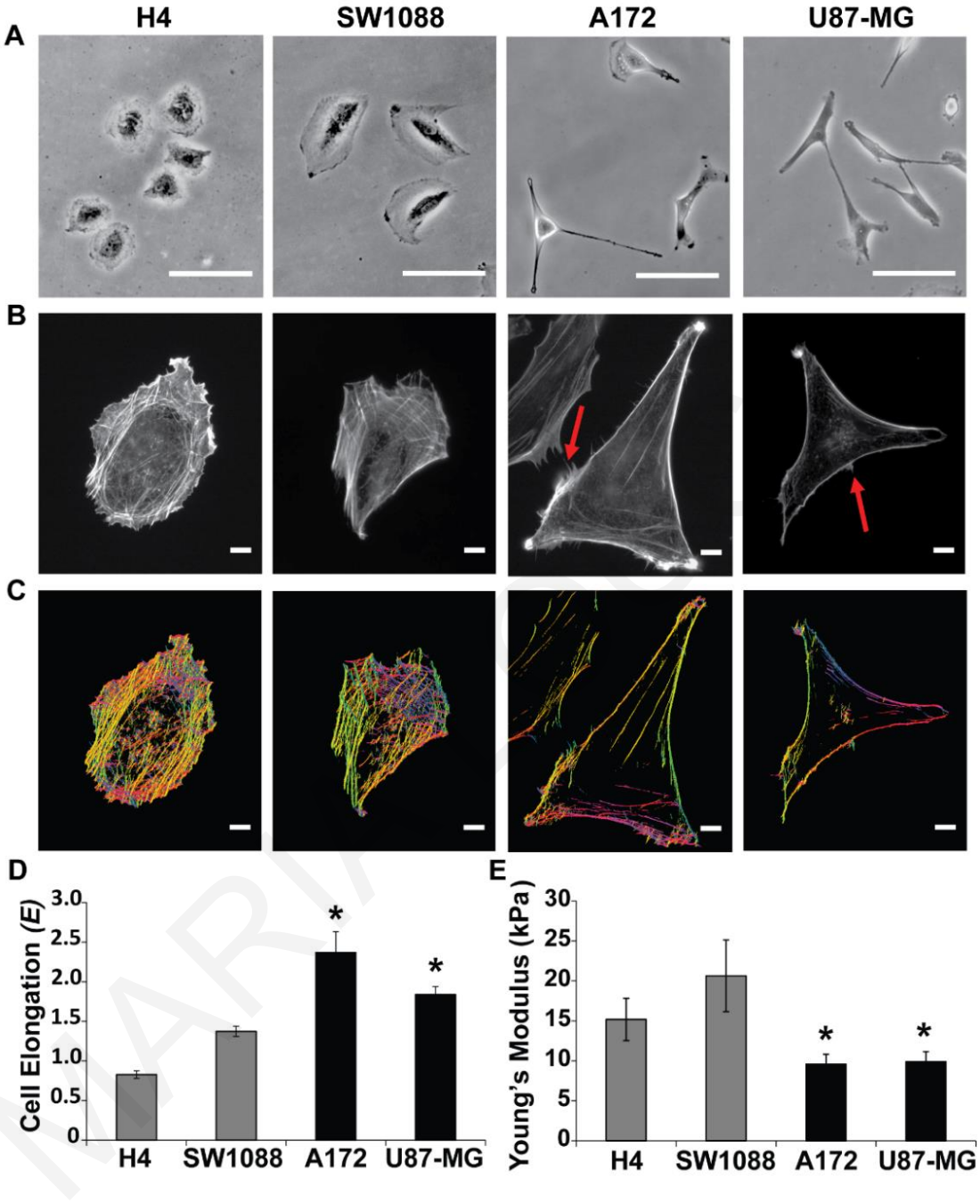

Figure 2-1. **Morphological characterization of glioma cells**. Representative images from **(A)** optical microscope imaging of H4, SW1088, A172 and U87-MG cells. Scale bar: 100µm **(B)** fluorescence microscope imaging of phalloidin-stained cells and **(C)** stress fiber orientation analysis using the FilamentSensor tool software where each color matches to a different fiber orientation (n=30 from each cell line and each group). Scale bar: 10µm **(D)** Cells elongation quantification, factor E was calculated from optical microscopy images of live cells, and **(E)** Young's modulus measurements using AFM. Asterisks denote a statistically significant difference ($p<0.05$) compared to H4 data.

Elongated and softer glioma cells are more invasive. Intrigued by the finding that A172 and U87-MG have morphological characteristics that differentiate them from H4 and SW1088, we sought to find out whether their stiffness was also related to their invasive potential. Several studies in the literature have connected these two, showing that the softer the cell the more likely it is to exhibit malignant characteristics[85]. For this purpose, AFM was used to measure cell stiffness of the four glioma cell lines. We found that A172 and U87-MG cells were softer than H4 and SW1088 **(Figure 2-1E)**, as demonstrated by the reduced Young's modulus value. The absolute values of the cell's Young's modulus were found to be H4:15.2±2.6 kPa, SW1088:20.6±4.5 kPa, A172:9.6±1.2 kPa and U87-MG:9.9±1.3 kPa (Young's Modulus Absolute Value= Average ± Standard Error), which lie within the expected values for live cells[107, 108] .

To test our hypothesis that cell stiffness is related to malignant characteristics, such as cell migration and invasion, a transwell invasion assay was performed. Over a 24-h period, the number of cells that invaded through matrigel differed among the four glioma cell lines **(Figure 2-2A&2C)**. The total number of cells invading through matrigel in average per transwell is presented in **Figure 2-2C**. The more aggressive U87-MG and A172 cells showed a statistically significant increase in invasion compared to the less aggressive H4 and SW1088.

To corroborate the data obtained from the transwell invasion assay, glioma cancer cell spheroids were generated from all four cell lines under study and embedded in 1mg/ml collagen I gels – the experimental procedure is presented in [59]. Notably, the rate of tumor spheroid invasion was dramatically different between the cell lines, further verifying that A172 and U87-MG are more invasive than H4 and SW1088. **Figure 2-3A** shows

representative images of H4 and A172 spheroids at their corresponding times. Specifically, A172 and U87-MG tumor spheroids invaded quickly and started dissociating from the original spheroid mass within 6h, while H4 spheroids reached a similar state at 16h, and SW1088 spheroids at 12h **(Figure 2-3B)**. Thus, the incubation time needed for spheroid invasion was correlated with the aggressiveness of cells and their invasive potential.

Aggressive cells construct colonies in unfavorable conditions. As our findings indicated that A172 and U87-MG cells were more elongated, softer, and formed tumor spheroids that invaded faster through collagen gels than H4 and SW1088 cells, we next examined the degree of their aggressiveness using the standard soft agar assay **(Figure 2-2B)**. The number of colonies formed on soft agar by the four glioma cell lines at the end of the 30-day period was measured and results are shown in **Figure2-2D**. U87-MG and A172 cells formed multiple large colonies on agar, while the other two cell lines only formed a few small colonies **(Figure 2-2E)**. Notably, U87-MG cells formed colonies of the largest size. These results further confirm that A172 and U87-MG exhibit a more invasive phenotype than H4 and SW1088.

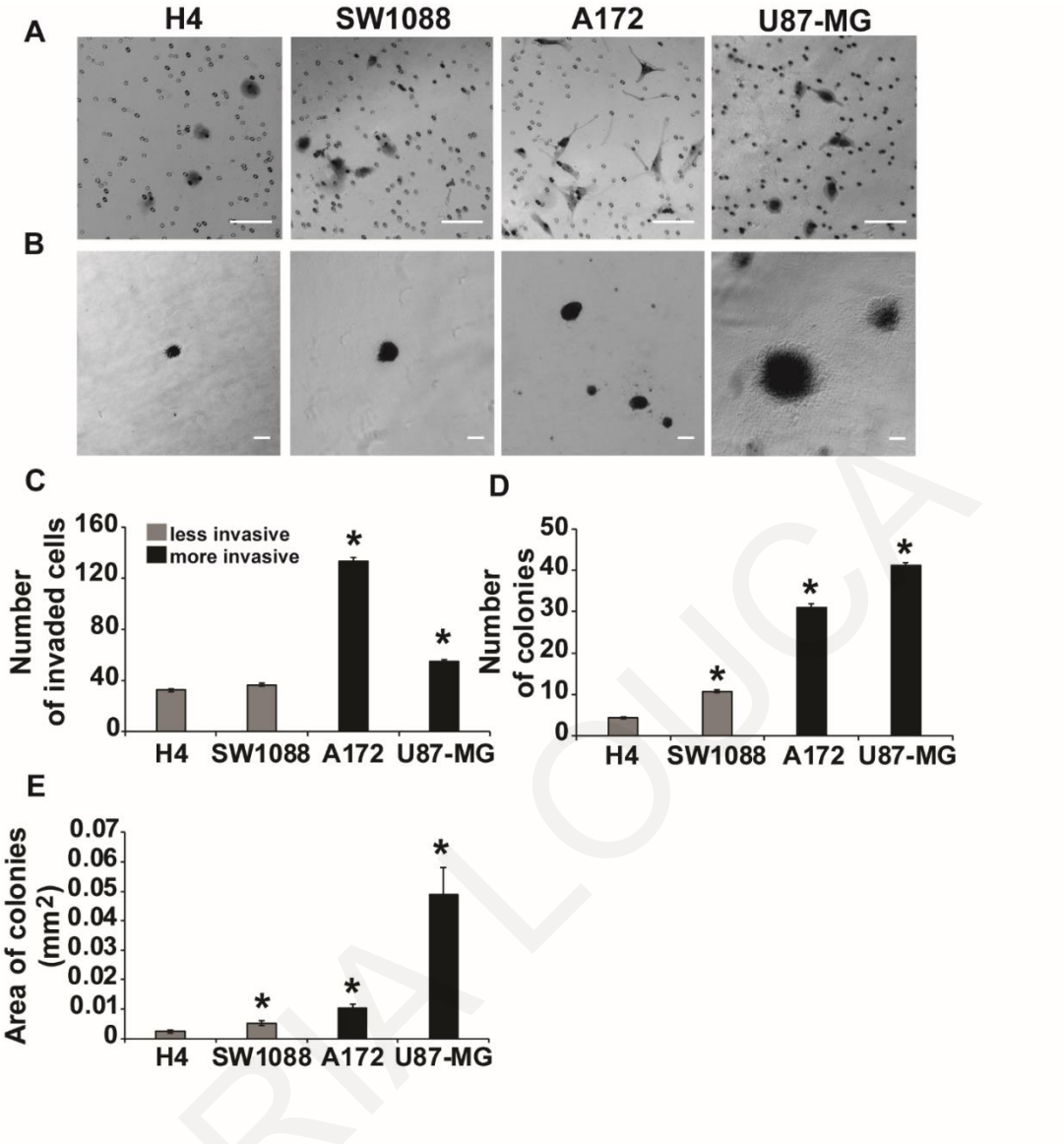

Figure 2-2. **Aggressiveness of glioma cells. (A)** Representative images of a transwell invasion assay using matrigel-coated inserts. The experiment was performed for 24h and the invading cells were counted in nine (9) randomly chosen microscopic fields per transwell. **(B)** Representative images of soft agar assay for 30 days. For quantitative analysis, five (5) images per well were taken with inverted microscope. Scale bar:100μm **(C)** Mean of total number of invaded cells per transwell of cell invasion compared to H4 cell line. Each sample was run in triplicate and three (3) independent experiments were performed. **(D)** Mean of total number of colonies per well compared to H4 cell line. Each sample was run in triplicate. **(E)** Area of colonies in mm^2 in average per well. Asterisks denote a statistically significant difference ($p<0.05$) compared to H4 data.

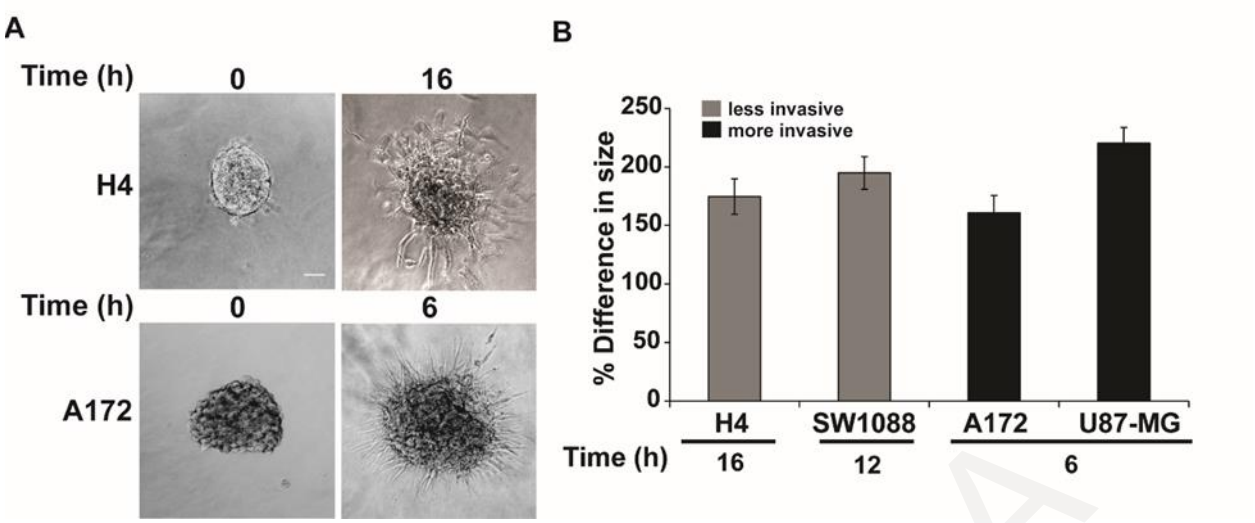

Figure 2-3. **Tumor spheroid invasion assay in collagen.** Spheroids (in average n=15 spheroids per cell line) were embedded in 1mg/ml collagen I gel and left to invade through the gel for different time periods depending on the aggressiveness of each cell line. **(A)** Representative images of H4 (least invasive) and A172 (most invasive) cells for 16h and 6 h, respectively. **(B)** The percentage of tumor spheroid invasion in each case was assessed by measuring the difference of each spheroid size ((major+minor axis)/2) within the corresponding hours following placement of the spheroid in the collagen gel (time zero).

RSU-1 protein and mRNA expressions are elevated in the aggressive glioma cells. As *RSU-1* has been previously reported to be overexpressed in metastatic breast cancer samples as well as highly invasive breast cancer and hepatocellular carcinoma cell lines [58, 67], we investigated if it is differentially expressed in our glioma cell lines and if its expression is correlated with invasiveness. In that regard, we first tested the expression of *RSU-1* at the mRNA level. Real-Time PCR was performed for the *RSU-1* gene using actin as housekeeping gene and H4 cell line as calibrator **(Figure 2-4A).** Our results showed that the more aggressive A172 and U87-MG cell lines overexpressed *RSU-1* compared to the less aggressive H4 and SW1088 cell lines. Real-Time PCR results were also validated by immunoblotting (**Figure 2- 4B&4C**, note lanes 3 and 4 compared to lanes 1 and 2).

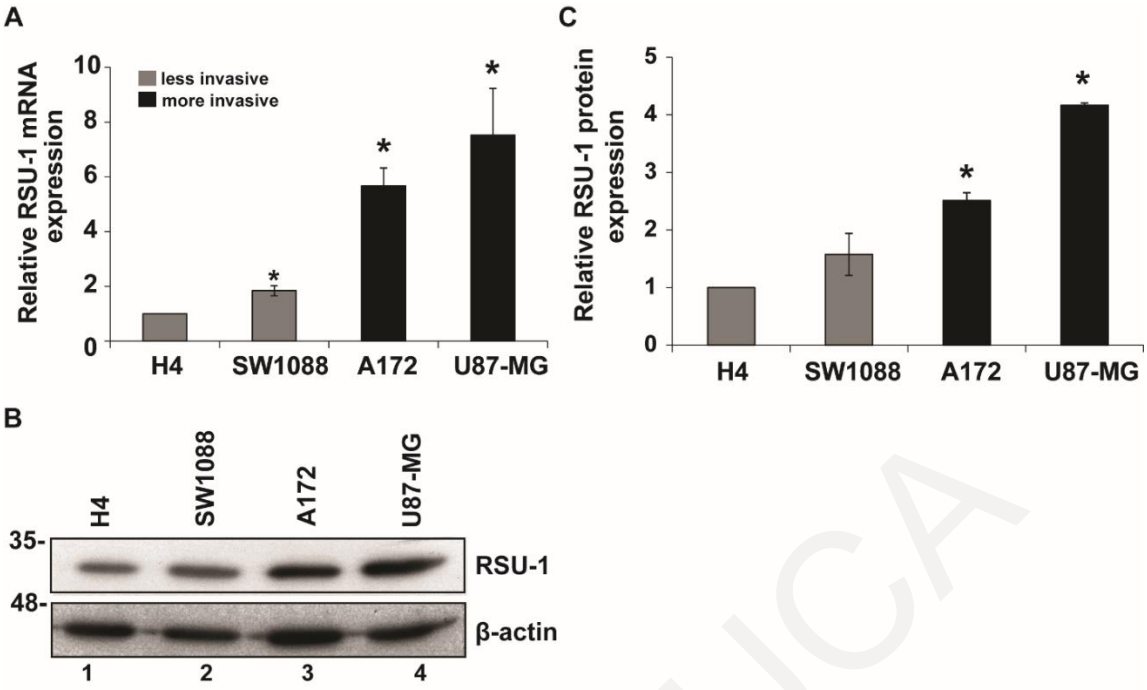

Figure 2-4. **RSU-1 expression is elevated in more invasive glioma cells. (A)** Relative *RSU-1* mRNA expression for the four glioma cell lines under study. Four independent Real Time PCR experiments were performed, and data were analyzed using the ΔΔCt method **(B)** Western blot for *RSU-1* protein expression, using β-actin as a loading control and H4 as a sample control **(C)** Graph shows the quantification of *RSU-1* protein expression by ImageJ software from three different western blots. Asterisks denote a statistically significant difference ($p<0.05$) compared to H4 data.

Elimination of RSU-1 from glioma cells differentially affects their motility. To identify the role of RSU-1 in the metastatic properties of glioma cells, it was silenced using siRNA-mediated silencing using a non-specific control siRNA (NSC) as transfection control. *RSU-1* was effectively silenced both at the mRNA **(Figure 2-5A)** and protein **(Figure 2-5B&5C)** level. Then, transwell migration assay was performed to find out how *RSU-1* silencing affects cell motility. The number of cells that migrated through the transwell pores was counted 24h after the addition of cells in the transwell and 48h after siRNA transfection. Surprisingly, *RSU-1* silencing did not have the same effect in all four glioma cell lines tested. Interestingly enough though, the migratory response of cells was associated with the degree of malignancy to which we assigned them based on the results

of morphological analysis, AFM measurements, soft agar growth and spheroid invasion. The least aggressive glioma cells (H4 and SW1088) exhibited increased motility following *RSU-1* silencing in contrast to the most aggressive glioma cells (A172 and U87-MG), which exhibited decreased motility after *RSU-1* silencing **(Figure 2-6A&6B)**.

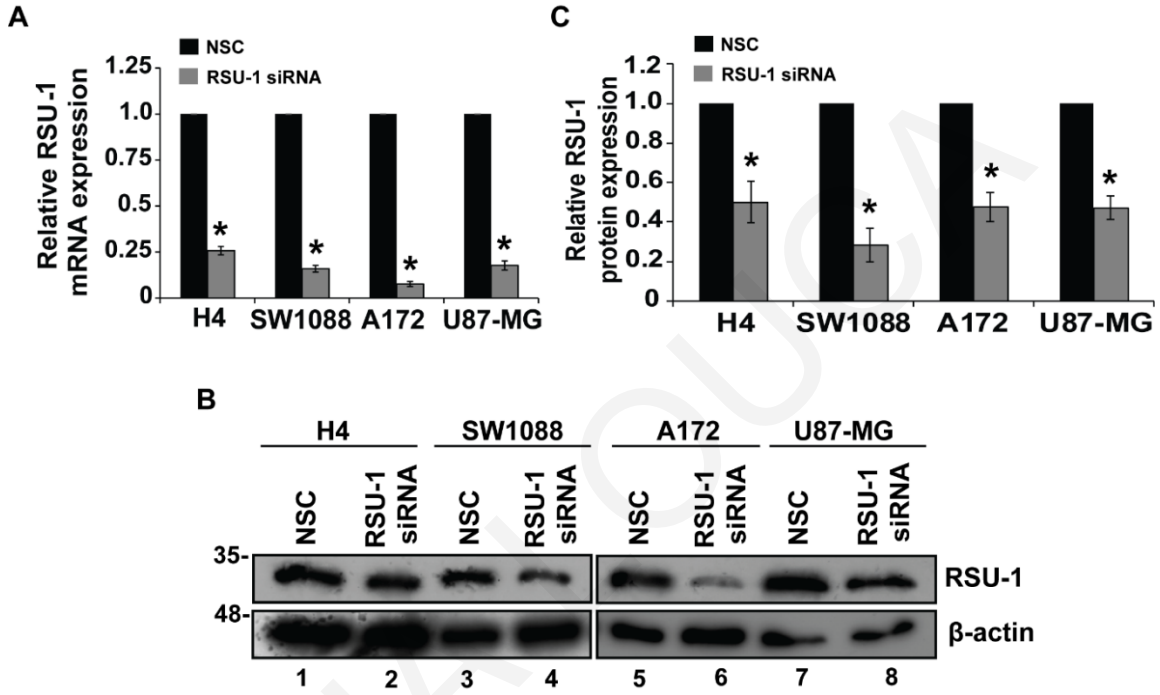

Figure 2-5. **RSU-1 is effectively silenced both at the mRNA level and protein level.** ***(*****A)** Relative mRNA expression of *RSU-1* in H4, SW1088, A172 and U87-MG cells upon treatment with NSC or RSU-1 siRNA for at least 48h. Eleven (11) independent RT-PCR experiments were performed and data were analyzed using the ΔΔCt method, having NSC treated cells as a calibrator sample for each cell line. **(B)** Representative immunoblot showing RSU1 expression at the protein level following treatment with NSC or *RSU-1* siRNA in all four glioma cell lines studied. **(C)** Graph representing quantification of RSU-1 protein expression normalized to β-actin for each cell line using ImageJ software. Immunoblots from four (4) independent experiments were used for the quantification. Asterisks denote a statistically significant difference ($p<0.05$) compared to NSC data.

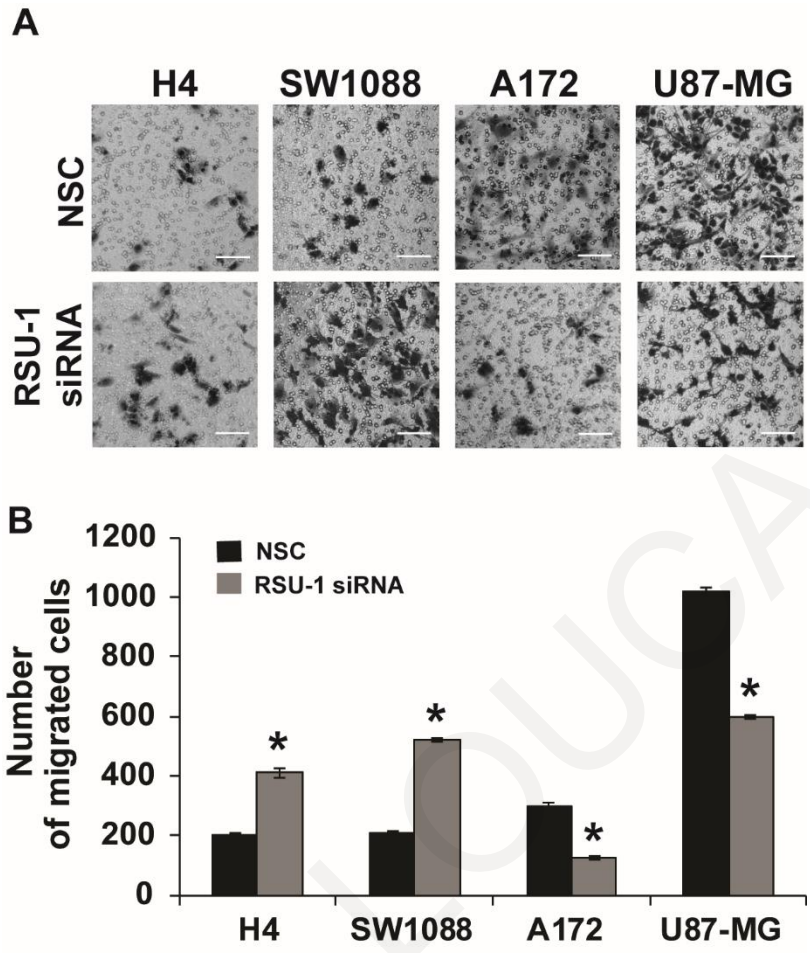

Figure 2-6. **RSU-1 silencing increased migration of the non-aggressive glioma cells but decreased migration of the aggressive cells. (A)** Representative images of a transwell migration assay that was performed for 24h for the four glioma cell lines with NSC or RSU-1 siRNA treatment. Scale bar: 100μm. The migrating cells were counted in nine (9) randomly chosen microscopic fields per transwell. **(B)** Total number of migrated cells compared to NSC for each cell line per transwell. Each sample was run in triplicate and three (3) independent experiments were performed. Asterisks denote a statistically significant difference ($p<0.05$) compared to NSC data.

RSU-1 enhances the invasion potential of aggressive glioma cells through MMP13, in contrast to non-aggressive glioma cells. Next, transwell invasion assay was performed following *RSU-1* silencing in all glioma cell lines. In accordance with cell motility results, invasion capacity was also found to be decreased upon *RSU-1* silencing in the most aggressive glioma cells, whereas it was increased in the least aggressive cells **(Figure 2-7A)**. **Figure 2-7B** indicates the mean of the total number of invaded cells per transwell for each cell line upon *RSU-1* silencing.

Finally, we tested whether *RSU-1* silencing affects key molecules involved in matrix degradation, an important aspect of cell invasion. Thus, following *RSU-1* silencing, we tested the mRNA expression of matrix metalloproteinase13 (MMP13) a fundamental protease in cancer cell metastasis, known to be involved in collagen I degradation [109, 110] that was previously shown to be regulated by *RSU-1* silencing in breast cancer cells [65]. We found that MMP13 mRNA expression was following a pattern identical to that of cell migration and invasion, corroborating our findings **(Figure 2-7C)**. Quantitative PCR results were validated further at the protein level by immunoblotting as shown in **Figure 2-7D&7E)**.

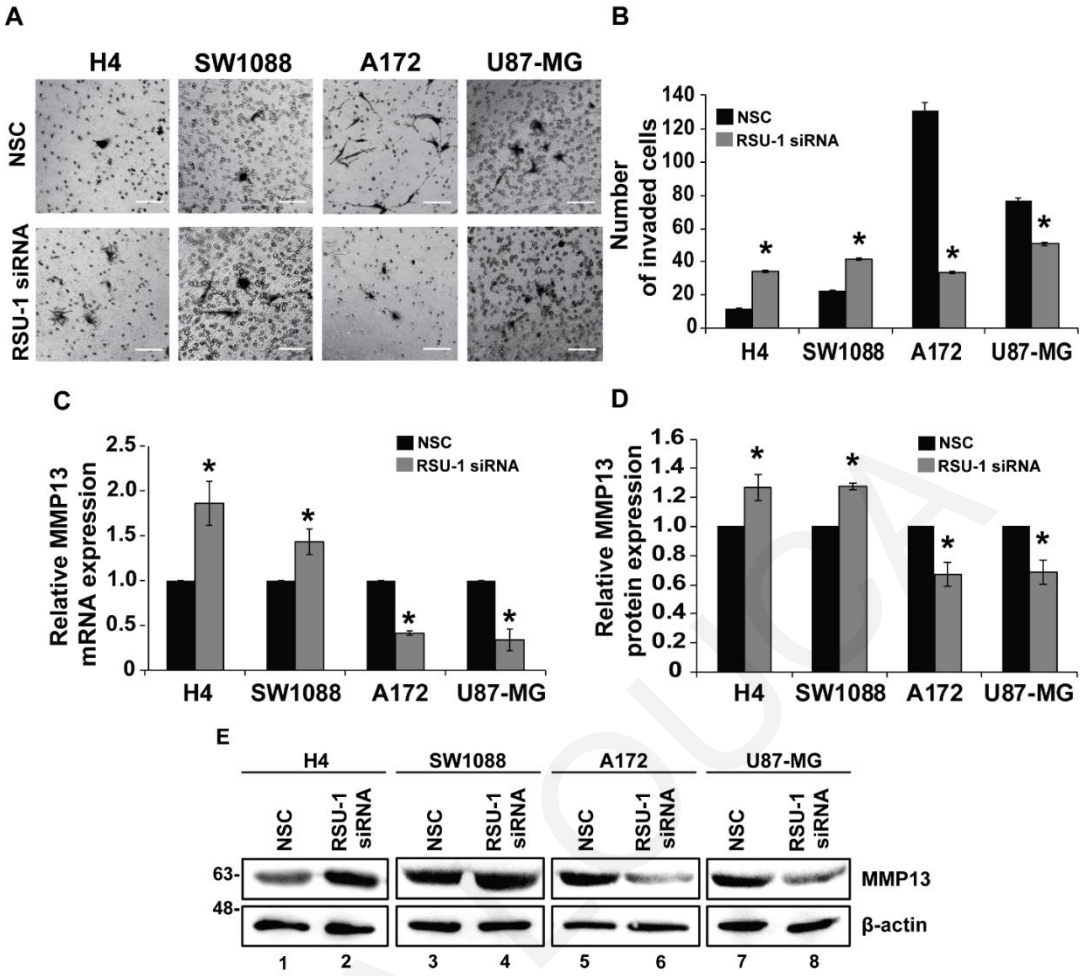

***Figure 2-7*. RSU-1 silencing increased invasion of non-aggressive glioma cells while decreased invasion of aggressive glioma cells through reduction in MMP-13. (A)** Representative images of a transwell invasion assay that was performed for 24h for the four glioma cell lines with NSC or RSU-1 siRNA treatment. The invading cells were counted in nine (9) randomly chosen microscopic fields per transwell. Scale bar: 100μm. **(B)** Total number of invaded cells compared to NSC for each cell line per transwell. Each sample was run in triplicate and at least three (3) independent experiments were performed. **(C)** Relative MMP13 mRNA expression following RSU-1 silencing for the four studying glioma cells was measured by RT-PCR and quantification was done using as NSC as the calibrator sample. **(D)** Graph representing quantification of MMP13 protein expression normalized to β-actin for each cell line following treatment with NSC or RSU-1 siRNA in all four glioma cell lines studied. Immunoblots from three independent experiments were used for the quantification using ImageJ software. **(E)** Representative immunoblot showing MMP13 protein expression. Asterisks denote a statistically significant difference ($p<0.05$) compared to NSC data.

RSU-1 silencing exerts its effect on glioma cell invasion through STAT6 phosphorylation regulation. Although the connection between cell invasion and MMP13 expression is well-established, we investigated whether other signaling molecules are mediating the effect of *RSU-1* silencing on cell invasion. To that regard, we selected the least invasive (H4) and one of the most invasive (A172) cells from the glioma cell panel, treated them with NSC or *RSU-1* siRNA and analyzed their protein expression using a Multiplexed Assay specifically designed to detect the 21 most influential phospho-proteins. Analysis of the Multiplex assay **(Figure 2-8A)** showed that only Signal Transducer and Activator of Transcription6 (STAT6) exhibited changes in phosphorylation that were consistent with the observed invasion pattern as well as with recently published data showing STAT6 to promote invasion in glioma cells [111]. More specifically, the least invasive cells (H4) treated with *RSU-1* siRNA had an increased level of phospho-STAT6 and a more invasive potential **(Figure 2-8B)**, whereas the more invasive cells (A172) treated with *RSU-1* siRNA exhibited decrease d phospho-STAT6 levels and a less invasive capacity **(Figure 2-8A&8B)**. The multiplex assay results were validated further by immunoblotting for H4 and A172 cell lines **(Figure 2-8C)** as well as SW1088 and U87-MG cell lines. To test whether STAT-6 phosphorylation is crucially involved in glioma cell invasion, we inhibited it in H4 and A172 cells by varying the concentration (100, 200 & 300nM) of the AS1517499 inhibitor, and we found that their invasive capacity was reduced upon inhibition of STAT-6 phosphorylation in a dose-dependent manner in both cell lines **(Figure 2-9A&9B).** These results were then validated in SW1088 and U87-MG cells using only the optimum concentration of the AS1517499 (300nM) as shown in **Figure 2-10**.

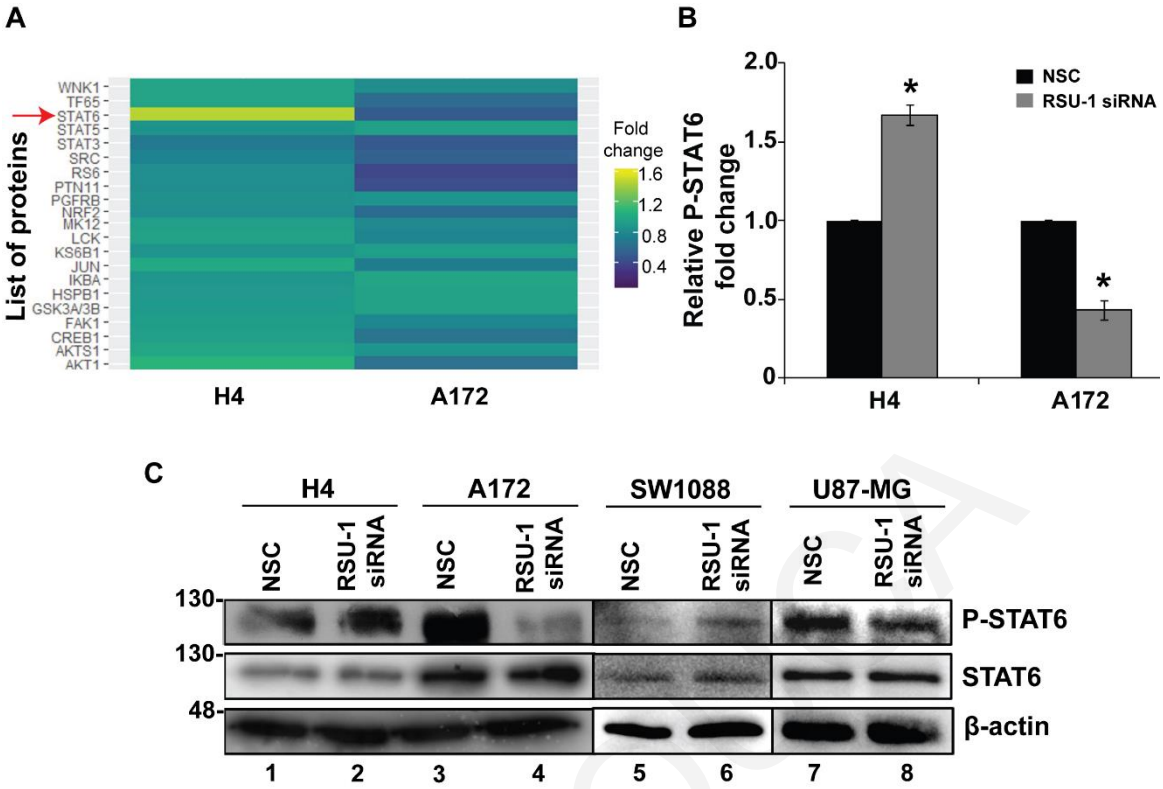

***Figure 2-8*. RSU-1 silencing enhanced STAT6 phosphorylation in non-aggressive glioma cells while diminished STAT6 phosphorylation in aggressive glioma cells. (A)** The heatmap depicts mean fold change results from the phosphoproteomic analysis performed for 21 phospho-proteins in two independent experiments between the treated (RSU-1 siRNA) and control cells (NSC siRNA) for both H4 and A172 cell lines. Red arrow indicates the most significant change in phosphorylation status upon RSU-1 knockdown **(B)** Quantification of the phosphoprotein analysis data for P-STAT6 following RSU-1 silencing using NSC as the control sample. **(C)** Representative immunoblot validating the phosphorylation status of STAT6 for the same protein samples as in (A) and Representative immunoblot showing the phosphorylation status of STAT6 in SW1088 cell line (upregulation) and in U87-MG cell line (downregulation) after RSU-1 silencing. Asterisks denote a statistically significant difference ($p<0.05$) compared to NSC.

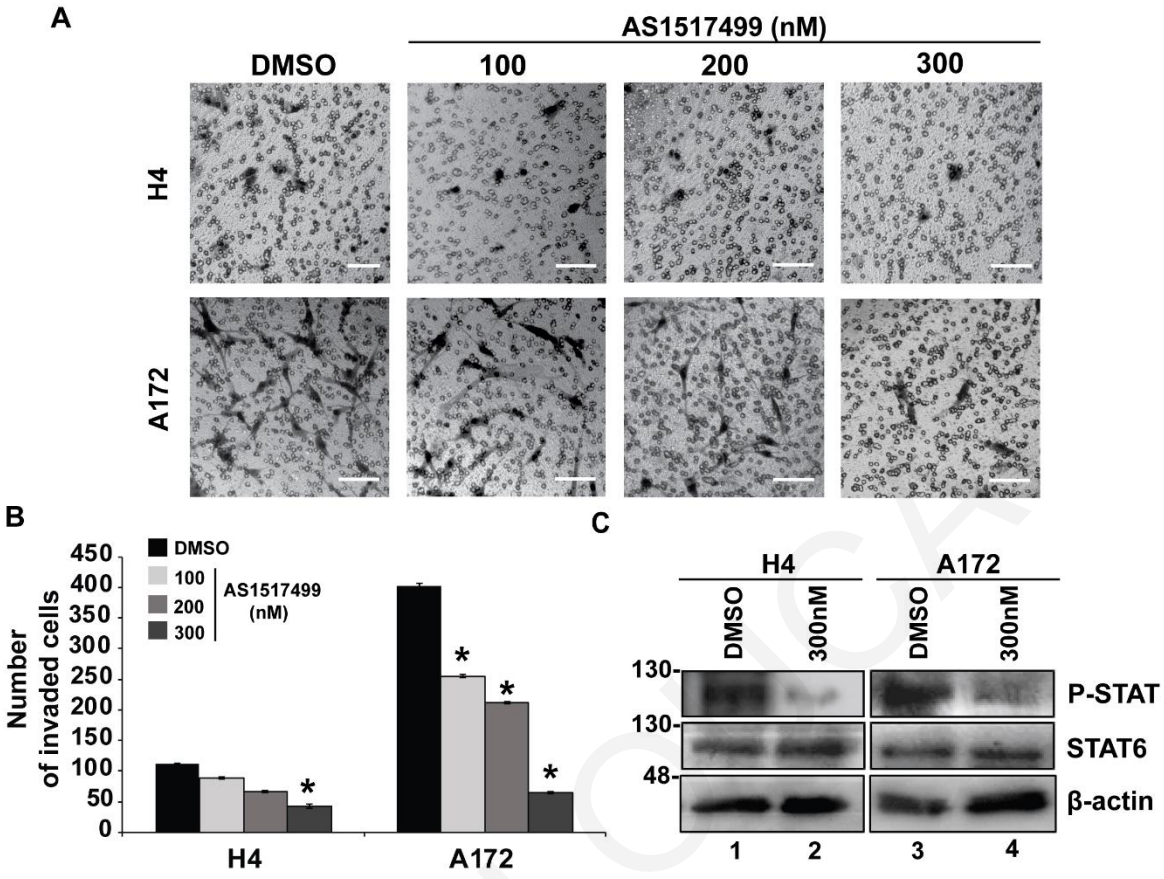

Figure 2-9. **In vitro effects of the phospho-STAT6 inhibitor (AS1517499), in glioma cell (H4 and A172) invasion. (A)** Representative images of transwell invasion assay performed following treatment with phospho-STAT6 inhibitor, AS1517499 (at 100, 200 or 300nM) or DMSO for 24h.Cells were left to invade for an additional 24h time period with inhibitor. The invading cells were counted in nine (9) randomly chosen microscopic fields per transwell. Scale bar: 100μm. **(B)** Total number of invaded cells compared to DMSO for each cell line per transwell. Two transwells were included per sample and at least two (2) independent experiments were performed. **(C)** Representative images of Western blot results of STAT6 phosphorylation in glioma cell lines (H4 and A172) following treatment with DMSO or 300nM of AS1517499. Asterisks denote a statistically significant difference ($p<0.05$) compared to DMSO.

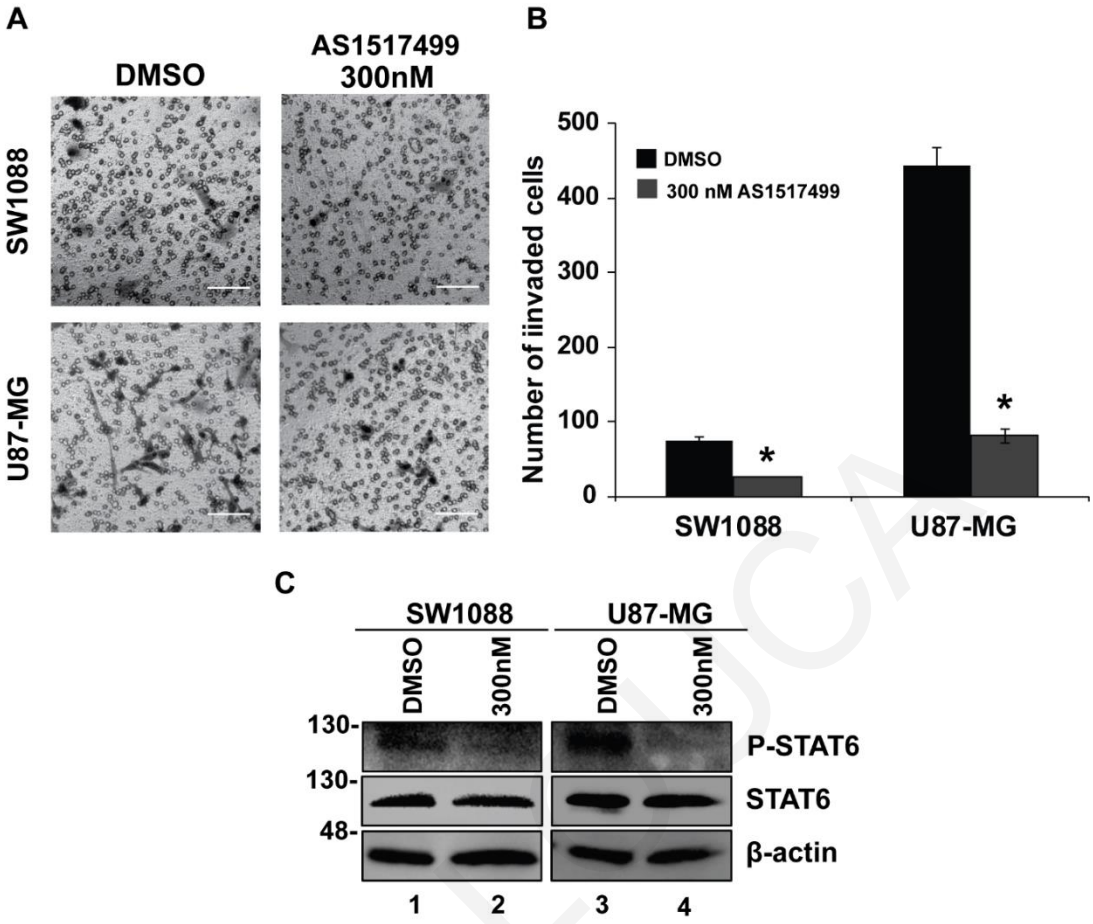

***Figure 2-10*. The effect of the phospho-STAT6 inhibitor (AS1517499) in SW1088 and U87-MG cell invasion. (A)** Representative images of transwell invasion assay performed following treatment with phosphor-STAT6 inhibitor, AS1517499 (300nM) or DMSO for 24h. Cells were left to invade for an additional 24h time period in the presence of the inhibitor. The invading cells were counted in nine (9) randomly selected microscope fields per transwell. Scale bar: 100μm. **(B)** Total number of invaded cells compared to DMSO for each cell line per transwell. Three transwells were included per sample. **(C)** Representative images of western blot results of STAT6 phosphorylation in SW1088 and U87-MG cells following treatment with DMSO or 300nM of AS1517499. Asterisks denote a statistically significant difference ($p<0.05$) compared to DMSO.

2.4 Discussion

In the current study, we used four glioma cell lines, namely H4, SW1088, U87-MG and A172 [103-105, 112] and we first characterized them based on their morphology, actin cytoskeleton organization, stiffness and invasion capacity. Our results show that A172 and U87-MG cells, which cause malignant tumors, were more elongated **(Figure 2-1)**, exhibited well-organized actin fibers, increased invasion in transwells **(Figure 2-2A)** and in collagen-embedded spheroids **(Figure 2-3)** and increased formation of colonies in soft agar **(Figure 2-2B)** showing metastatic abilities and capability for anchorage independent growth, respectively. Conversely, H4 and SW1088 cells were less elongated **(Figure 2-1A&ID)**, presented random orientation of actin stress fibers **(Figure 2-1C)**, reduced invasion **(Figure 2-2A)** and inability to grow in soft agar **(Figure 2-2B)**. Moreover, AFM measurements demonstrated that A172 and U87-MG cells exhibited statistically significant lower Young's modulus than H4 and SW1088, indicating that malignant glioma cells are softer than H4 and SW1088 a property that enables them to migrate faster **(Figure 2-1E)**. These findings are consistent with the results of pertinent studies in other cancer cell lines, which also showed that highly aggressive cancer cells are generally softer than non-malignant cells [108, 113, 114]. Interesting, the ratio of the Young's modulus value of the less invasive cells (non-tumorigenic, H4) to the Young's value of the other cell lines are: H4/SW1088= 0.73, H4/A172=1.58, H4/U87-MG=1.53. These results are similar to the results found in the literature[108, 115] and especially to the ratio (1.4–1.8) between healthy and breast cancer cells where similar spherical probes were used[116]. We then tested the expression of RSU-1, a FA protein that was previously shown to be implicated in breast cancer cell invasion promoting breast cancer cell metastasis, introducing RSU-1 as a potential metastasis marker [65]. We found here that *RSU-1* is upregulated in cell lines exhibiting higher invasion capacity (A172

and U87-MG) compared to the less invasive cells (H4 and SW1088) both at the mRNA **(Figure 2-4A)** and protein level **(Figure 2-4B&4C)**. Interestingly, we showed for the first time that *RSU-1* silencing has an opposite effect on glioma cell line invasion depending on whether the cell line is aggressive or not **(Figure 2-7A&7B)**. More specifically, *RSU-1* silencing in A172 and U87-MG cell lines inhibited their invasion, whereas it promoted invasion of H4 and SW1088 cells. Interestingly, *MMP13* expression followed an almost identical pattern **(Figure 2-7C& 7D).** Finally, we also showed through multiplex analysis of phospho-proteins that STAT6 phosphorylation was increased in the H4 cell line upon *RSU-1* silencing in contrast to A172 cells in which STAT6 phosphorylation was decreased **(Figure 2-8A&B)**. Multiplex results were validated by immunoblotting further confirming the involvement of STAT6 in glioma cell invasion **(Figure 2-8C)** as demonstrated in other cancer types[117]. Interestingly, we also found that the invasive capacity of H4 and A172 glioma cells was decreased following inhibition of STAT6 phosphorylation in a dose-dependent manner **(Figure 2-9A&9B)**. This result is in accordance with other previously published studies, showing that STAT-6 promotes glioma cells invasion [111], although this is the first time that *RSU-1* is being associated with STAT6 regulation as shown in **Figure 2-11**.

In conclusion, the present study provides the first evidence that RSU-1 has distinct roles in glioma cell invasion depending on the cells' aggressiveness. In fact, our finding that depletion of *RSU-1* from the highly invasive A172 cells -that normally express RSU-1 in high levels- inhibits cell invasion, whereas depletion of *RSU-1* from the non-invasive H4 cells –that normally express RSU-1 at minimal levels-enhances cell invasion indicates that there exists a type of regulation that is level-dependent. This is reminiscent of other cases in which the expression level of a FA protein is correlated with differential regulation of cell

migration[118], and definitely warrants further investigation. Further investigation is, of course, warranted in order to decipher the exact mechanism of action of RSU-1 in gliomas and the regulator of RSU-1 levels and how their coordinated expression affects the malignancy of glioma cells. Moreover, validation of the current findings in human glioma patients, especially of varying tumor grade would be rather valuable and might render RSU-1 a predictor of gliomas progression potentially contributing to the development of novel therapeutic interventions targeting it. Hence, patients with elevated *RSU-1* expression would be expected to have aggressive gliomas and would benefit from a treatment that includes blocking *RSU-1* whereas patients with reduced *RSU-1* expression would be expected to have less aggressive tumors and would thus benefit from a conventional treatment.

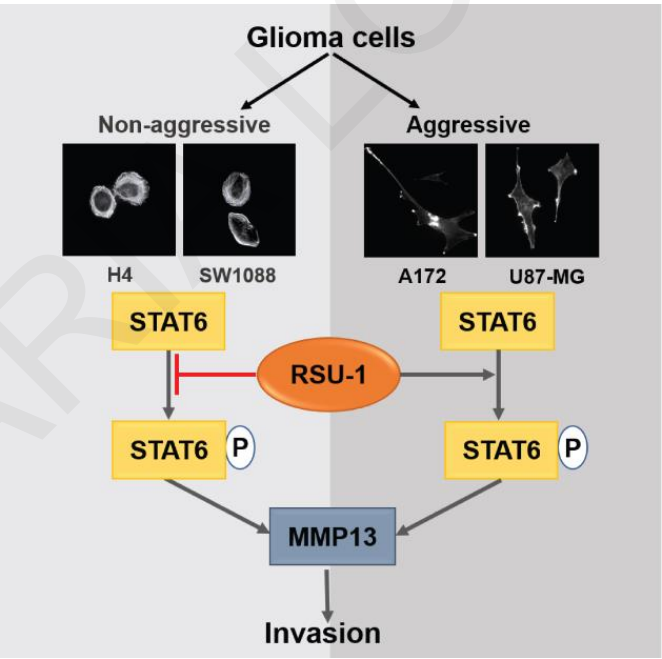

Figure 2-11. **Schematic diagram illustrating the significant findings of this work.** RSU-1 protein promotes the invasion capacity of aggressive glioma cells (A172 and U87-MG) through phosphorylation of STAT6 and overexpression of MMP13. However, in non-aggressive glioma cells (H4 and SW1088) RSU-1 protein suppress the phosphorylation of STAT6 and the expression of MMP13 with consequence the reducing of cells invasion.

Chapter 3

3 Coordinated Expression of Ras Suppressor 1 (RSU-1) and Growth Differentiation Factor 15 (GDF15) Affects Glioma Cell Invasion

This research has been published in *Cancers*: **Maria Louca**, Vasiliki Gkretsi and Triantafyllos Stylianopoulos. Coordinated Expression of Ras Suppressor 1 (RSU-1) and Growth Differentiation Factor 15 (GDF15) Affects Glioma Cell Invasion. *Cancers* volume 11, Article number: 1159 (2019) [doi:10.3390/cancers11081159].

3.1 Introduction

Glioblastoma multiform aggressive nature makes the identification of the precise molecular mechanism involved in its pathogenesis imperative. A number of studies have given emphasis to the significance of cell-ECM interactions on the progression and invasive potential of human astrocytic tumors [20, 78, 119]. More specifically, FA proteins, localized at cell-ECM adhesion sites maintain direct or indirect connections with actin cytoskeleton [120, 121] and thus, they are critically involved in many physiological and pathological processes including the regulation of the migratory and invasive capacity of glioma cells [122, 123].

As also mentioned in **Section 1.3.1**, RSU-1 is a FA protein initially identified as a suppressor of Ras-dependent oncogenic transformation [43, 46, 57, 69, 79] but it was recently shown to interact with the LIM5 domain of the PINCH-1 at FA sites [66, 124]. As it was referred in **Section 1.3** PINCH1 directly binds to ILK, which in turn binds to PARVA forming a stable ternary complex at FAs that is also tightly connected to the actin cytoskeleton through direct interaction of PARVA with actin [125-127]. Apart from the effect of FAs on actin cytoskeleton reorganization, Rho-GTPases which are downstream targets of Ras, are also involved in actin cytoskeleton reorganization and have been implicated in glioma cell

migration, and invasion, as well as in tumor progression [128-130]. Also, several recent studies have indicated that *RSU-1* silencing inhibits migration and invasion of hepatocellular carcinoma, breast and colon cancer cells [51, 59, 67, 81, 131]. Despite the fact that there is a connection between *Ras* oncogene and cancer cell aggressiveness, the exact role of RSU-1 with regard to the metastatic properties of cancer cells remains unclear.

Regarding the role of RSU-1 in the central nervous system [47, 53, 54], not much is known either. Interestingly though, our recent work **(Section 2)** demonstrated a differential regulation of cell migration and invasion of glioma cells by RSU-1 based on their aggressiveness [132]. Thus, RSU-1 was shown to promote the invasion capacity of aggressive glioma cells (A172 and U87-MG) but inhibit that of non-aggressive cells (H4 and SW1088), indicating that a complex molecular mechanism is in place.

Growth differentiation factor (GDF15), also known as macrophages inhibitory cytokine (MIC-1) [133], Placental bone morphogenetic protein (PLAB) [134], Placental transforming growth factor B (P-TGFβ) [135], Prostate-derived factor (PDF) [136], and Non-steroidal anti-inflammatory drug-activated gene-1 (*NAG1*) [137] is a member of the Transforming growth factor beta (TGF-β) superfamily of proteins known to be secreted in low levels in all normal tissues other than placenta in which it is quite abundant [138]. Interestingly, GDF15 has been reported to be involved in actin cytoskeleton reorganization and remodeling [62] while at the same time being implicated in the regulation of proliferation and invasion in breast, prostate, colon, liver and pancreatic cancer cells [61, 63, 72, 102, 139-141]. More importantly, glioblastoma patients have been shown to have increased GDF15 levels in their blood [141] while higher *GDF15* mRNA expression inside the tumor has been associated with poor survival [142], suggesting that GDF15 likely possesses tumor-promoting

properties. On the other hand, there has been evidence that GDF15 acts as tumor suppressor in glioma cells [143, 144].

Taking all the above into consideration, the role of GDF15 with regard to cancer cell development and progression is still vague and it could depend on the cell-type, its expression levels or its interaction with other proteins [145, 146].

In a recent *in vitro* study performed in breast cancer cells, we showed that *RSU-1* silencing downregulates several actin-modulating genes, namely *PARVA*, *RhoA*, *Rho associated kinase-1 (ROCK)* and *Fascin-1* and leads to inhibition of breast cancer cell migration and invasion [60]. Notably, however, treatment with human recombinant GDF15 (hrGDF15) completely reverses both the inhibition in gene expression and the functional effects on cell migration and invasion [60].

As this connection, between RSU-1 and GDF15 is not yet well-defined, in this chapter we aimed to investigate the interplay between RSU-1 and GDF15 in glioma cell lines and the effect of their expression on glioma cell migration and invasion.

3.2 Methods

Cell culture. H4, SW1088 and A172 human cells were obtained from American Type Culture Collection (ATCC). All cells were grown in high-glucose Dulbecco's modified Eagle's medium (DMEM) supplemented with 10% fetal bovine serum and 1% antibiotic/antimycotic and were cultured at 37 °C in a 5% CO2 humidified atmosphere.

Antibodies and reagents. Anti-PINCH1 antibody was purchased from Cell Signaling Technology, anti-GDF15 was from Santa Cruz Biotechnology. Anti-tubulin was obtained from Developmental Studies Hybridoma Bank. RSU-1 siRNA and GDF-15 siRNA were purchased from Santa Cruz Biotechnology as referred **in Section 2.2**. Lipofectamine 2000 was purchased from Invitrogen Life Technologies and Alamar Blue reagent was obtained from Thermo Scientific. Transwell inserts were obtained from Greiner Bio-One, and Matrigel was from Corning. QIAzol Lysis Reagent was purchased from QIAGEN, GDF15 human recombinant protein (hrGDF15) was obtained from R&D systems, and G-LISA RhoA Activation Assay was purchased from Cytoskeleton. Collagen I was obtained from Corning as mentioned in **Section 2.2**.

Tranwell Migration and Invasion Assays. Cell migration and invasion assays were performed as described in **Section 2.2**. Experiments were run in duplicate and four independent experiments were performed.

Tumor spheroids formation in collagen gels. Following transfection with NSC or *RSU-1* or *GDF15* siRNA, a suspension of 2.5×10^4 was used for generating drops of 20 μL containing 500 cells each [96]. Drops were left for 24 h so that spheroids are formed and spheroids were then embedded in 1 mg/mL collagen I gels inside wells of a 96-well plate [132]. Pictures were taken at time zero and at 6, 12 or 16 h later, depending on the cells'

aggressiveness. The spheroids' size was determined using the ImageJ software and differences between the time zero and final time point were measured.

Transfection with siRNA. Cells seeded at a density of approximately 50% were transfected with 100 nM siRNA against *RSU-1*, or *GDF15* or with a control NSC siRNA, using the Lipofectamine 2000 reagent (7 μL per 35 mm dish) according to the manufacturer's guidelines. Cells were harvested 48 h post-transfection or replated into transwells 24 h later and left to migrate/invade for an additional 24 h (total 48 h following siRNA transfection) [60].

Treatment with hrGDF15. For the experiments that included treatment with hrGDF15, H4, SW1088 and A172 cells were grown until they reached 70% confluency and were then cultured for 24 h in low serum DMEM supplemented with 0.5% fetal bovine serum (FBS). Cells were then subjected to treatment with hrGDF15 (10 ng/mL) or the control solvent in which hrGDF15 was dissolved (4 mM HCI containing 0.1% bovine serum albumin) for 24 h[60].

Cell viability assay. H4 and A172 cells transfected with *RSU-1* or *GDF15* siRNA and H4, SW1088 and A172 cells treated with hrGDF15 were subjected to cell viability assay using the Alamar Blue reagent for at least 2 h, according to the manufacturer's instructions. The absorbance was then measured using Rayto spectrophotometer at 570 and 600 nm. Finally, results were analyzed and compared to the control samples.

RNA isolation and Real-Time Polymerase Chain Reaction (PCR). RNA isolation and Real-Time PCR was performed as described in **Section 2.2**. The primers used for each gene are shown in **Table 1, in Appendices**.

Protein extraction and Western blotting. Whole protein cell lysates were extracted as descripted in **Section 2.2**. The detection of antibodies was performed as mentioned in **Section 2.2.** The protein expression was quantified compared to the β-actin loading control using the National Institute of Health (NIH) ImageJ software. The mean intensity of respective protein bands from three different immunoblots was used for the quantification, as indicated.

RhoA activation assay. RhoA activation was assessed using the G-LISA RhoA activation assay kit (Cytoskeleton) according to the manufacturer's instructions.

3.3 Results

Growth Differentiation Factor 15 (GDF15) mRNA expression is reduced in more aggressive glioma cells. Since the role of GDF15 in cancer progression is controversial and not fully elucidated yet [143, 144], we first tested *GDF15* expression in three cell lines H4, SW1088, and A172 both at the mRNA **(Figure 3-1A)** and protein level **(Figure 3-1B &1C)**. In our previous work [132], we have shown that A172 cells that cause GBM are very aggressive having a strong invasive capacity in contrast to SW1088 cells, which cause astrocytoma and are less invasive, and H4 cells which are almost non-invasive neuroglioma cells. Here, we show that H4 cells express *GDF15* at higher levels than SW1088 and A172 cells both at the mRNA and protein level **(Figure 3-1)**, whereas *RSU-1* expression follows the exact opposite pattern, being elevated as the aggressiveness of cells increases **(Figure 3-1D–1F)**.

Intrigued by this finding, we wondered whether *RSU-1* and *GDF-15* are collaborating in regulating glioma cell invasion through a common molecular pathway, as both genes are

indirectly associated with actin cytoskeleton reorganization and aggressive cancer cell behavior [126, 140].

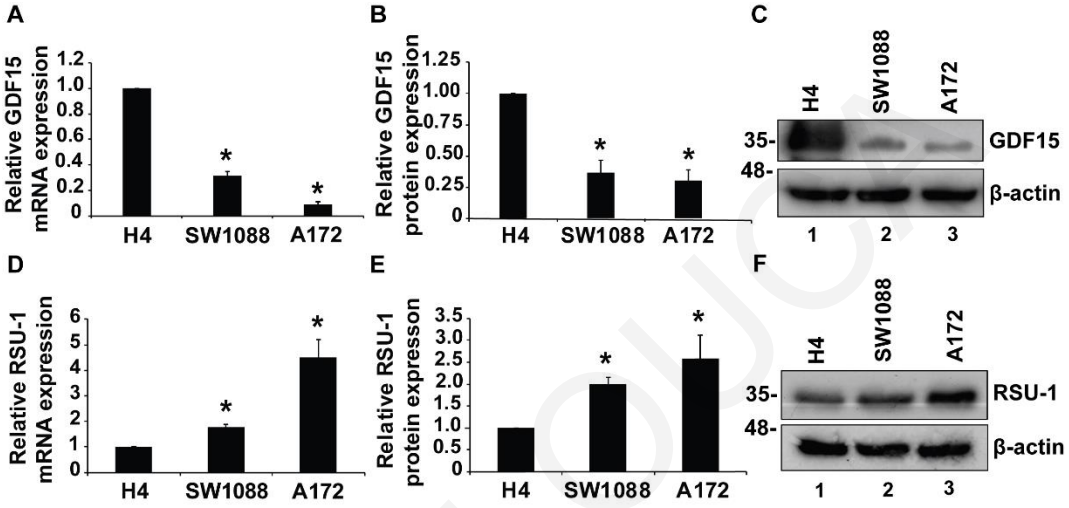

Figure 3-1. **Growth differentiation factor (GDF15) expression decreases from the less aggressive (H4) towards the more aggressive (A172) cells, whereas the RSU-1 expression follows the opposite pattern. (A–D)** Relative GDF15 and RSU-1 mRNA expression in three brain cell lines (H4, SW1088 and A172). Three independent real-time polymerase chain reaction (PCR) experiments were performed. **(B–E)** Western blot for GDF15 and RSU-1 protein expression with H4 cell line as the sample control and β-actin as the loading control. **(C–F)** Graphs show the quantification of GDF15 and RSU-1 protein expression with ImageJ software from two different Western blots. Asterisks denote a statistically significant difference ($p < 0.05$) compared to the H4 data.

Human Recombinant GDF15 (hrGDF15) treatment protein differentially affects motility and invasive capacity of cells depending on cell aggressiveness. To evaluate the role of GDF15 in regulating the motility and invasion of glioma cells, H4, SW1088, and A172 cells were treated with human recombinant hrGDF15 (10 ng/mL) for 24 h and were then subjected to transwell migration and invasion assays. As shown in **Figure 3-2**, hrGDF-15 treatment increased both

the invasion (**Figure 3-2A&2B**) and migration (**Figure 3-2C**) of the less invasive H4 cells and inhibited that of the more invasive A172 cells without any alteration in cell viability (**Figure 3-2D**). Notably, SW1088 cells, which have intermediate invasive capacity and *GDF15* basal level expression, did not show any statistically significant changes in invasion (**Figure 3-2B**) and migration (**Figure 3-2C**) following hrGDF15 treatment.

In order to identify possible connections between GDF15 and RSU-1 with regard to glioma cell invasion, we examined the *RSU-1* mRNA expression upon hrGDF-15 treatment and found that in H4 cells, which express low *RSU-1* and high *GDF-15* levels, *RSU-1* was strongly upregulated following hrGDF-15 treatment both at the mRNA (**Figure 3-3A**) and protein level (**Figure 3-3B&C**). By contrast, in A172 cells that already express high *RSU-1* and low *GDF15* levels, hrGDF15 treatment affected *RSU-1* expression to a lesser extent, presumably due to the fact that it is already highly expressed in these cells.

Since RSU-1 is known to directly interact with PINCH1 [66, 124], we wondered whether *PINCH1* expression is also affected by hrGDF15 treatment. As shown in **Figure 3-3**, hrGDF15 treatment led to upregulation of *PINCH1* in H4 cells which was not true for A172 cells (**Figure 3-3D–3F**).

Subsequently, to determine whether the increased invasiveness of H4 cells and the decreased invasiveness of A172 cells observed upon hrGDF15 treatment involved Rho GTPases activity, we assessed RhoA activity by a G-LISA RhoA activation assay, as RhoA is known to be modulated by *Ras* oncogene and plays central role in actin cytoskeleton reorganization [147]. RhoA activity was increased in H4 cells and decreased in A172 cells compared to the control (**Figure 3-3H**), following an identical expression pattern (**Figure 3-3G**) with that of *PINCH1* (**Figure 3-3D**). We also tested whether major proteases are also affected by hrGDF15 treatment, and thus we examined the expression of *MMP13,* a metalloproteinase

with a crucial role in glioma cell invasion as well as in other cancer types. Consistent with the changes observed in cell invasion, we found that *MMP13* mRNA (**Figure 3-3I**) and MMP13 protein (**Figure 3-3K**) in H4 and A172 cell lines follows the exact same pattern. **Figure 3-4** shows the relative mRNA expression for *RSU-1*, *PINCH1*, *MMP13* and *RhoA* in SW1088 cells, which express intermediate levels of both RSU-1 and GDF15, following hrGDF15 treatment. No clear inhibitory or promoting pattern can be observed in any of the genes tested in SW1088 which supports the invasion and migration results showing no effect of hrGDF15 treatment on these cellular properties (**Figure3-2**).

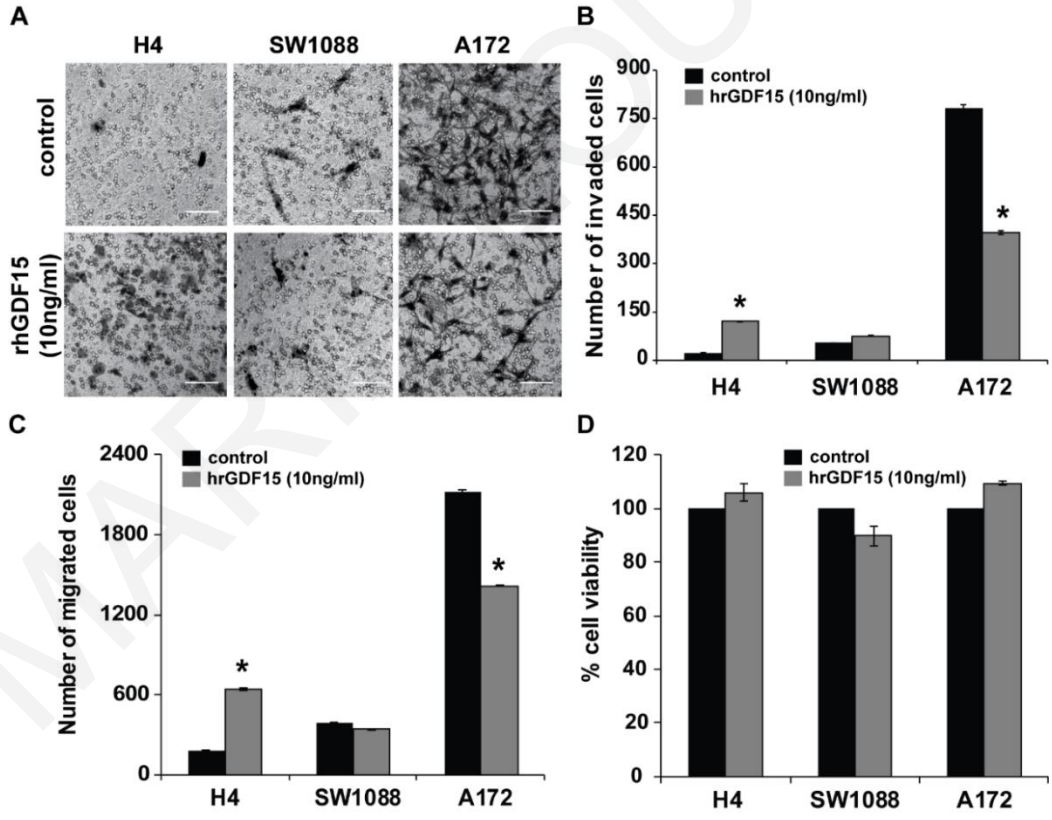

***Figure 3-2*. hrGDF15 treatment promotes migration and invasion of less invasive cells and inhibits that of the highly invasive cells without affecting cell survival.** (**A**) Control and hrGDF15 (10 ng/mL) treated cells (H4, SW1088 and A172) were subjected to transwell invasion assay 24 h post-treatment. Scale bar: 100 μm. (**B**) Diagrammatic representation of results from invasion assays which depicts the total number of invading glioma cells per transwell for each group (nine randomly chosen microscopic fields per transwell). (**C**) Diagram showing the total

number of migrated cells per transwell. Supplementary Figure S1 shows representative images of migration through the transwell for H4, SW1088 and A172 cells. For the invasion and migration assays three independent experiments were performed and each sample was run in duplicate. (**D**) Graph representing the percentage of cell viability as measured by Alamar blue assay 24 h post hrGDF15 treatment for the three cell lines. Each sample was run in triplicate and three independent experiments were performed. Asterisks denote a statistically significant difference ($p < 0.05$).

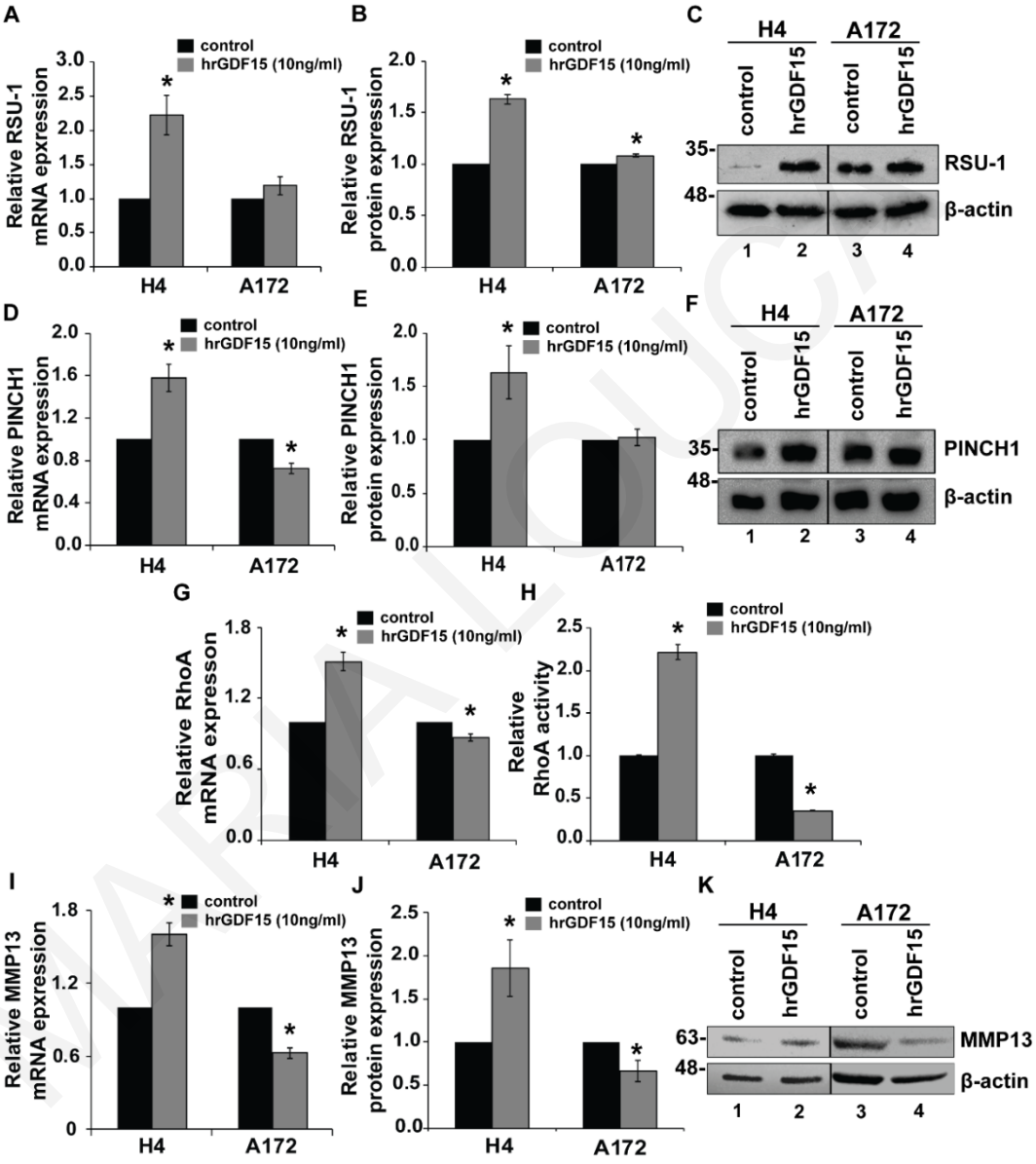

***Figure 3-3*. hrGDF-15 treatment upregulates *RSU-1* expression and promotes or suppresses invasion of glioma cells through upregulation or downregulation of PINCH1, RhoA, and MMP13 respectively.** (**A**,**D**,**G**,**I**) Relative mRNA expression of *RSU-1*, *PINCH1*, *RhoA* and *MMP13* respectively in H4 and A172 cell line upon treatment with hrGDF15 (10 ng/mL) for 24 h. Four independent real-time PCR experiments were performed and data were analyzed using the ΔΔCt method using control-treated cells as a calibrator sample for each cell line. (**H**) Relative RhoA activity 24 h post rhGDF15 treatment on H4 and A172 cell lines. (**B**,**E**,**K**) Representative pictures

of Western blot displaying RSU-1, PINCH1 and MMP13 protein expression following hrGDF15 treatment for 24 h. (**C**,**F,J**) Graphs representing quantification of RSU-1 and PINCH1 protein expression respectively for each cell line using ImageJ software and β-actin as loading control. Mean band intensity from two immunoblots from independent experiments was used for the quantification. Asterisks indicate a statistically significant difference ($p < 0.05$) compared to control data.

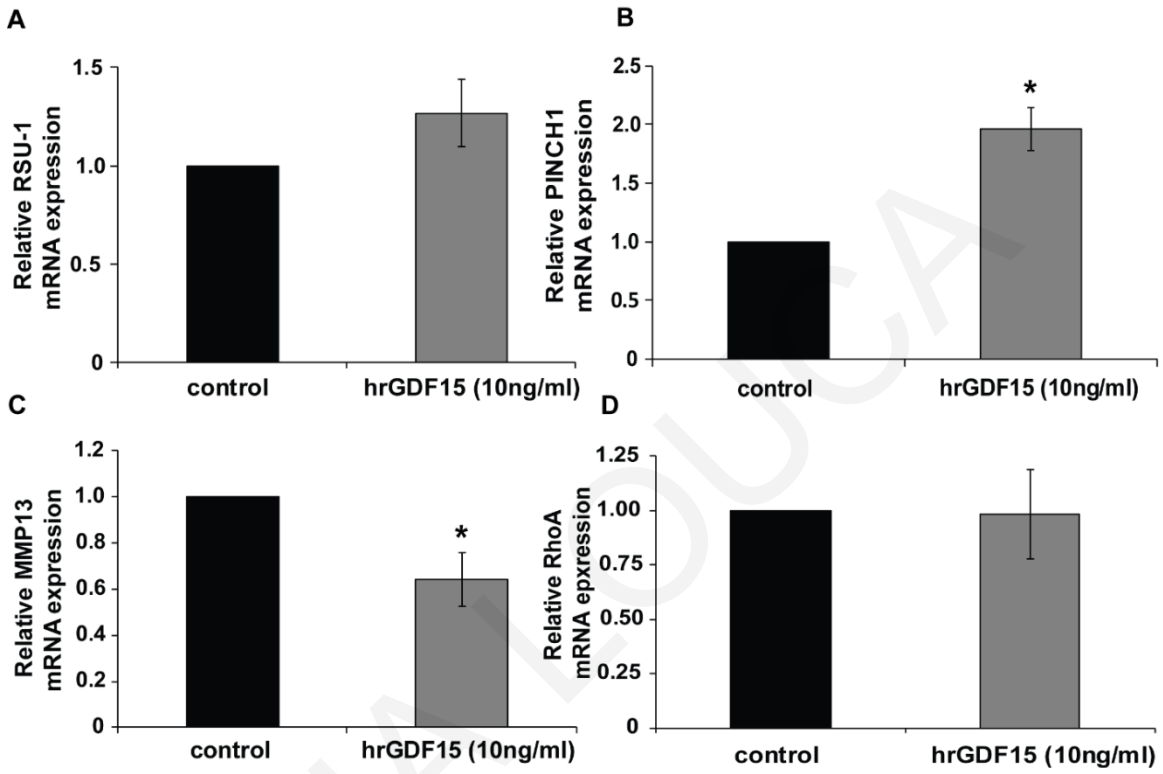

***Figure 3-4*. Gene expression of RSU-1. PINCH1, MMP13 and RhoA in SW1088 cell line upon hrGDF15 treatment.** Relative mRNA expression following hrGDF15 treatmen**t** for *Rsu-1* **(A)**, *PINCH1* **(B)**, *MMP13* **(C)** and *RhoA* **(D)** for SW1088 cell line 48h post -hrGDF15 treatment. Two (2) independent experiment were performed and quantification was done using a control as the calibrator sample. Asterisks denote statistically significant changes ($p<0.05$) compared to control data.

RSU-1 silencing regulates GDF15 expression and differentially affects cell invasiveness and the expression of PINCH1, RhoA and MMP13. In an attempt to elucidate the interplay between GDF15 and RSU-1 in glioma cell invasion and the molecular pathway involved, we first assessed the invasion capacity of H4, SW1088 and A172 cells using a 3-dimensional (3D) spheroid formation assay in collagen (**Figure 3-5**) following *RSU-1* silencing. Our results show that H4 and

SW1088 cells become more invasive after silencing, whereas the invasiveness of A172 decreases. Also, we tested the expression of GDF15, PINCH1, RhoA, and MMP13 in H4, SW1088 and A172 cells following *RSU-1* silencing for 48 h. As shown in **Figure 3-6**, RSU-1 was silenced both at the mRNA (**Figure 3-6A**) and protein level (**Figure 3-6B&6C**). **Figure 3-7** shows the effect of RSU-1 silencing at the mRNA expression of SW1088 cells.

Interestingly, a dramatic increase in *GDF15* mRNA expression was observed following RSU-1 silencing in A172 glioma cells, which have low endogenous GDF15 levels (**Figure 3-6D**) versus non-specific control (NSC) sample, while a smaller increase was observed in H4 cells, which have higher endogenous GDF15 levels. Western blotting analysis verified the mRNA data at the protein level (**Figure 3-6E&6F**). Also, in the SW1088 cell line that has lower endogenous RSU-1 levels, no effect was observed in GDF15 expression upon further reduction of RSU-1 mRNA (**Figure 3-7B**).

Next, we tested the effect of *RSU-1* silencing on *PINCH1*, *RhoA*, and *MMP13* expression. *RSU-1* silencing resulted in upregulation of PINCH1 (**Figure 3-6G**), RhoA (**Figure 3-6J**) and MMP13 (**Figure 3-6L**) in H4 cells and SW1088 cells (**Figure 3-7**) respectively, and downregulation in A172 cells (**Figure 3-6G–6L**). RhoA activation assay was also performed 48 h post RSU-1 silencing (**Figure 3-6K**) and our results followed the same pattern as *RhoA* mRNA expression in H4 and A172 cell lines (**Figure 3-6J**).

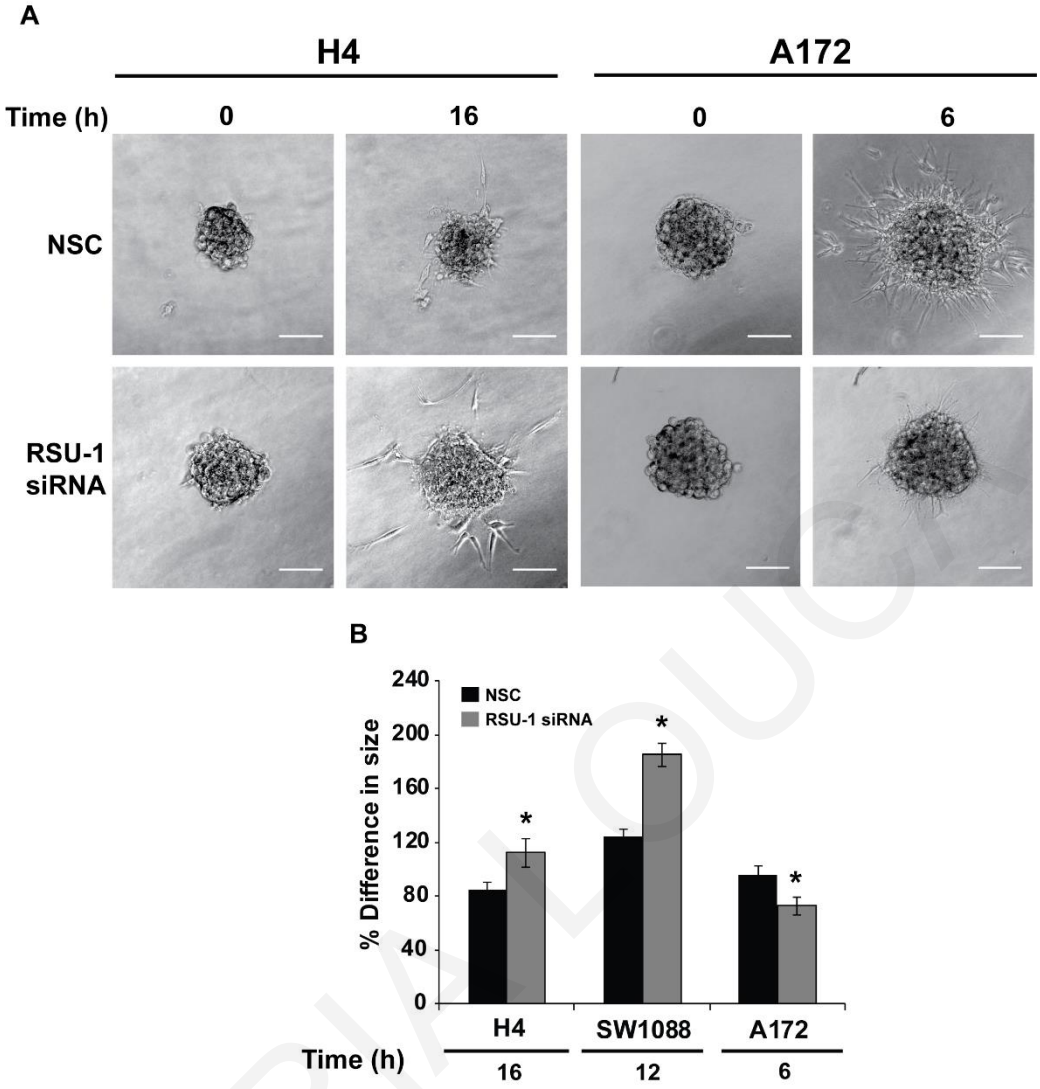

Figure 3-5. **Tumor spheroid invasion assay after NSC and *RSU-1* siRNA transfection in spheroids embedded in collagen I gels.** Spheroids (in average n=20 spheroids per cell line) were embedded in 1mg/ml collagen I gel and left to invade through the gel for different time periods depending on the aggressiveness of each cell line. **(A)** Representative images of H4 (least invasive) and A172 (most invasive) cells for 16h and 6 h, respectively. **(B)** The percentage of tumor spheroid invasion for H4, SW1088 and A172 cell line was assessed by measuring the difference of each spheroid size ((major+minor axis)/2) within the corresponding hours following placement of the spheroid in the collagen gel (time zero). Three (3) independent experiment were performed and quantification was done using the NSC as the control sample. Asterisks denote statistically significant changes ($p<0.05$) compared to NSC data.

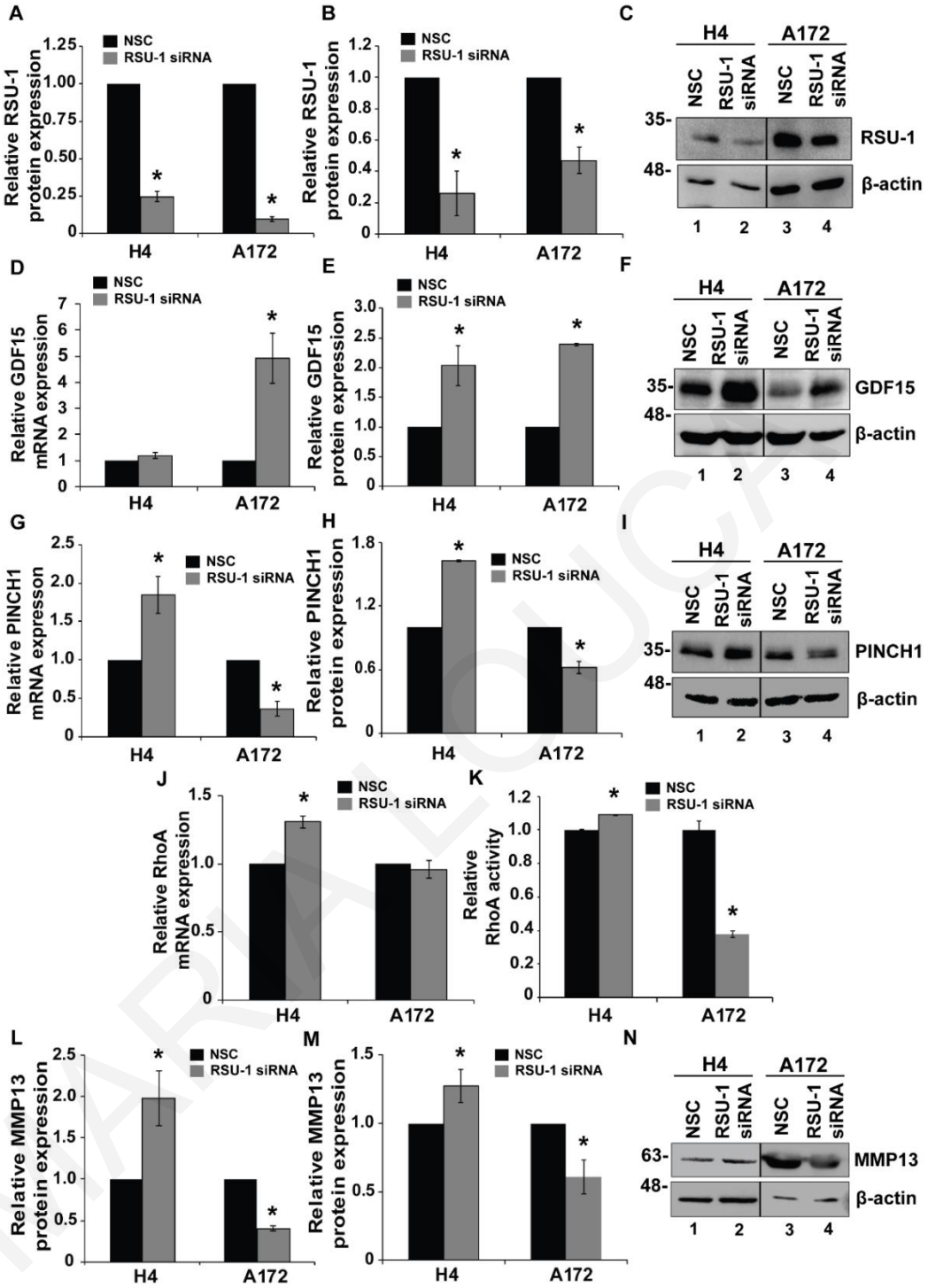

***Figure 3-6*. RSU-1 silencing upregulates GDF15 expression and regulates PINCH1, RhoA and MMP13 expression.** (**A**,**D**,**G**,**J**,**L**) Relative mRNA expression of *RSU-1*, *GDF15*, *PINCH1*, *RhoA* and *MMP13* respectively in the H4 and A172 cell lines upon *RSU-1* silencing. Four independent real-time PCR experiments were performed and data were analyzed using the ΔΔCt method, while non-specific control (NSC) treated cells were used as the calibrator sample for each cell line. (**B**,**E**,**H**,**M**) Relative RSU-1, GDF15, PINCH1 and MMP13 protein expression respectively after treatment with NSC or RSU-1 siRNA for 48 h in H4 and A172 cells. Quantification was performed using the NIH ImageJ software and the mean band intensity was

calculated from two different immunoblots. (**C**,**F**,**I**,**N**) Representative pictures from Western blot displaying RSU-1, GDF15, PINCH1 and MMP13 expression at the protein level after *RSU-1* silencing for H4 and A172 cell lines. (**K**) Relative RhoA activity 48 h post RSU-1 silencing for H4 and A172 cell lines. Asterisks indicate a statistically significant difference ($p < 0.05$) compared to NSC data.

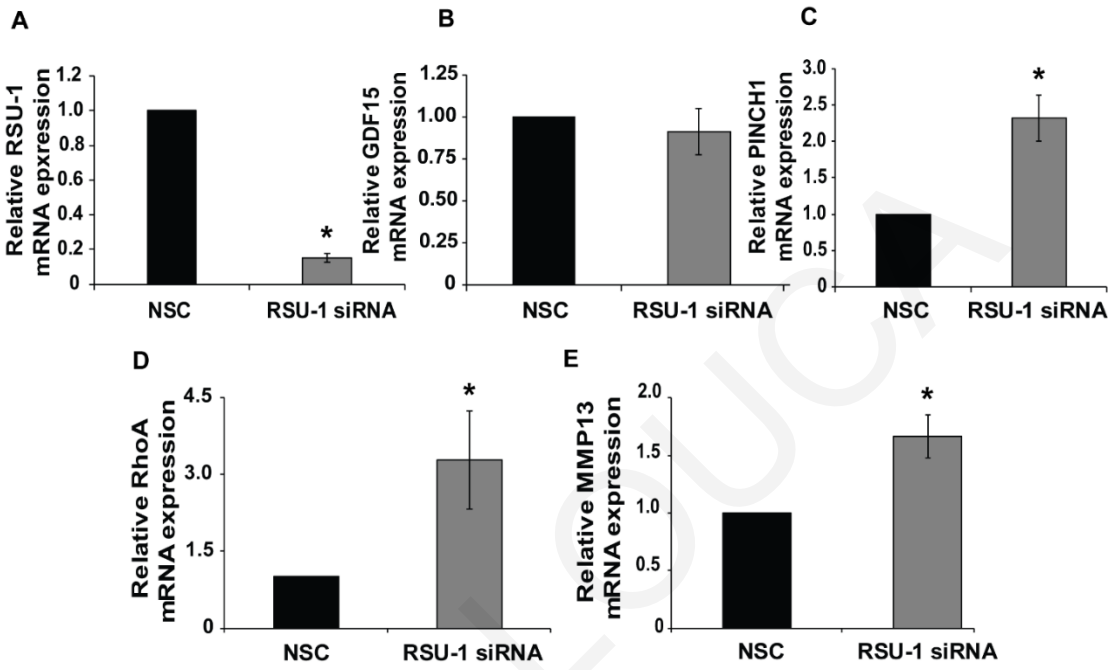

Figure 3-7. **Relative mRNA expression in SW1088 cells following *RSU-1* silencing. (A)** *RSU-1*, **(B)** *GDF15*, **(C)** *PINCH1*, **(D)** *RhoA* and **(E)** *MMP13* mRNA expression 48h post treatment with NSC and *RSU-1* siRNA. At least Four (4) independent experiment were performed and quantification was done using the NSC as the calibrator sample. Asterisks symbolize statistically significant changes ($p<0.05$) compared to control data.

GDF15 Silencing Leads to Reduced Invasion in More Invasive Cells but Does not Affect Less Invasive Cells. We have shown so far in our study that GDF15-treated cells (H4 and A172) exhibited distinct invasive behavior that was correlated with changes in expression of *RSU-1*, *PINCH1*, *RhoA* and *MMP13*, and that silencing of *RSU-1* leads H4, SW1088 and A172 cells to behave similarly to the GDF15-treated cells with the same alterations in gene expression (*PINCH1*, *RhoA* and *MMP13).* Subsequently, we investigated the effect of *GDF15* silencing on these parameters. For this

purpose, H4 and A172 cell were transfected with NSC or GDF15 siRNA for 48 h. As shown in **Figure 3-8**, *GDF15* silencing was successful both at the mRNA (**Figure 3-8A**) and protein level (**Figure 3-8A&8B**). Following *GDF15* silencing, cells were subjected to transwell migration and invasion assays (**Figure 3-8**). Our results show that *GDF15* silencing reduced the migration and invasion capacity of the aggressive A172 cells, whereas invasion and migration of H4 cells was not affected (**Figure 3-8D**). These results were consistent with 3D spheroids invasion assay (**Figure 3-9**). Cell viability assay was performed to exclude the possibility of reduced cell migration and invasion due to cell death. As depicted in **Figure 3-8G**, cell survival was not affected by *GDF15* silencing further strengthening our findings that *GDF15* silencing inhibits migration and invasion in A172 cells. Moreover, gene expression analysis further corroborated our data showing that although *RSU-1* was downregulated (**Figure 3-10A-10C**) in both cell lines after *GDF15* silencing, the expression of *PINCH1* (**Figure 3-10D–10F**), *RhoA* (**Figure 3-10G&10H**) and *MMP13* (**Figure 3-10I–10K**) followed a pattern similar to that of cell invasion, being reduced only in A172 cells.

Finally, to better understand the molecular mechanism governing RSU-1 and GDF-15 in glioma cells, we proceeded to silence *RSU-1* for 24 h and then treated the cells with hrGDF-15 for another 24 h. As shown in supplementary **Figure 3-11**, hrGDF15 treatment enhances the effects of *RSU-1* siRNA on H4 and A172 cells, suggesting that they have the same end result and they are likely involved in a common signaling pathway.

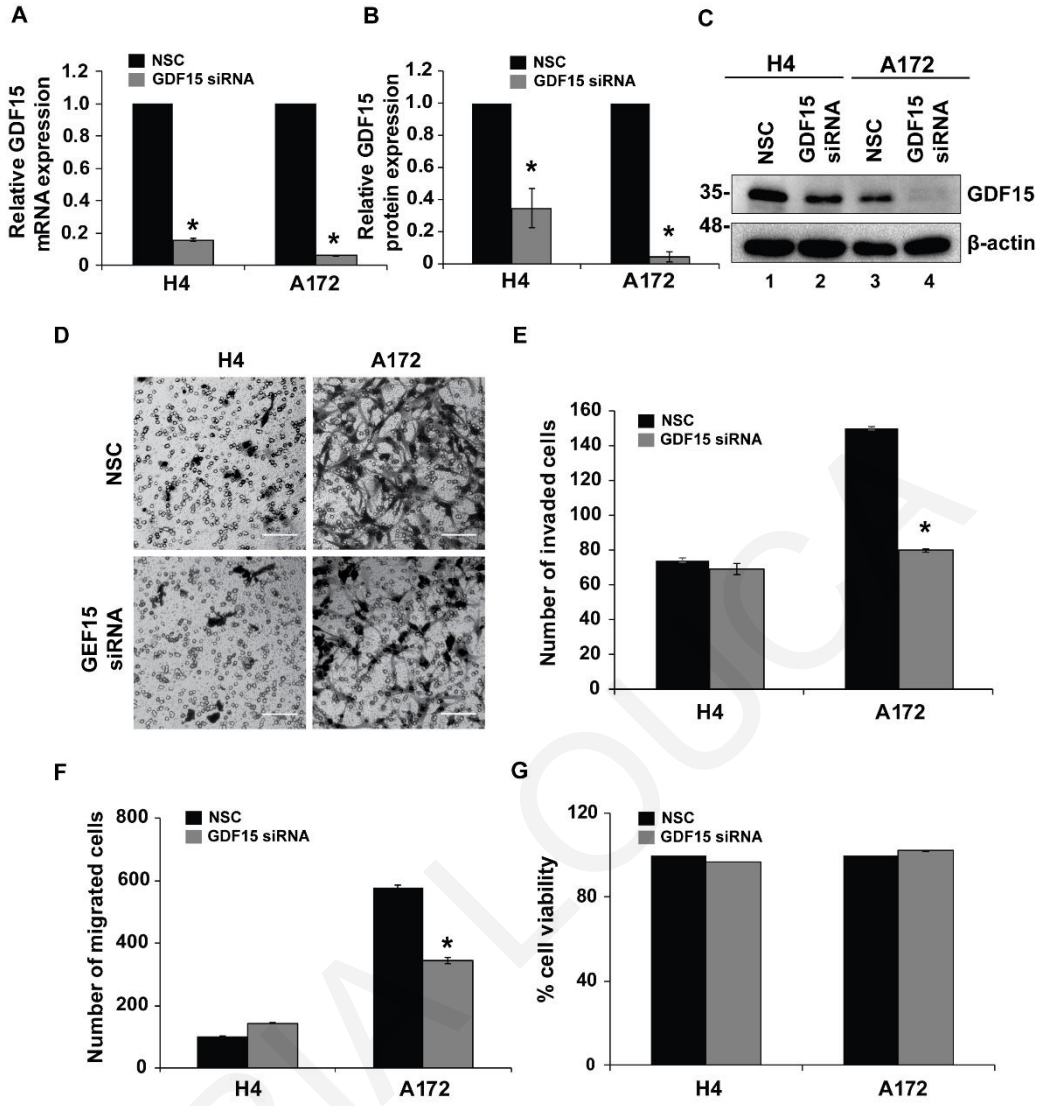

***Figure 3-8. GDF15* silencing does not interfere with cell survival but inhibits cell invasion and migration of the aggressive cell line (A172), whereas it does not affect the non-invasive cell line (H4).** (**A**) Relative *GDF15* mRNA expression in H4 and A172 after NSC or *GDF15* siRNA transfection for 48 h. Three independent real-time PCR experiments were performed and data were analyzed using the ΔΔCt method, with NSC as a calibrator sample for each cell line. (**B**) Quantification of GDF15 protein expression using three different immunoblots. Analysis was performed using NIH ImageJ software. (**C**) Representative picture of Western blot showing the silencing of GDF15 protein after NSC or *GDF15* siRNA for 48 h in H4 and A172. (**D**) NSC and *GDF15* siRNA treated H4 and A172 cells were subjected to invasion assay 24 h post-transfection. Scale bar: 100 µm. (**E**) Diagram showing the total number of invading glioma cells per transwell in each group (nine randomly chosen microscopic fields per transwell). (**F**) Diagram showing the total number of migrated cells per transwell assessed as described above. For invasion and migration assays three independent experiments were performed and each sample was run in duplicate. (**G**) Graph representing the percentage of cell viability assessed by Alamar blue assay 48 h post *GDF-15* siRNA transfection for the two cell lines compared to NSC. Each sample was run in triplicate. Asterisks denote a statistically significant difference ($p < 0.05$) compared to NSC data for each cell line.

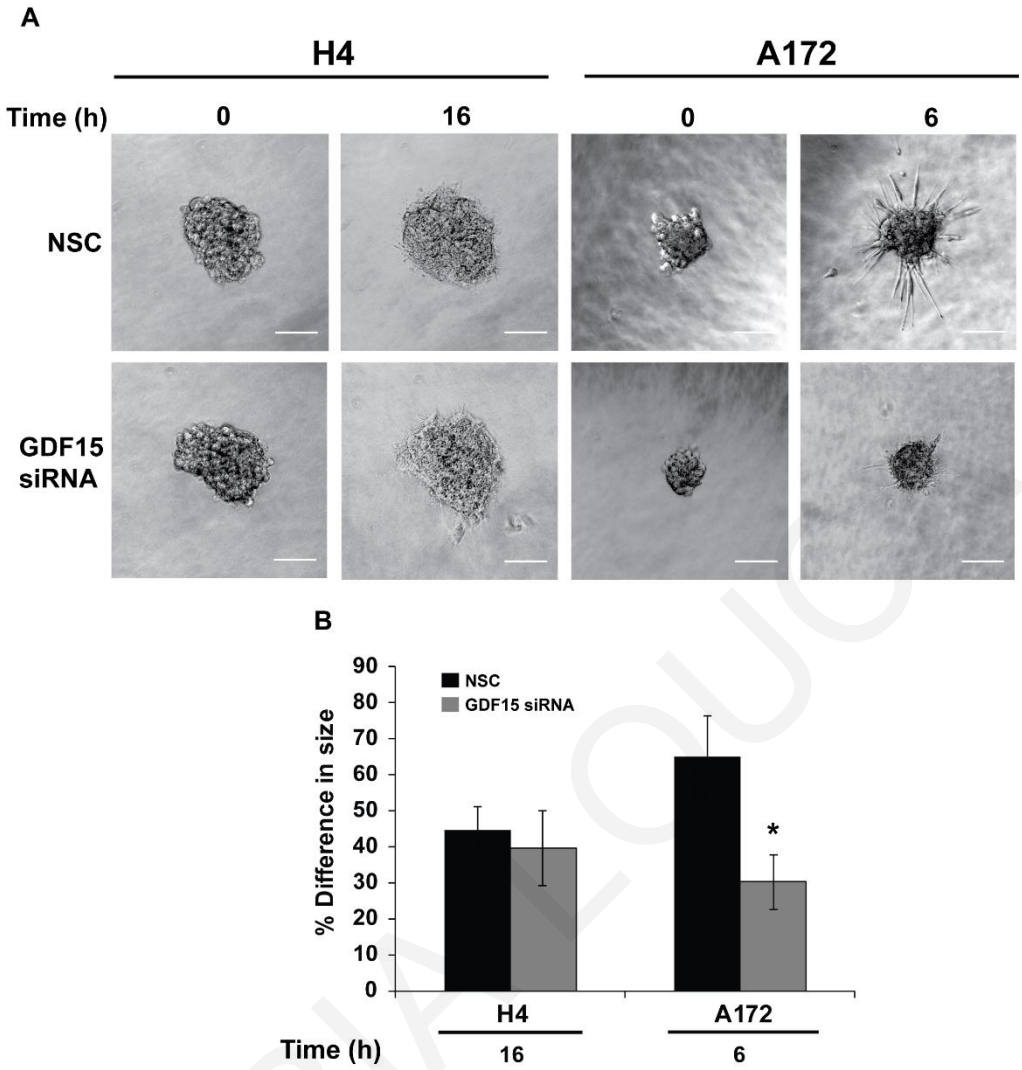

***Figure 3-9*. Tumor spheroid invasion assay after NSC and *GDF15* siRNA tansfection in spheroids embedded in collagen I gels.** Spheroids (in average n=10 spheroids per cell line) were embedded in 1mg/ml collagen I gel and left to invade through the gel for different time periods depending on the aggressiveness of each cell line. **(A)** Representative images of H4 (least invasive) and A172 (most invasive) cells for 16h and 6 h, respectively. **(B)** The percentage of tumor spheroid invasion for H4 and A172 cell line was assessed by measuring the difference of each spheroid size ((major+minor axis)/2) within the corresponding hours following placement of the spheroid in the collagen gel (time zero). Two (2) independent experiment were performed and quantification was done using the NSC as the control sample. Asterisks denote statistically significant changes ($p<0.05$) compared to NSC data.

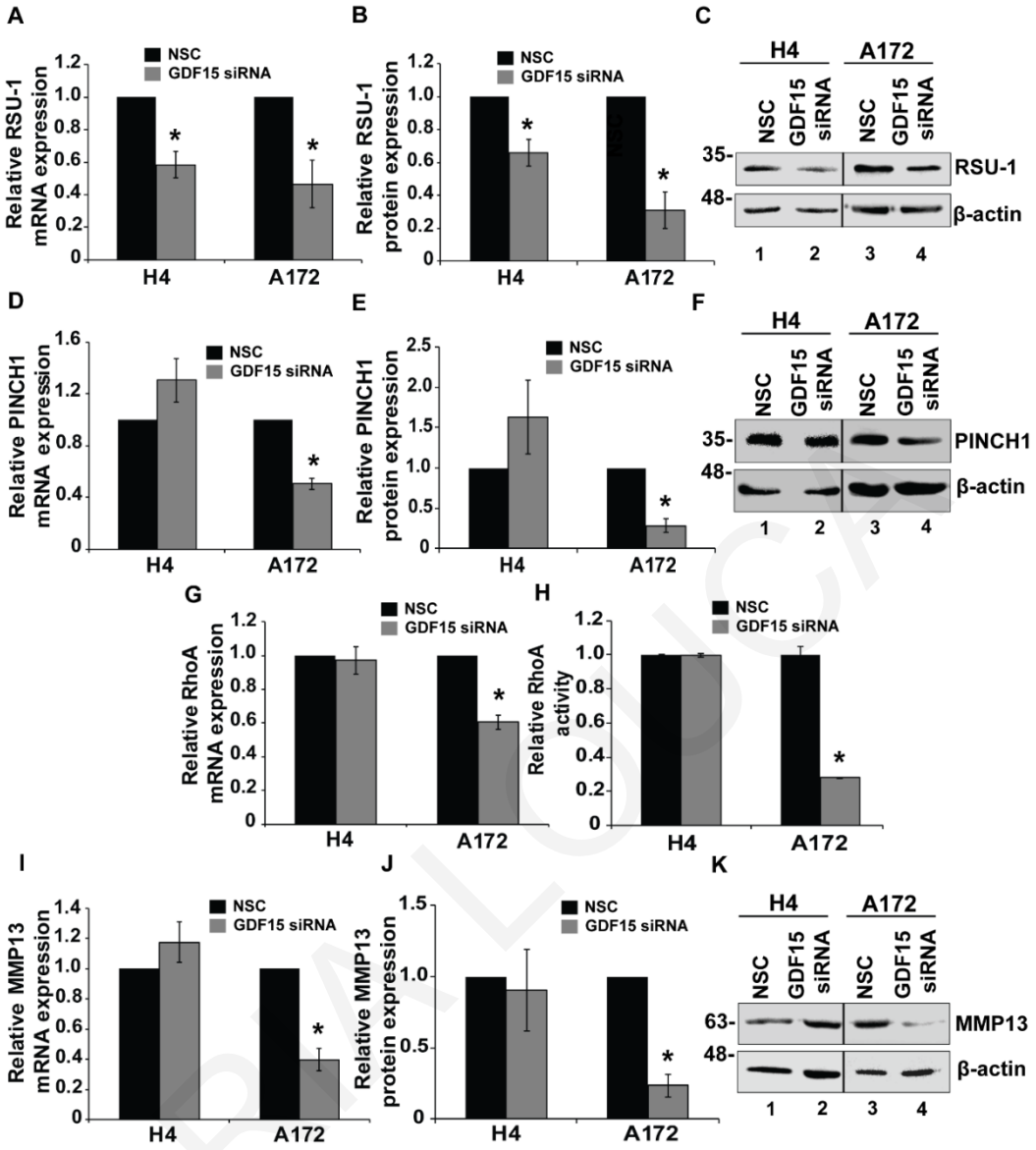

***Figure 3-10*. Effect of *GDF15* silencing on *RSU-1, PINCH1, RhoA* and *MMP-13* expression.** (**A**,**D**,**G**,**I**) Relative *GDF15*, *PINCH1*, *RhoA* and *MMP13* mRNA expression respectively in H4 and A172 cells upon *GDF15* silencing. Three independent real-time PCR experiments were conducted and data were analyzed using the ΔΔCt method having control-treated cells as calibrators for each cell line. (**H**) Relative RhoA activity 24 h post rhGDF15 treatment on H4 and A172 cell lines. (**C**,**F**,**K**) Representative image from Western blot analysis displaying RSU, PINCH1 and MMP13 protein expression after *GDF15* silencing. (**B**,**E**,**J**) Graphs representing quantification of RSU-1, PINCH1 and MMP13 protein expression for each cell line using ImageJ software. Two immunoblots from independent experiments were used for the quantification. Asterisks indicate a statistically significant difference ($p < 0.05$) compared to NSC data.

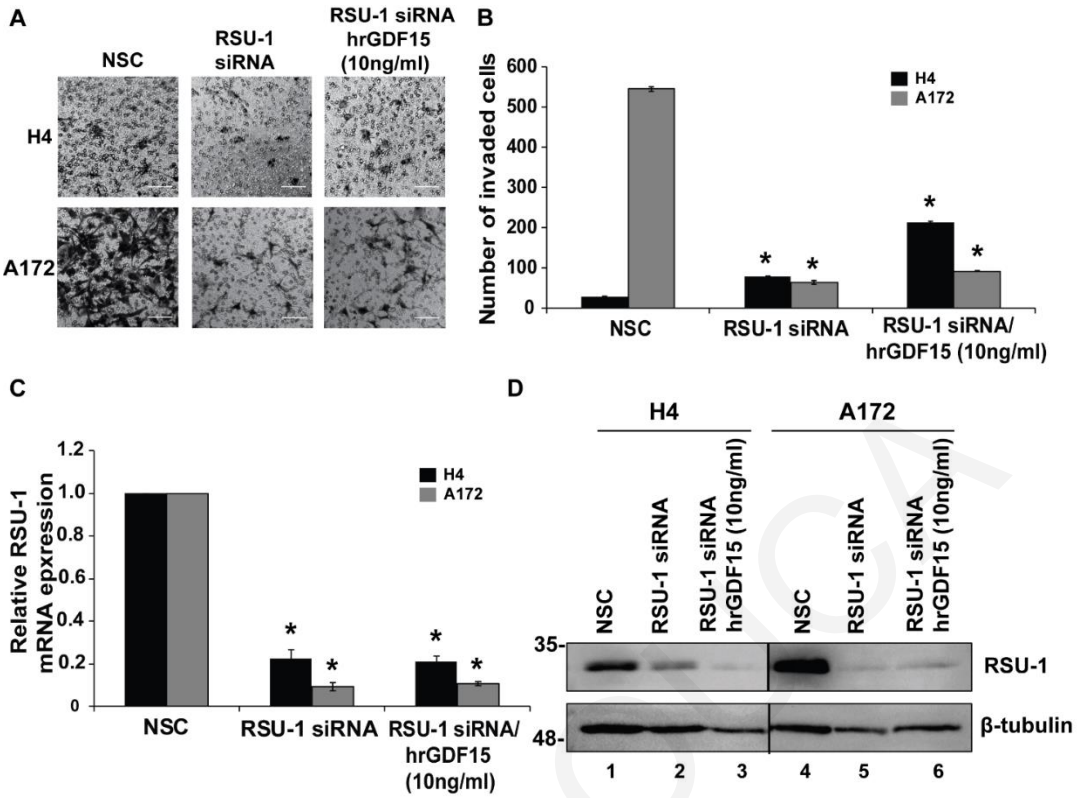

***Figure 3-11*. Combination of *RSU-1* silencing and treatment with hrGDF15 (10ng/ml) has the same effect with *RSU-1* silencing on its own on transwell invasion assay and on RSU-1 expression for H4 and A172 glioma cell lines. (A)** Representative images of a transwell invasion assay that was performed for 24h for H4 and A172 cell lines with NSC, *RSU-1* siRNA, or the combination *RSU-1*siRNA and treatment with hrGDF15 (10ng/ml). The invading cells were counted in nine (9) randomly chosen microscopic field per transwell. Scale bar: 100μm. **(B)** Total number of invaded cells compared to NSC for *RSU-1* siRNA and the *RSU-1* siRNA for *RSU-1* siRNA/GDF15 treatment (10ng/ml) for each cell line per transwell. Each sample was run in duplicate and two (2) independent experiments were performed. **(C)** Relative *RSU-1* mRNA expression for H4 and A172 cell lines with NSC, *RSU-1* siRNA, or the combination *RSU-1*siRNA and treatment with hrGDF15 (10ng/ml). Three independent Real-Time PCR experiments were performed and data were analyzed using the ΔΔCt method, while NSC treated cells were used as the calibrator sample for each cell line. **(D)** Representative pictures from Western blot analysis displaying RSU-1 expression at the protein level following transfection with NSC, *RSU-1* siRNA, or the combination *RSU-1*siRNA and treatment with hrGDF15 (10ng/ml) for H4 and A172 cell lines. Asterisks symbolize statistically significant changes ($p<0.05$) upon *RSU-1* siRNA and *RSU-1*siRNA/ hrGDF15 compared to NSC sample for each cell line.

3.4 Discussion

Migration and invasion assays (**Figure 3-8**). Our results show that *GDF15* silencing reduced the migration RSU-1, which binds to PINCH1 at FA sites [123] has been previously found to be upregulated in more invasive breast and brain cancer cells [59, 131]. Moreover, we recently demonstrated a differential regulation of cell migration and invasion of glioma cells by RSU-1 based on their aggressiveness, with RSU-1 promoting an invasive behavior in aggressive cells (A172 and U87-MG) and inhibiting them in the less aggressive ones (H4 and SW1088) [131]. This by itself indicates the existence of a complex molecular mechanism that governs glioma cell invasion in vitro. Moreover, *GDF15* is downregulated in aggressive glioma cell lines (SW1088 and A172) in contrast to non-aggressive neuroglioma cells (H4) and its expression is exactly opposite from that of *RSU-1* in glioma cells (**Figure 3-1**). This, combined with the fact that *GDF15* is involved in actin cytoskeleton organization [62], prompted us to investigate the interplay between this protein and RSU-1 with regard to glioma cell aggressiveness in vitro. Although, there are many studies documenting the role of *GDF-15* on proliferation, invasion and migration of cancer cells [63, 141, 143], these results are contradictory tending to indicate that its function is, to a certain extent, cell type-specific. Here, we provided evidence for the role of *GDF15*, in glioma cell invasion and for its correlation with RSU-1 in this process.

To investigate the interplay and possible connection between *RSU-1* and *GDF15* in glioma cells, we used three different brain cell lines, namely H4, SW1088 and A172, which have different tumoral origin, properties and proteins expression level [131, 148, 149]. and four different experimental approaches; (a) hrGDF15 treatment, (b) *RSU-1* silencing, (c) *GDF15* silencing, and (d) combined hrGDF15 treatment and *RSU-1* silencing. In all four approaches, the expression of *RSU-1*, *GDF15*, *PINCH1*, *RhoA* and *MMP-13* as well as the effect on cell

migration and invasion was investigated. **Figure 3-12** presents a diagrammatic summary of the molecular interactions, based on our findings. As shown in the diagram, in cells with high GDF15 and low RSU-1 expression (H4 cells), hrGDF15 treatment upregulates *RSU-1* (which is very low at an endogenous level), *PINCH1*, *RhoA* and *MMP-13* and promotes migration and invasion, whereas in cells with low GDF15 and high RSU-1 expression (A172 cells) the effect is the opposite. Interestingly, in SW1088 cells with intermediate expression level of RSU-1 and GDF15, insignificant changes were noticed following hrGDF15 treatment both with regard to invasion (**Figure 3-2B**) and migration (**Figure 3-2C**) as well as gene expression (**Figure 3-4**). Thus, *GDF15* promotes invasion in H4 cells and inhibits it in A172 through alterations in *PINCH1*, *RhoA* and *MMP-13* expression, which are known to regulate cell migration and invasion.

To test the hypothesis that *GDF15* and *RSU-1* are implicated in the same molecular mechanism to regulate H4, SW1088 and A172 cells invasion, we silenced *RSU-1* (**Figure 3-6**) and observed a strong upregulation of *GDF15* in the A172 cell line, which has low endogenous GDF15 levels (**Figure 3-6D–6F**) and a smaller change was observed in H4 cells in which GDF15 is abundant. These results suggest that RSU-1 inhibits GDF15 in A172 cells in which *RSU-1* expression levels are higher and GDF15 treatment promotes *RSU-1* expression in H4 cells in which GDF15 levels are higher. Also, the SW1088 cell line has intermediate motility behavior and this is in accordance with the relative endogenous level of RSU-1 and GDF15.

By silencing *RSU-1*, we showed that migration and invasion (**Figure 3-5**) are increased in H4 and decreased in A172 [131] suggesting that *RSU-1* by itself inhibits migration and invasion in H4 and promotes them in A172 again through regulation of *PINCH1*, *RhoA* and *MMP-13* expression (**Figure 3-6**). This is not surprising as *PINCH1* is in direct

interaction with *RSU-1* and of course it is very possible any change in *RSU-1* expression also affects *PINCH1* [123]. Moreover, RhoA is known to promote the formation of actin fibers and to be implicated in cell migration [150] and as it is shown in **Figure 3-3H**, its activation was following the same pattern with the mRNA expression after hrGDF15 treatment.

In an effort to investigate the exact molecular mechanism underlying the *RSU-1* function by *GDF15* regulation, we finally silenced *GDF15* by siRNA-mediated silencing (**Figure 3-8**). Our results show that *GDF15* silencing inhibited cell migration and invasion of A172 cells and did not affect the mobility of H4 cells. As shown in **Figure 3-12**, if GDF15 is missing from the pathway then migration and invasion are regulated by RSU-1, which differentially regulates them in the two cell lines. Interestingly, the expression of *PINCH1*, *RhoA* and *MMP13* also followed identical pattern **(Figure 3-10D–10G,10I–10K**), while *RSU-1* was downregulated upon *GDF15* silencing in both cell lines (**Figure 3-10A–10C**). These results suggest that *GDF15* silencing in the less invasive H4 cells with lower RSU-1 expression downregulates *RSU-1* further without affecting invasion and gene expression. On the other hand, *GDF15* silencing in the more invasive A172 cells leads to reduced *RSU-1* expression that is in agreement with the cell invasion pattern being also consistent with the findings obtained from direct *RSU-1* silencing (**Figure 3-6**).

To summarize, the data presented in this study provide evidence that there is a strong connection between *RSU-1* and *GDF15* in H4 and A172 cells, which is different from the one observed in breast cancer cells [60], further corroborating the idea that GDF15's function is, to a great extent, cell-type specific. More importantly, this work points out the significance of the relative expression of these two proteins in affecting the ability of cells to migrate and invade in brain parenchyma. Moreover, our knowledge of the molecular mechanism in which GDF15 and RSU-1 are involved will facilitate the identification of

therapeutic targets in signalling pathways that are crucial to cancer development and progression. Future studies are thus needed in order to better clarify the exact mechanism in which *RSU-1* and *GDF15* take part in gliomas and evaluate the diagnostic potential of their expression levels.

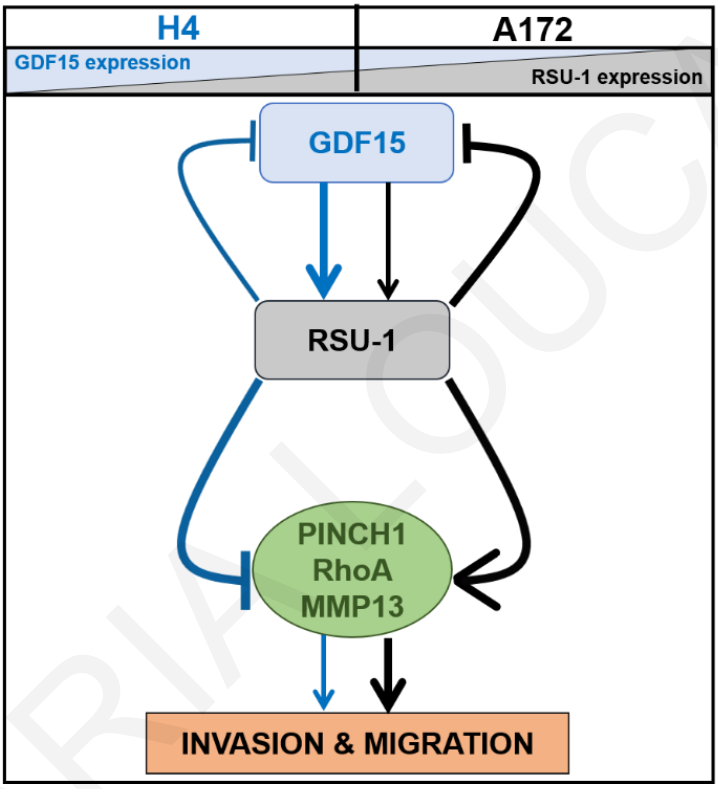

***Figure 3-12*. Schematic representation of the involvement of *RSU-1* and *GDF15* in regulating of H4 and A172 cell migration and invasion.** The non-invasive H4 cells, endogenously express high levels of GDF15 and low levels of RSU-1 in contrast to the highly invasive A172 cells which endogenously express high RSU-1 and low GDF15 levels. This differential expression leads to a different behavior with regard to brain cell migration and invasion. In H4 cells, *GDF15* induces *RSU-1*, which in turn inhibits migration and invasion by inhibiting *PINCH1*, *RhoA* and *MMP-13* (solid blue arrows and lines). In the invasive A172 cells, *GDF15* promotes *RSU-1* which enhances migration and invasion through upregulation of *PINCH1*, *RhoA*, and *MMP-13* (solid black arrows and lines). Arrows used in the diagram are of different weight, so that thick arrows indicate stronger effect while thin arrows indicate weaker effect, further emphasizing the concept that expression levels of both RSU-1 and GDF15 are crucial in regulating glioma cell migration and invasion.

4 Chapter 4: ILK silencing inhibits migration and invasion of more invasive glioma cells by downregulating ROCK-1 and Fascin-1

This research is under review in *Frontiers in Oncology*: **Maria Louca**, Apostolos Zaravinos, Triantafyllos Stylianopoulos and Vasiliki Gkretsi.

4.1 Introduction

As mentioned **in Chapter 1** tumor malignancy and cancer cell invasiveness is greatly dependent upon the interaction of cancer cells with the ECM through integrins [151-153]. Integrins are heterodimeric cell membrane receptors consisting of a and β subunits, which when activated are capable of transmitting signals from the ECM and tumor microenvironment to the interior of the cell and determine cell behavior by regulating processes such as cell differentiation, migration, invasion, apoptosis and proliferation [154-157]. This is accomplished through the binding of integrins to a complex network of focal adhesion proteins at cell-ECM adhesion sites that comprise the cell's "adhesome". Notably, the cell's adhesome is also found in close contact with the actin cytoskeleton to better coordinate various cellular responses to extracellular stimuli [20, 22, 28, 158].

In **Chapters 2** and **3**, I described my work on the role of RSU-1 in glioma cells aggressiveness and its regulation by the GDF15 protein. However, RSU-1 was shown previously to interact with PINCH1, which is a protein of the IPP complex and in turn it interacts with ILK[30, 35, 51].

ILK, a highly conserved serine-threonine pseudo-kinase, was firstly identified in 1996 as a cytoplasmic domain interactor with integrin β1 and β3 subunits, and was later shown to

regulate multiple cellular processes upon integrin activation, including cell motility, apoptosis, proliferation and tissue morphogenesis[29, 35, 153, 159-161]. Interestingly, ILK expression has been previously associated with advanced tumor grade in many malignancies including gliomas [29, 34, 160, 162-165]. Moreover, ILK depletion has been shown to lead to adhesion and spreading defects through downregulation of Rho-associated kinase (ROCK-1), a principle effector, known to modulate actin cytoskeleton and promote cell motility [166-170] . In fact, elevated ROCK-1 expression has been also associated with shorter survival in pancreatic cancer patients and malignant progression in breast cancer and glioblastoma cells [171-173].

Fascin-1 is an actin-bundling functional protein-target of ROCK-1 and is also upregulated in many human carcinomas, such as colon and breast as well as in glioma, promoting cell migration, invasion and metastasis[174-178]. The main objective of the present work was to determine *in vitro* the role of ILK in glioma cell invasiveness. To this end we used two different cell lines, the H4 non-invasive cells and the A172, highly invasive cells [132, 179], and we have found that ILK silencing inhibits cell migration and invasion of the A172 cells through downregulation of ROCK-1 and Fascin-1.

4.2 **Methods**

TCGA data extraction and RNA-seq analysis. RNA-seq data (read counts) were extracted from the Cancer Genome Atlas Glioblastoma Multiforme (TCGA-GBM) dataset (163 untreated glioblastomas and 5 normal brain samples), using the Genomic Data Commons (GDC) Data Portal. Normal samples were also extracted from the Genotype-Tissue Expression project (GTEx), totaling 207 normal brain samples. Read counts were normalized to transcripts per million (TPM) mapped reads, as previously reported[180]. Briefly, read counts were initially divided by the length of each gene in kilobases (reads per

kilobase, RPK) and were then counted up and divided by 1,000,000 («per million» scaling factor), producing the TPM values for each gene, in each tumor sample, and a small offset was added to avoid taking log of zero. The $\log_2(TPM + 1)$ scale was used to compare between brain cancer and normal samples. The mRNA expression level of ILK was evaluated using the limma R package with the cut-offs being $\log_2FC=1$ and q-value=0.01.

Data availability.

The glioblastoma multiforme RNA-Seq data that were analyzed for this study were extracted from the TCGA-GBM dataset can be found in the GDC Data portal of the National Cancer Institute (NIH) (portal.gdc.cancer.gov/projects/TCGA-GBM). The RNA-Seq data from the normal brain samples were extracted from the GTEx project and can be found here: gtexportal.org[181].

Cell lines. The human brain cell lines H4 and A172 were maintained in Dulbecco's Modified Eagle Medium (DMEM) supplemented with 10% Fetal Bovine Serum (FBS) and 1% antibiotic-antimycotic, as described previously [132] .

Antibodies and reagents. The anti-ILK, anti-ROCK-1 and anti-Fascin-1 antibodies were purchased from Cell Signaling Technology. Anti-MMP13 was purchased from Abcam, anti-β-actin was from Santa Cruz Biotechnology and anti-tubulin from Developmental Studies Hybridoma Bank as referred in **Section 2.2**. ILK siRNA was obtained from Santa Cruz Biotechnology, Lipofectamine 2000 from Invitrogen Life Technologies and Alamar Blue reagent from Thermo Scientific. Transwell chambers were obtained from Greiner Bio-One and Matrigel as well as Collagen I were purchased from Corning. QIAzol Lysis Reagent was obtained from QIAGEN, Superscript Reverse Transcriptase from Invitrogen and SYBR Green Supermix from KAPA Biosystems as referred in **Section 2.2**.

siRNA transfection. H4 and A172 cells were seeded in 6-well plates and were grown in complete culture medium until they reached a cell density of approximately 50%. DMEM was then replaced with medium without antibiotic-antimycotic and cells were transfected with appropriate siRNA with specific sequences for NSC (Non-specific-control) and ILK using the Lipofectamine 2000 reagent according to the manufacture's guidelines. Cells were harvested 48h post-transfection and were used further for other assays, as specified [179].

Cell invasion and migration assays. Cell invasion and migration assays were performed as described in **Section 3.2.**

Tumor spheroids formation in collagen gels. Spheroids were formed using the hanging drop method, as described previously [132, 179]. Briefly, $2.5x10^4$ H4 or A172 cells 24h post-siRNA transfection, were suspended in DMEM and then placed on the cover of a cell culture plate in the form of drops (each drop containing 500 cells). Spheroids were left to grow at 37°C for an additional 24h. Then, individual spheroids were embedded in 1.0 mg/ml collagen I in 96-well plate. Pictures were taken at time zero, and at either 16h for the H4 cells, or at 6h for the A172 cells, respectively, using a Nikon Eclipse optical microscope. The size of the spheroids (average of the major and minor axis length) was calculated using the ImageJ software and compared to their initial size at time zero. At least 8 spheroids were analyzed per condition and at least two independent experiments were performed for each cell line.

Cell viability assay. The Alamar blue reagent was used to measure cell viability after transfection of brain cells with ILK siRNA according to the company's guidelines. Briefly, equal numbers of H4 and A172 cells were seeded in 6-well plates 48h post siRNA treatment. Alamar blue reagent was added and cells were incubated with the reagent for 2h at 37°C [179]. Absorbance was finally measured at 450nm and 600nm using Rayto

spectrophotometer. All experiments were run in triplicates for each cell line. NSC-treated samples served as control.

Quantitative PCR. RNA isolation from brain cancer cells and gene expression analysis was performed as described in **Section 2.2**. The primers used for each target gene are shown in **Table 1 in Appendices**.

Western Blotting and protein quantification. Whole protein cell lysates were extracted as mentioned in **Section 2.2**. Membranes were incubated with anti-ILK, or anti-ROCK-1, or anti-Fascin-1, or anti-MMP13 antibodies overnight. Antibody against β-tubulin was used as loading control. The detection of the antibody was done using ChemiDoc XRS+ Imaging System (BioRad) and protein expression was quantified compared to the β-actin or β-tubulin loading control using the ImageJ software. The mean intensity of respective protein bands from four different immunoblots was used for the quantification, as indicated.

Statistical analysis. Comparisons between the expression of gene pairs were performed using regression variable plots. and correlated pair-wise using the Pearson's test. Pearson's correlation coefficient (rho) was used as a measure of the linear correlation between two variables. All statistical analyses were performed using IBM SPSS Statistics v.24.0.0.1. Overall statistical significance of differences from the experiments was tested using the Student's t test. All statistically significant differences ($p < 0.05$) are marked with an asterisk (*).

4.3 Results

ILK expression is dramatically elevated in glioblastoma multiforme patient samples and invasive cells. We first examined the expression of ILK in glioblastoma tissues using the publicly available data on the TCGA-GBM dataset. As shown in **Figure 4-1A**, human glioblastoma tissues have significantly higher ILK expression compared to the normal tissues. In accordance with this finding, we found that ILK is upregulated in A172 highly invasive glioblastoma cells compared to the non-invasive H4 neuroglioma cells, both at the mRNA (**Figure 4-1B**) and protein levels (**Figure 4-1B&1C**).

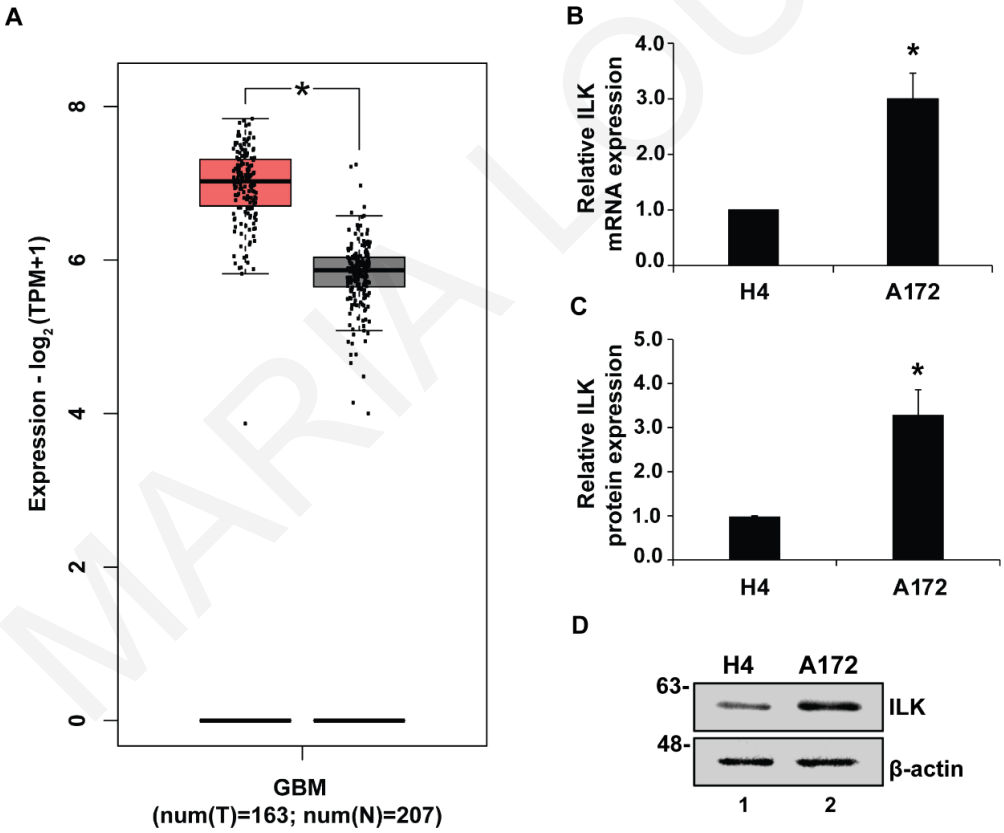

Figure 4-1. **ILK is overexpressed in glioblastoma tissues and invasive cells compared to normal tissues and neuroglioma cells. (A)** ILK expression in glioblastoma multiforme patients, T = Glioblastoma multiforme tissue samples; N = Solid normal brain tissue samples. **(B)** Relative *ILK* mRNA expression in H4 non-invasive neuroglioma and A172 highly invasive neuroblastoma cells. Three independent Real-Time PCR experiments were performed, and data were analyzed using the ΔΔCt method having β-actin as housekeeping gene. The H4 cells served as the calibrator for the analysis. **(C)** Relative ILK protein expression from four different western blots using β-

actin as the loading control and H4 as the sample control. Asterisks correspond to statistically significant differences with a p-value of <0.05. **(D)** Representative images from Western blots displaying ILK expression at the protein level. B-actin served as loading control**.**

ILK silencing significantly impairs the motility of the more aggressive glioblastoma cells but not that of the non-aggressive glioma cells. In order to investigate the role of *ILK* in the motility of glioma cells, we proceeded in its silencing using siRNA-mediated silencing. As shown in **Figure 4-2**, ILK was effectively silenced both at the mRNA (**Figure 4-2A**) and protein (**Figure 4-2B-2C**) levels. Then, 24h post-transfection, cells were subjected to transwell migration assay for another 24h. Interestingly, *ILK* silencing greatly impaired the migratory capacity of the highly invasive A172 cells without affecting the migratory behavior of the non-invasive H4 cells (**Figure 4-3A-3B**). To exclude the possibility that the observed inhibition in the migratory capacity of A172 cells upon *ILK* silencing was due to cell death, we performed viability assay, and observed no detrimental effects (**Figure 4-3C**).

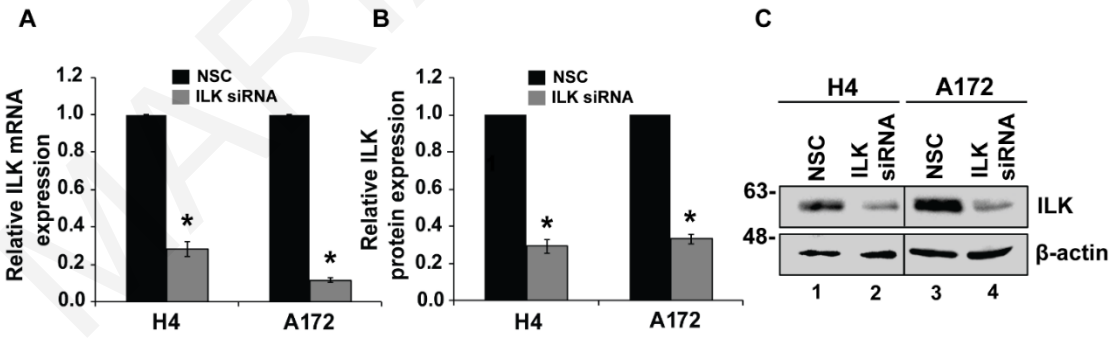

***Figure 4-2*. ILK is effectively silenced both at the mRNA and protein level. (A)** Real-time PCR analysis of ILK mRNA levels in H4 and A172 cells. Gene expression was normalized to β-actin, analyzed using the ΔΔCt method and expressed as relative changes compared to NSC treated samples for each cell line. **(B)** Relative ILK protein expression after treatment with NSC or ILK siRNA for 48h in H4 and A172. Quantification was performed from four different immunoblots using the NIH ImageJ software and actin served as a loading control. **(C)** Representative picture

of western blot showing ILK downregulation at the protein level following *ILK* silencing for the two cell lines under study. *P<0.05 indicates statistically significant differences compared to the NSC treated samples.

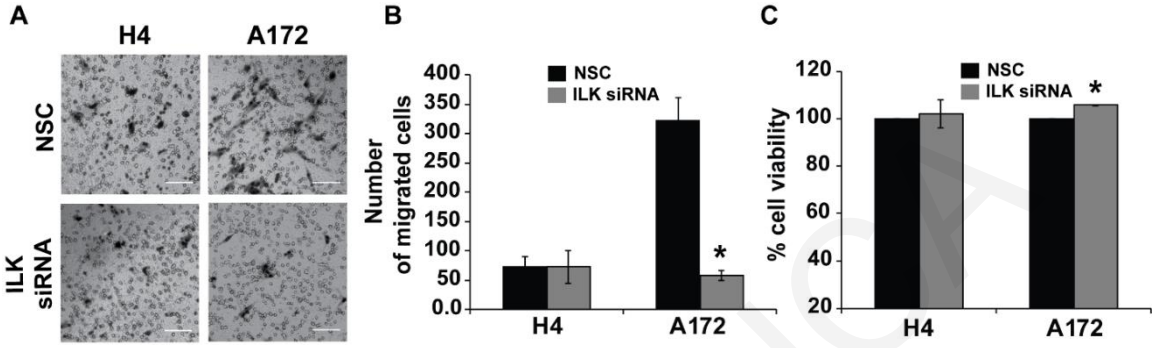

Figure *4-3. ILK* silencing significantly reduces the migratory capacity only in glioblastoma cells (A172) without affecting that of neuroglioma's (H4) behavior. (A) Representative images from H4 and A172 cells subjected to transwell migration assay following transfection with NSC or ILK siRNA. Migratory capacity of cells was measured under the optical microscope within 24h as described in Material and Methods. **(B)** Total number of migrated cells compared to NSC for each cell line per transwell. Two independent experiments were performed. **(C)** Alamar blue assay revealed that *ILK* silencing did not affect the viability of H4 and A172 cells. *P<0.05 indicates statistically significant differences compared to the NSC treated samples.

ILK silencing inhibits the invasive capacity of more aggressive cells but does not affect that of non-aggressive cells. To test whether cell invasion is affected in a similar way by *ILK* silencing, we examined the effect of *ILK* silencing on glioma cell invasion using two approaches: transwell-invasion assay and tumor spheroids invasion assay. Consistent with the migration results (**Figure 4-3**), both cell invasion approaches clearly demonstrated that *ILK* silencing impairs the invasion of the highly invasive A172 cells but does not affect that of the non-invasive H4 cells. More specifically, transwell invasion capacity was inhibited only in A172 cells upon ILK knockdown, whereas in H4 cells, which were characterized by lower basal ILK levels (**Figure 4-1B**), invasion was not affected (**Figure 4-4A&4B**).

This finding was also verified using tumor-spheroid invasion assay, a more physiologically relevant approach that involves growth of cancer cells in tumor-like spheroids that are embedded within matrix and are allowed to grow in three dimensions (3D) and not in monolayers as in the case of the transwell invasion assay [179]. Specifically, tumor spheroids of H4 and A172 cells lacking ILK, were embedded in 3D collagen I gels and left to invade through the matrix for 16h and 6h, respectively, depending on their aggressiveness. Our results (**Figure 4-4C&4D**) validated those of cell migration and transwell invasion assay, showing that *ILK* silencing affects only the more invasive glioblastoma cells (A172) which have been shown to express ILK at higher levels (**Figure 4-1B**) and does not affect the less invasive glioma cells (H4) which have lower ILK basal levels (**Figure 4-1B**).

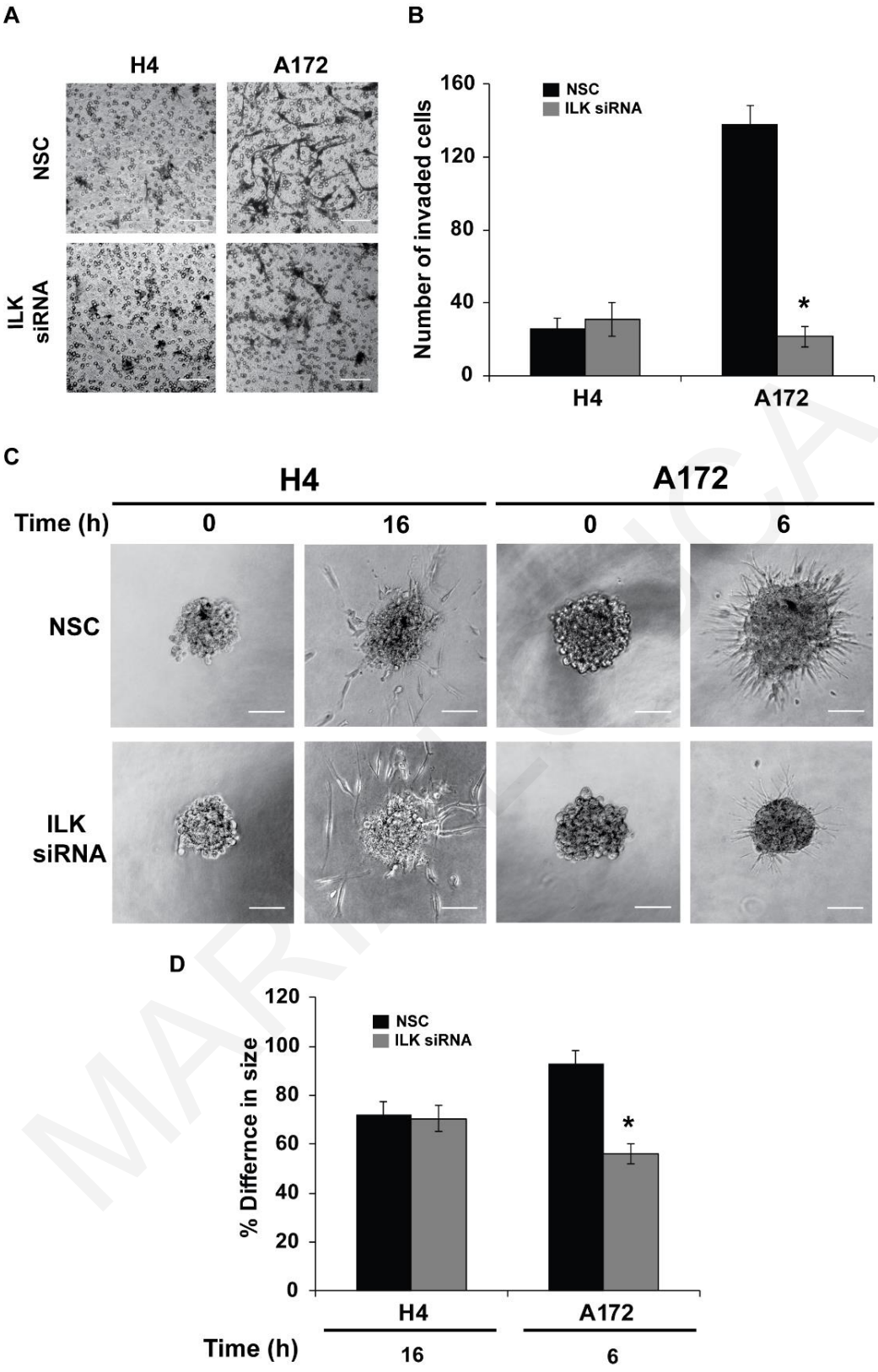
A
H4
A172
NSC
ILK siRNA
B
Number of invaded cells
160
120
80
40
0
NSC
ILK siRNA
*
H4
A172
C
H4
A172
Time (h)
0
16
0
6
NSC
ILK siRNA
D
% Differnce in size
120
100
80
60
40
20
0
NSC
ILK siRNA
*
H4
A172
Time (h)
16
6

***Figure 4-4*. The effect of ILK elimination for H4 and A172 cells on *in vitro* invasion assays. (A)** Representative images of transwell-invasion assay from inverted microscope in the presence of ILK siRNA or absence (NSC siRNA) for 24h in the two cell lines under study. **(B)** Quantification of the cell invasion results per transwell from three independent experiments. **(C)** Representative pictures of tumor spheroid invasion assay performed after NSC and ILK siRNA knockdown for each cell line (H4 and A172) at time zero and 16h or 6h respectively post embedding into 1mg/ml collagen I gel. **(D)**The percentage of tumor spheroids invasion per each cell line was calculated by measuring the difference of each spheroid size ((major+minor axis)/2) within the corresponding hours following placement of the spheroid in the collagen I gel (time zero). Four (4) independent experiment were performed and quantification was assessed for ILK siRNA samples compared to NSC samples. *P<0.05 indicates statistically significant differences compared to the NSC treated samples.

ILK depletion downregulates ROCK-1, Fascin-1 and MMP13 in A172 but not H4 cell.

To shed some more light upon the molecular mechanism involved, we first examined the expression of ROCK-1 (**Figure 4-5A-5C**) in H4 and A172 cells, following *ILK* silencing. ROCK-1 is known to be actively involved in actin cytoskeleton organization and modulation of cell migration and invasion [182], while being directly activated by ILK [168, 169]. Furthermore, the expression of Fascin-1 was also determined (**Figure 4-5D-5F**) as it is a key actin-bundling protein, promoting the formation of invadopodia that is also found upregulated in more malignant astrocytoma and glioblastoma patients and has been shown to be activated by ROCK-1 [183, 184]. As shown in **Figure 4-5**, *ILK* silencing led to downregulation of ROCK-1 and Fascin-1 in A172 cells but did not affect their expression in H4 cells, further corroborating the findings from the migration (**Figure 4-3**) and invasion assays (**Figure 4-4**). Finally, we tested the expression of MMP13 following *ILK* silencing, since it is a known effector protease that is crucially involved in glioma cell invasion [132]. The expression of MMP13 follows an identical pattern to that of ROCK-1 and Fascin-1 (**Figure 4-5G-5I**).

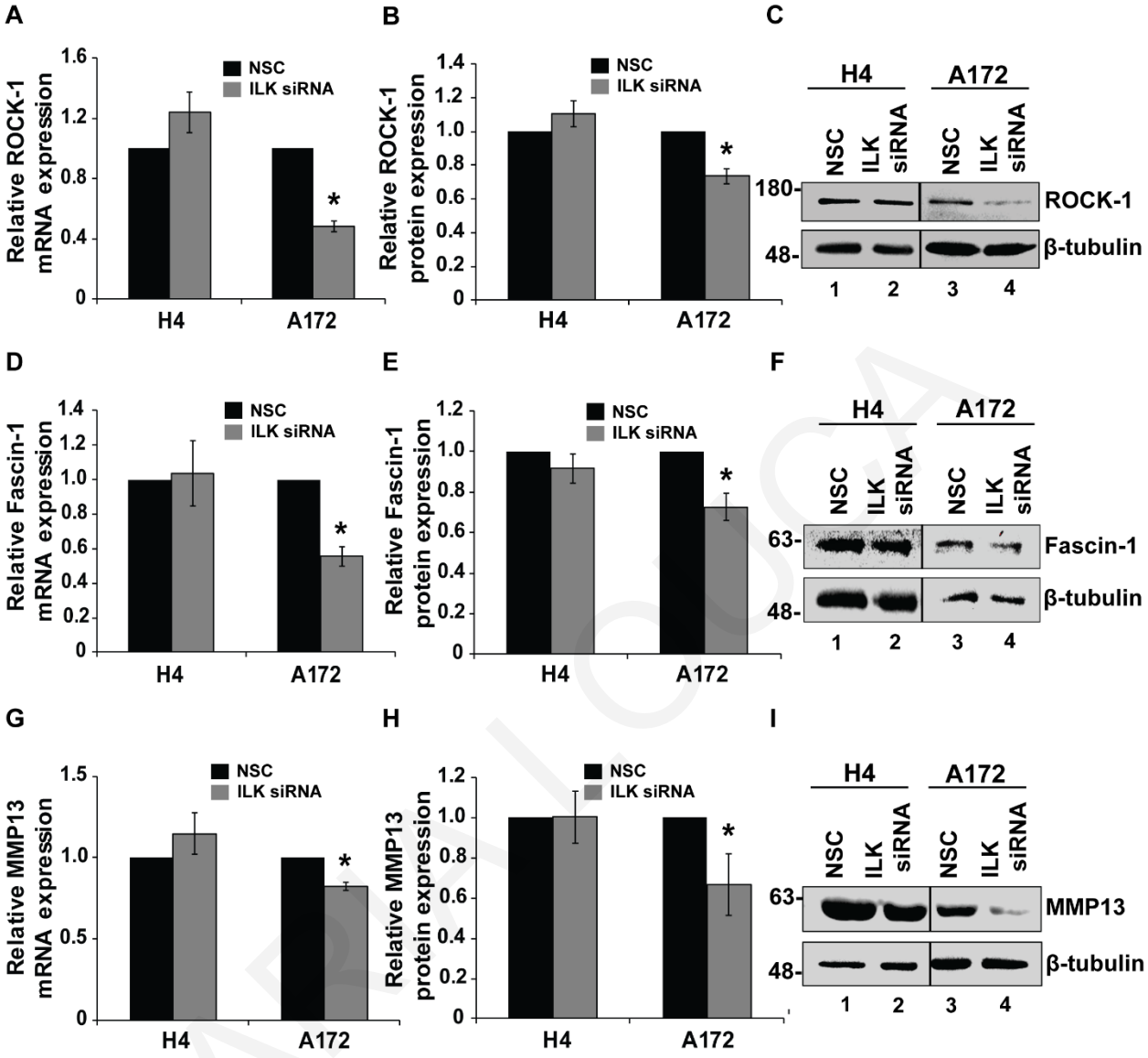

***Figure 4-5. ILK* silencing suppresses cell migration and invasion of glioblastoma cells (A172) through downregulation of ROCK-1, Fascin-1 and MMP13 without affecting the behavior and gene expression of neuroglioma cells (H4). (A, D&G)** Quantification of the mRNA expression of ROCK-1-, Fascin-1 and MMP13 post of NSC or ILK siRNA transfection for H4 and A172 cell lines. **(B, E &H)** Western blot analysis for ROCK-1-1, Fascin and MMP13 respectively. **(C, F, & I)** Representative immunoblots of 3 independent experiments showing ROCK-1, Fascin-1 and MMP13 respectively protein expression. *P<0.05 denotes statistically significant differences compared to the NSC treated samples.

Pairwise correlations of the expression of ILK, ROCK-1, Fascin-1, MMP13 in the TCGA-GBM patient dataset. To further enhance our findings, we performed a pairwise correlation analysis of the expression of ILK, ROCK-1, Fascin-1 and MMP13 in the TCGA-GBM patient dataset. The expression of *ILK*, *ROCK-1* and *Fascin-1* was significantly correlated (Pearson's rho>0.4; p<0.01); whereas, that between the gene pairs ILK and MMP13; ROCK-1 and MMP13; or Fascin-1 and MMP13, was not (**Figure 4-6**).

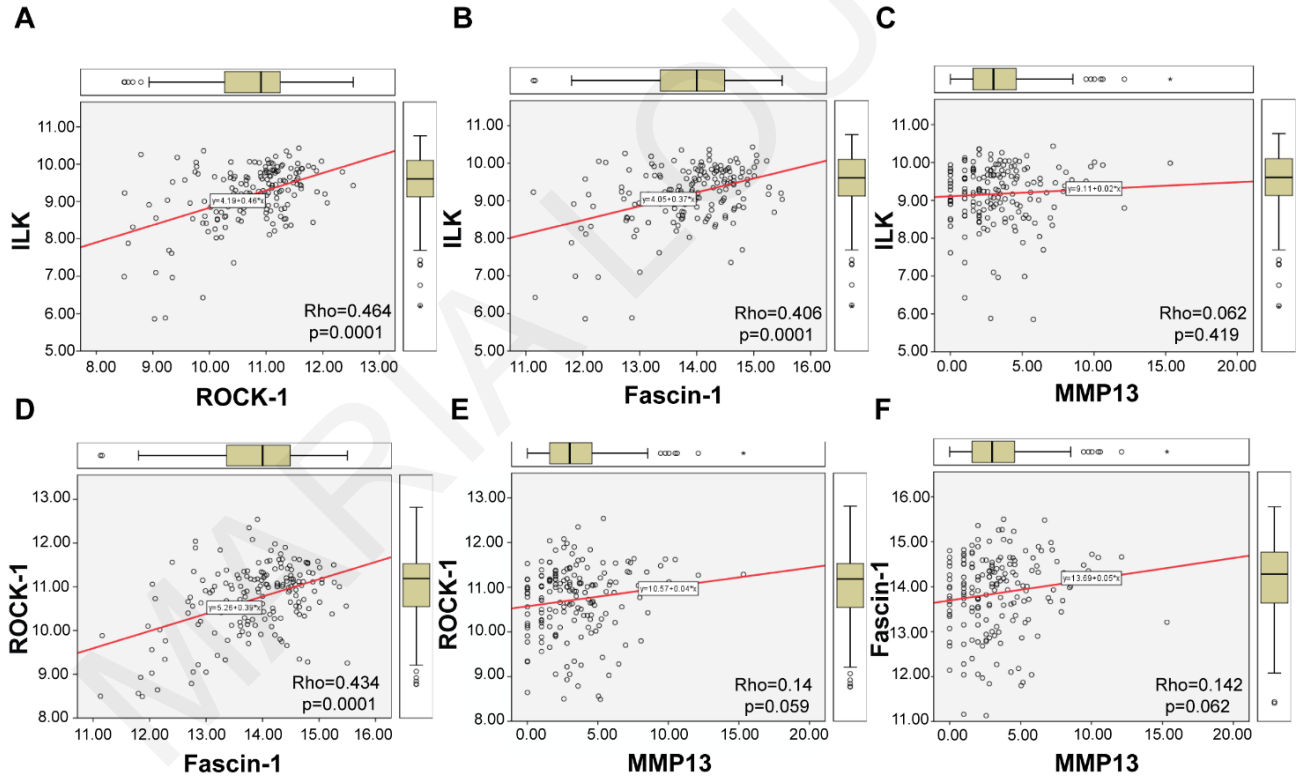

***Figure 4-6*. Correlations between the expression of the genes ILK, ROCK-1, Fascin-1 and MMP13 using TCGA-GBM dataset.** Regression variable plots illustrating the significant correlations between the expression of the genes ILK and ROCK-1 **(A)**, ILK and Fascin-1 **(B)**, and ROCK1 and Fascin-1 **(D)**. The gene pairs ILK and MMP13 **(C)**; ROCK-1 and MMP13 **(E)**; or Fascin-1 and MMP13 **(F)** were not correlated between them. Rho, Pearson's rho; p, p-value. The linear fit line is highlighted in red color.

4.4 Discussion

Several studies demonstrate a significant role of ILK in regulating many physiological cellular functions, but numerous other studies have also implicated ILK in tumor biology and specifically in cancer cell apoptosis, proliferation, migration and invasion [159-161]. Cell migration and invasion, in particular, play a crucial role in tumor recurrence and metastasis and are thought to account for reduced survival in patients with glioblastoma [185]. Despite intensive research on the role of ILK in health and disease, little is known regarding its involvement in glioblastoma pathogenesis [160, 165].

In the present work, we used two brain cell lines, the H4 non-invasive neuroglioma cells and the A172 highly invasive glioblastoma cells, to decipher ILK's involvement in glioblastoma aggressiveness. We found that ILK expression is elevated in the highly invasive cell line compared to the non-invasive one. This was also supported by TCGA data, showing that ILK is significantly upregulated in GBM patients compared to the normal brain. These findings indicate that ILK is crucially involved in glioblastoma pathogenesis.

By silencing *ILK*, we showed that both the migration and invasion capacity of A172 cells is dramatically impaired, while no alteration is observed in the respective properties of H4 neuroglioma cells. This, suggests that ILK depletion affects only the more invasive cell lines which also have higher basal ILK levels.

To better understand the involvement of ILK in glioblastoma pathogenesis, we investigated the molecular mechanism by which ILK promotes motility and invasion of glioblastoma cells. To that regard, we examined the expression of ROCK-1 and Fascin-1, two known actin-cytoskeleton modulators involved in determining the migratory behavior of cancer cells [186, 187]. Our results show that *ILK* silencing reduced the expression of both ROCK-1 and Fascin-1 only in A172 cells, which is in line with our results from the migration

and invasion assays. These results were also supported by analysis of the TCGA-GBM dataset, which provided us with a wider perspective of what is the situation in human tissues.

Finally, taking into consideration the fact that Fascin-1 promotes cancer cells invasion in an MMP-dependent manner [188] and that ROCK induces the migration and invasion of human cancer via MMP13 up-regulation [189], we further tested the expression of *MMP13*, following *ILK* silencing which also showed a similar expression pattern. Interestingly though, pairwise correlation analysis of *ILK*, *ROCK-1, Fascin-1* and *MMP13* expression in the TCGA-GBM patient dataset showed that the expression of *ILK*, *ROCK-1* and *Fascin-1* is significantly correlated while that was not true for the expression between the gene pairs of the respective genes with *MMP13* (*ILK* and *MMP13*; *ROCK-1* and *MMP13*; and *Fascin-1* and *MMP13*). This is not surprising but rather further verifies our data, as it indicates that *MMP13* is regulated by many other genes within the human body to fulfill its role as an effector protease. Thus, in isolated glioblastoma cells following targeted silencing of *ILK*, we observe dramatic reduction in the *MMP13* expression (**Figure 4-5**) which suggests that ILK promotes migration and invasion though the ROCK-1, Fascin-1, MMP13 axis (**Figure 4-7**). However, in the human samples analyzed from the TCGA-GBM dataset, things are more complicated, and while *ILK* expression is well-correlated with the direct-target genes *ROCK-1* and *Fascin-1*, the *MMP13* expression is not correlated in the same way (**Figure 4-6**) as it is also affected by many other signals inside the tissue[190, 191].

In conclusion, our data shows for the first time how ILK is implicated in the invasiveness of glioblastoma cells. We also provide the first evidence on the regulation of ROCK-1 and Fascin-1 by ILK and as a subsequent MMP13 activation, thus, leading to invasive behavior of glioblastoma cells. All in all, our findings will enhance our understanding of the role of ILK dynamics in human glioblastomas, and demonstrate that

ILK should be further evaluated as a potential candidate target for achieving better therapeutic outcome in GBM patients.

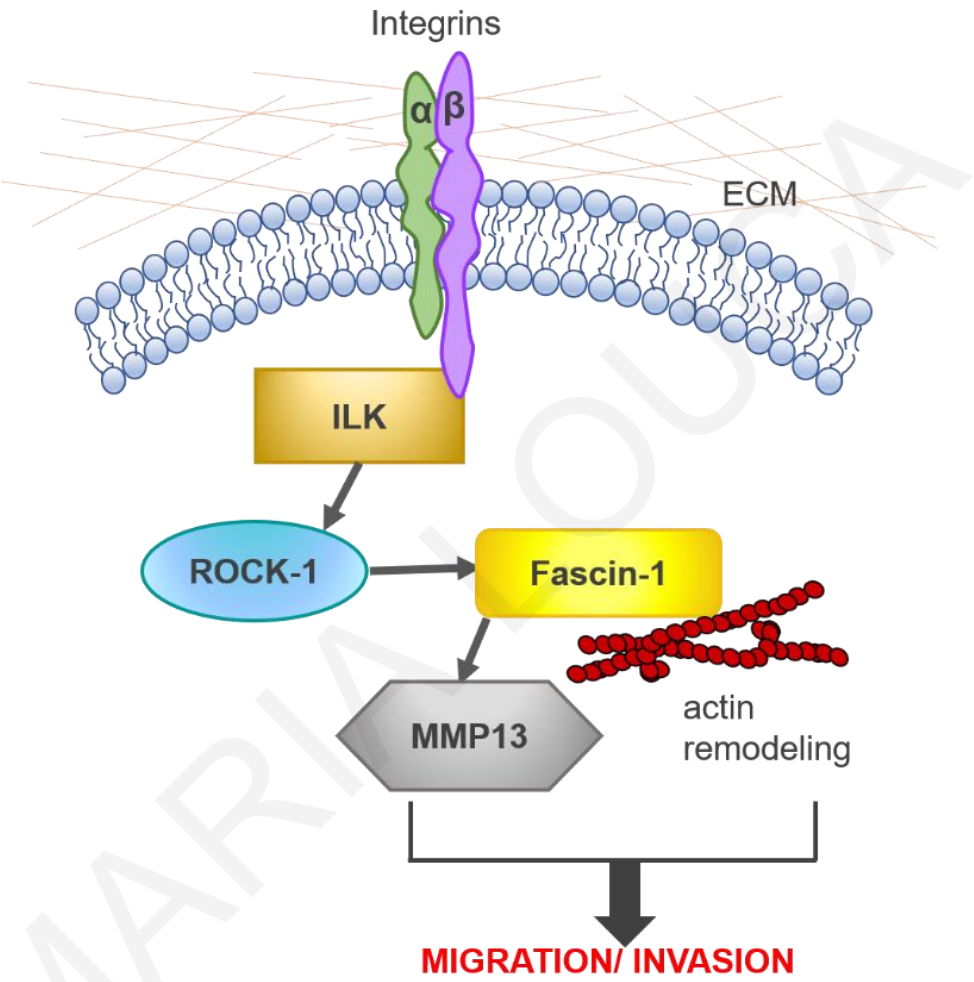

***Figure 4-7*. Diagrammatic representation of the putative molecular mechanism of ILK's action in regulating glioblastoma cells migration/invasion *in vitro*.** ROCK-1 protein can be activated by ILK and then Fascin-1 upregulates the expression of MMP13 which induces the migration and invasion of glioblastoma cells.

5 Conclusions and Future Directions

5.1 Conclusions

In this dissertation study, the role of RSU-1 and ILK was investigated with regard to glioma cell aggressiveness. Also, the interplay between RSU-1 and GDF-15 was studied in glioma cells. For that purpose, this research work combined several different *in vitro* approaches using not only 2D but also 3D culture models in an attempt to better mimic the physiological conditions and the actual tumor setting.

Firstly, four glioma cell lines of varying aggressiveness (H4, SW1088, A172 and U87-MG) were characterized in terms of morphology, cytoskeleton organization and stiffness, and their migratory and invasive potential was evaluated by performing colony formation assays as well as a series of transwell migration and invasion assays and 3D tumor spheroid invasion assays. Based on the initial findings, glioma cell lines were categorized in two distinct groups; aggressive cell lines (A172 and U87-MG cells) which were characterized by more elongated, and softer cells that exhibited higher invasion and migration capacity, and non-aggressive cell lines (H4 and SW1088) which were characterized by less elongated, harder cells with minimum migratory and invasive potential.

Moreover, *RSU-1* was found to be dramatically upregulated in the more aggressive glioblastoma cells (A172 and U87-MG) compared to less invasive ones (H4 and SW1088) which indicated fundamental involvement of RSU-1 towards a more aggressive phenotype. Notably, RSU-1 silencing had opposite effects on glioma cell motility depending on the cells' aggressiveness which was accompanied by respective changes in the expression of specific proteins that are part of the RSU-1-activated-molecular signaling pathway. More specifically, *RSU-1* silencing in aggressive cells led to decreased invasive capacity,

decreased STAT6 phosphorylation and decreased MMP13 expression, suggesting that RSU-1 promotes a metastatic phenotype in aggressive cells that is why its inhibition halted migratory and invasive propensity. On the contrary, *RSU-1* silencing in less aggressive cells enhanced invasive capacity, induced STAT6 phosphorylation and upregulation of MMP13 expression, which indicated that RSU-1 has an inhibitory role in these cells with regard to their *in vitro* metastatic properties. This differential role of RSU-1 in glioma cells depending on the cell aggressiveness further signifies that RSU-1 expression level could serve as a predictor of glioma progression and metastasis.

To further test this hypothesis, the interplay between RSU-1 and GDF15 and their role in regulating glioma cell invasion was studied using three different glioma cell lines (H4, SW1088 and A172). Apart from the fact that these cell lines had increasing invasion capacity, they also exhibited opposite patterns of *RSU-1* and *GDF15* expression. More importantly, it was shown that glioma cells behave differently with regard to cell migration and invasion depending on the relative RSU-1 and GDF15 expression. Moreover, it was shown that PINCH1, RhoA and MMP13 play a crucial role being regulated by RSU-1/GDF15 interplay ultimately affecting the final invasive phenotype of glioma cells.

Finally, because RSU-1 is directly connected to ILK, the role of ILK in the aggressiveness of glioma cells *in vitro* was studied using the ILK silencing approach in H4 and A172 cells ILK silencing inhibited cell migration and invasion of the more aggressive A172 cells whereas it did not affect the motility and invasive ability of non-aggressive H4 cells. In addition, the expression of ROCK-1, Fascin-1 and MMP13 had respective changes. Also, all findings were verified by a bioinformatics analysis of the TCGA-GBM dataset. Concluding, ILK promotes glioblastoma cell invasion through activation of ROCK-1 and Fascin-1 *in vitro*, providing a more exact molecular mechanism for its action.

Collectively, this dissertation revealed that RSU-1 can differentially regulate the motility and invasive capacity of glioma cells, depending on its expression level and their aggressiveness, promoting the invasion of aggressive glioma cells (A172 and U87-MG), which have higher RSU-1 expression, and suppressing this capacity in less aggressive glioma cells (H4 and SW1088) which have lower RSU-1 expression. Thus, these findings suggest that targeting RSU-1 in the more aggressive glioma cells could be promising for the management of patients with brain tumors. This is the first work showing a connection between RSU-1 and GDF15 in malignant H4 and A172 cells that provides the basis for their future evaluation as potential novel therapeutic targets against glioma cell invasion.

5.2 **Future Directions**

Since the finding of the present work are promising, demonstrating that RSU-1 is critically involved in glioma cell invasive behavior and that its involvement may differ depending on its expression level and the cell type, it would be interesting to test in future studies whether the expression level of *RSU-1* in patients/tumor samples is also correlated with disease prognosis. Such a connection could render RSU-1 a prognostic biomarker for predicting the aggressiveness of gliomas while providing a potent novel therapeutic target.

Furthermore, the exact delineation of the molecular pathway by which RSU-1 regulates the malignant behavior of glioma cells is essential. Thus, future experiments would contribute to the identification of molecules associated with RSU-1 in glioma. For this purpose, a more targeted multiplex assay can be designed in order to detect alterations of influential phosphoproteins which may be implicated in glioma cell invasion and MMP13 expression. Additionally, co-immunoprecipitation experiments could be performed to identify potential proteins that directly interact with RSU-1.

Moreover, in this study, a strong inverse relationship between RSU-1 and GDF15 in H4 and A172 cells glioma cells was revealed. In that regard, an RSU-1 overexpression approach in non-invasive glioma cells (H4), which express low RSU-1 basal level, could complement the findings of the silencing approach.

Additionally, in this study ILK silencing was shown to affect the invasion capacity of aggressive glioblastoma A172 cells which express high ILK basal levels but did not alter the respective properties of non-aggressive glioma cells (H4). Thus, further experiments including ILK silencing in combination with a phosphoproteomic screening may facilitate the identification of the molecular mechanism by which ILK regulates glioma cell malignancy.

In conclusion, the fact that RSU-1 has differential role and expression in glioma cell lines highlights the need to include more glioma cell lines and of course human samples that will allow us to generalize our conclusions or get a better idea of the exact involvement of RSU-1 in glioma cell invasion. Also, it would be of fundamental importance to validate results *in vivo* and examine whether RSU-1 plays similar role in actual gliomas grown inside the whole animal. Thus studies in animal tumor models would be a highly advisable direction to be taken in the future.

Last but not least, this work showed that certain conclusions in cancer biology cannot be generalized as there are many cell-type specific factors affecting the final outcome. More specifically, the GDF15 level differently affects RSU-1 expression depending on the aggressiveness of glioma cells. This, in fact, is in concert with the idea of personalized medicine, as it is taking into account these cell-type specific differences that represent the heterogeneity found in human tissues and gets us closer to designing therapies that are custom made for each individual patient.

Concluding, the present dissertation provided evidence on the role of RSU-1, ILK and GDF15 in gliomas, pointing towards the direction that these proteins could be potential new biomarkers or therapeutic targets against invasion and metastasis which is the leading cause of death for cancer patients.

List of Tables

List of Figures

References

1. Bray, F. et al. Global cancer statistics 2018: GLOBOCAN estimates of incidence and mortality worldwide for 36 cancers in 185 countries. *CA: a cancer journal for clinicians* **68**, 394-424 (2018).
2. Siegel, R.L., Miller, K.D. & Jemal, A. Cancer statistics, 2016. *CA: a cancer journal for clinicians* **66**, 7-30 (2016).
3. Ferlay, J. et al. Estimating the global cancer incidence and mortality in 2018: GLOBOCAN sources and methods. *International journal of cancer* **144**, 1941-1953 (2019).
4. Louis, D.N. et al. The 2016 World Health Organization Classification of Tumors of the Central Nervous System: a summary. *Acta neuropathologica* **131**, 803-820 (2016).
5. Kleihues, P., Burger, P.C. & Scheithauer, B.W. The new WHO classification of brain tumours. *Brain pathology* **3**, 255-268 (1993).
6. Radner, H., Blumcke, I., Reifenberger, G. & Wiestler, O.D. [The new WHO classification of tumors of the nervous system 2000. Pathology and genetics]. *Der Pathologe* **23**, 260-283 (2002).
7. Kleihues, P. et al. The WHO classification of tumors of the nervous system. *Journal of neuropathology and experimental neurology* **61**, 215-225; discussion 226-219 (2002).
8. Reifenberger, G., Wirsching, H.G., Knobbe-Thomsen, C.B. & Weller, M. Advances in the molecular genetics of gliomas - implications for classification and therapy. *Nature reviews. Clinical oncology* **14**, 434-452 (2017).
9. Dang, L. et al. Cancer-associated IDH1 mutations produce 2-hydroxyglutarate. *Nature* **462**, 739-744 (2009).
10. Modrek, A.S., Bayin, N.S. & Placantonakis, D.G. Brain stem cells as the cell of origin in glioma. *World journal of stem cells* **6**, 43-52 (2014).
11. Ostrom, Q.T. et al. CBTRUS Statistical Report: Primary Brain and Other Central Nervous System Tumors Diagnosed in the United States in 2011-2015. *Neuro-oncology* **20**, iv1-iv86 (2018).
12. Buckner, J.C. et al. Central nervous system tumors. *Mayo Clin Proc* **82**, 1271-1286 (2007).
13. van den Bent, M.J. et al. A clinical perspective on the 2016 WHO brain tumor classification and routine molecular diagnostics. *Neuro-oncology* **19**, 614-624 (2017).
14. Balmain, A., Gray, J. & Ponder, B. The genetics and genomics of cancer. *Nature genetics* **33 Suppl**, 238-244 (2003).
15. Fidler, I.J. The pathogenesis of cancer metastasis: the 'seed and soil' hypothesis revisited. *Nature reviews. Cancer* **3**, 453-458 (2003).
16. Bacac, M. & Stamenkovic, I. Metastatic cancer cell. *Annual review of pathology* **3**, 221-247 (2008).
17. Minn, A.J. et al. Genes that mediate breast cancer metastasis to lung. *Nature* **436**, 518-524 (2005).
18. Bernstein, J.J. & Woodard, C.A. Glioblastoma cells do not intravasate into blood vessels. *Neurosurgery* **36**, 124-132; discussion 132 (1995).
19. Bacac, M. & Stamenkovic, I. Metastatic cancer cell. *Annual Review of Pathology-Mechanisms of Disease* **3**, 221-247 (2008).
20. Zaidel-Bar, R., Itzkovitz, S., Ma'ayan, A., Iyengar, R. & Geiger, B. Functional atlas of the integrin adhesome. *Nature cell biology* **9**, 858-867 (2007).
21. Hynes, R.O. Integrins: bidirectional, allosteric signaling machines. *Cell* **110**, 673-687 (2002).

22. Winograd-Katz, S.E., Fassler, R., Geiger, B. & Legate, K.R. The integrin adhesome: from genes and proteins to human disease. *Nature reviews. Molecular cell biology* **15**, 273-288 (2014).
23. Desgrosellier, J.S. & Cheresh, D.A. Integrins in cancer: biological implications and therapeutic opportunities. *Nature reviews. Cancer* **10**, 9-22 (2010).
24. Guo, W. & Giancotti, F.G. Integrin signalling during tumour progression. *Nature reviews. Molecular cell biology* **5**, 816-826 (2004).
25. Delon, I. & Brown, N.H. Integrins and the actin cytoskeleton. *Current opinion in cell biology* **19**, 43-50 (2007).
26. Brakebusch, C. & Fassler, R. The integrin-actin connection, an eternal love affair. *The EMBO journal* **22**, 2324-2333 (2003).
27. Brown, J., Kumbar, S. & Banik, B. Bio-instructive scaffolds for musculoskeletal tissue engineering and regenerative medicine. (Academic Press, 2016).
28. Elad, N. et al. The role of integrin-linked kinase in the molecular architecture of focal adhesions. *Journal of cell science* **126**, 4099-4107 (2013).
29. Hannigan, G.E. et al. Regulation of cell adhesion and anchorage-dependent growth by a new beta 1-integrin-linked protein kinase. *Nature* **379**, 91-96 (1996).
30. Wickstrom, S.A., Lange, A., Montanez, E. & Fassler, R. The ILK/PINCH/parvin complex: the kinase is dead, long live the pseudokinase! *The EMBO journal* **29**, 281-291 (2010).
31. Fukuda, K., Gupta, S., Chen, K., Wu, C. & Qin, J. The pseudoactive site of ILK is essential for its binding to alpha-Parvin and localization to focal adhesions. *Molecular cell* **36**, 819-830 (2009).
32. Ahmed, N. et al. Molecular pathways regulating EGF-induced epithelio-mesenchymal transition in human ovarian surface epithelium. *American journal of physiology. Cell physiology* **290**, C1532-1542 (2006).
33. Persad, S. & Dedhar, S. The role of integrin-linked kinase (ILK) in cancer progression. *Cancer metastasis reviews* **22**, 375-384 (2003).
34. Persad, S. et al. Inhibition of integrin-linked kinase (ILK) suppresses activation of protein kinase B/Akt and induces cell cycle arrest and apoptosis of PTEN-mutant prostate cancer cells. *Proceedings of the National Academy of Sciences of the United States of America* **97**, 3207-3212 (2000).
35. Legate, K.R., Montanez, E., Kudlacek, O. & Fassler, R. ILK, PINCH and parvin: the tIPP of integrin signalling. *Nature reviews. Molecular cell biology* **7**, 20-31 (2006).
36. Honda, S., Shirotani-Ikejima, H., Tadokoro, S., Tomiyama, Y. & Miyata, T. The integrin-linked kinase-PINCH-parvin complex supports integrin alphaIIbbeta3 activation. *PloS one* **8**, e85498 (2013).
37. Ghatak, S., Morgner, J. & Wickstrom, S.A. ILK: a pseudokinase with a unique function in the integrin-actin linkage. *Biochemical Society transactions* **41**, 995-1001 (2013).
38. Rooney, N. & Streuli, C.H. How integrins control mammary epithelial differentiation: a possible role for the ILK-PINCH-Parvin complex. *FEBS letters* **585**, 1663-1672 (2011).
39. Lange, A. et al. Integrin-linked kinase is an adaptor with essential functions during mouse development. *Nature* **461**, 1002-1006 (2009).
40. Tu, Y., Li, F., Goicoechea, S. & Wu, C. The LIM-only protein PINCH directly interacts with integrin-linked kinase and is recruited to integrin-rich sites in spreading cells. *Molecular and cellular biology* **19**, 2425-2434 (1999).
41. Zhang, Y., Chen, K., Tu, Y. & Wu, C. Distinct roles of two structurally closely related focal adhesion proteins, alpha-parvins and beta-parvins, in regulation of cell morphology and survival. *The Journal of biological chemistry* **279**, 41695-41705 (2004).

42. Ito, S. et al. The roles of two distinct regions of PINCH-1 in the regulation of cell attachment and spreading. *Molecular biology of the cell* **21**, 4120-4129 (2010).
43. Tsuda, T. & Cutler, M.L. Human RSU1 is highly homologous to mouse Rsu-1 and localizes to human chromosome 10. *Genomics* **18**, 461-462 (1993).
44. Cutler, M.L., Bassin, R.H., Zanoni, L. & Talbot, N. Isolation of rsp-1, a novel cDNA capable of suppressing v-Ras transformation. *Molecular and cellular biology* **12**, 3750-3756 (1992).
45. Dougherty, G.W., Chopp, T., Qi, S.M. & Cutler, M.L. The Ras suppressor Rsu-1 binds to the LIM 5 domain of the adaptor protein PINCH1 and participates in adhesion-related functions. *Experimental cell research* **306**, 168-179 (2005).
46. Masuelli, L. & Cutler, M.L. Increased expression of the Ras suppressor Rsu-1 enhances Erk-2 activation and inhibits Jun kinase activation. *Molecular and cellular biology* **16**, 5466-5476 (1996).
47. Masuelli, L., Ettenberg, S., Vasaturo, F., Vestergaard-Sykes, K. & Cutler, M.L. The ras suppressor, RSU-1, enhances nerve growth factor-induced differentiation of PC12 cells and induces p21CIP expression. *Cell growth & differentiation : the molecular biology journal of the American Association for Cancer Research* **10**, 555-564 (1999).
48. Montanez, E., Karakose, E., Tischner, D., Villunger, A. & Fassler, R. PINCH-1 promotes Bcl-2-dependent survival signalling and inhibits JNK-mediated apoptosis in the primitive endoderm. *Journal of cell science* **125**, 5233-5240 (2012).
49. Kadrmas, J.L. et al. The integrin effector PINCH regulates JNK activity and epithelial migration in concert with Ras suppressor 1. *The Journal of cell biology* **167**, 1019-1024 (2004).
50. Elias, M.C., Pronovost, S.M., Cahill, K.J., Beckerle, M.C. & Kadrmas, J.L. A crucial role for Ras suppressor-1 (RSU-1) revealed when PINCH and ILK binding is disrupted. *Journal of cell science* **125**, 3185-3194 (2012).
51. Gonzalez-Nieves, R., Desantis, A.I. & Cutler, M.L. Rsu1 contributes to regulation of cell adhesion and spreading by PINCH1-dependent and - independent mechanisms. *Journal of cell communication and signaling* **7**, 279-293 (2013).
52. Kim, Y.C., Gonzalez-Nieves, R. & Cutler, M.L. Rsu1-dependent control of PTEN expression is regulated via ATF2 and cJun. *Journal of cell communication and signaling* (2019).
53. Porcheri, C., Suter, U. & Jessberger, S. Dissecting integrin-dependent regulation of neural stem cell proliferation in the adult brain. *The Journal of neuroscience : the official journal of the Society for Neuroscience* **34**, 5222-5232 (2014).
54. Pierron, M., Pinan-Lucarre, B. & Bessereau, J.L. Preventing Illegitimate Extrasynaptic Acetylcholine Receptor Clustering Requires the RSU-1 Protein. *The Journal of neuroscience : the official journal of the Society for Neuroscience* **36**, 6525-6537 (2016).
55. Tajiri, H. et al. Targeting Ras-Driven Cancer Cell Survival and Invasion through Selective Inhibition of DOCK1. *Cell reports* **19**, 969-980 (2017).
56. Sahai, E. & Marshall, C.J. RHO-GTPases and cancer. *Nature reviews. Cancer* **2**, 133-142 (2002).
57. Vasaturo, F., Dougherty, G.W. & Cutler, M.L. Ectopic expression of Rsu-1 results in elevation of p21CIP and inhibits anchorage-independent growth of MCF7 breast cancer cells. *Breast cancer research and treatment* **61**, 69-78 (2000).
58. Giotopoulou, N. et al. Ras suppressor-1 promotes apoptosis in breast cancer cells by inhibiting PINCH-1 and activating p53-upregulated-modulator of apoptosis (PUMA); verification from metastatic breast cancer human samples. *Clinical & experimental metastasis* **32**, 255-265 (2015).

59. Gkretsi, V., Stylianou, A., Louca, M. & Stylianopoulos, T. Identification of Ras suppressor-1 (RSU-1) as a potential breast cancer metastasis biomarker using a three-dimensional in vitro approach. *Oncotarget*, 27364-27379 (2017).
60. Gkretsi, V. et al. Inhibition of Breast Cancer Cell Invasion by Ras Suppressor-1 (RSU-1) Silencing Is Reversed by Growth Differentiation Factor-15 (GDF-15). *International journal of molecular sciences* **20** (2019).
61. Ji, H. et al. Twist promotes invasion and cisplatin resistance in pancreatic cancer cells through growth differentiation factor 15. *Molecular medicine reports* **12**, 3841-3848 (2015).
62. Aw Yong, K.M. et al. Morphological effects on expression of growth differentiation factor 15 (GDF15), a marker of metastasis. *Journal of cellular physiology* **229**, 362-373 (2014).
63. Wallin, U. et al. Growth differentiation factor 15: a prognostic marker for recurrence in colorectal cancer. *British journal of cancer* **104**, 1619-1627 (2011).
64. Chunduru, S. et al. Identification of an alternatively spliced RNA for the Ras suppressor RSU-1 in human gliomas. *Journal of neuro-oncology* **60**, 201-211 (2002).
65. Gkretsi, V., Stylianou, A., Louca, M. & Stylianopoulos, T. Identification of Ras suppressor-1 (RSU-1) as a potential breast cancer metastasis biomarker using a three-dimensional in vitro approach. *Oncotarget* **8**, 27364-27379 (2017).
66. Donthamsetty, S. et al. Role of PINCH and its partner tumor suppressor Rsu-1 in regulating liver size and tumorigenesis. *PloS one* **8**, e74625 (2013).
67. Gkretsi, V. & Bogdanos, D.P. Elimination of Ras Suppressor-1 from hepatocellular carcinoma cells hinders their in vitro metastatic properties. *Anticancer research* **35**, 1509-1512 (2015).
68. Aizaki, H. et al. Expression profiling of liver cell lines expressing entire or parts of hepatitis C virus open reading frame. *Hepatology* **36**, 1431-1438 (2002).
69. Tsuda, T., Marinetti, M.R., Masuelli, L. & Cutler, M.L. The Ras suppressor RSU-1 localizes to 10p13 and its expression in the U251 glioblastoma cell line correlates with a decrease in growth rate and tumorigenic potential. *Oncogene* **11**, 397-403 (1995).
70. Gkretsi, V. et al. Depletion of Ras Suppressor-1 (RSU-1) promotes cell invasion of breast cancer cells through a compensatory upregulation of a truncated isoform. *Scientific reports* **9**, 10050 (2019).
71. Stupp, R. et al. Effect of Tumor-Treating Fields Plus Maintenance Temozolomide vs Maintenance Temozolomide Alone on Survival in Patients With Glioblastoma: A Randomized Clinical Trial. *Jama* **318**, 2306-2316 (2017).
72. Xu, Q. et al. Growth differentiation factor 15 induces growth and metastasis of human liver cancer stem-like cells via AKT/GSK-3beta/beta-catenin signaling. *Oncotarget* **8**, 16972-16987 (2017).
73. Ma, Y.S. et al. DRR1 promotes glioblastoma cell invasion and epithelial-mesenchymal transition via regulating AKT activation. *Cancer letters* **423**, 86-94 (2018).
74. de Groot, J.F. et al. Tumor invasion after treatment of glioblastoma with bevacizumab: radiographic and pathologic correlation in humans and mice. *Neuro-oncology* **12**, 233-242 (2010).
75. Johnson, D.R. & O'Neill, B.P. Glioblastoma survival in the United States before and during the temozolomide era. *Journal of neuro-oncology* **107**, 359-364 (2012).
76. Stupp, R. et al. Radiotherapy plus concomitant and adjuvant temozolomide for glioblastoma. *The New England journal of medicine* **352**, 987-996 (2005).
77. Scherer, H. The forms of growth in gliomas and their practical significance. *Brain* **63**, 1-35 (1940).

78. Sun, L.H. et al. Overexpression of Paxillin Correlates with Tumor Progression and Predicts Poor Survival in Glioblastoma. *CNS Neurosci Ther* **23**, 69-75 (2017).
79. Cutler, M.L., Bassin, R.H., Zanoni, L. & Talbot, N. Isolation of Rsp-1, a Novel Cdna Capable of Suppressing V-Ras Transformation. *Molecular and cellular biology* **12**, 3750-3756 (1992).
80. Dougherty, G.W., Jose, C., Gimona, M. & Cutler, M.L. The Rsu-1-PINCH1-ILK complex is regulated by Ras activation in tumor cells. *Eur J Cell Biol* **87**, 721-734 (2008).
81. Zacharia, L.C., Stylianopoulos, T. & Gkretsi, V. Ras Suppressor-1 (RSU-1) in Cancer Cell Metastasis: Friend or Foe? *Crit Rev Oncog* **22**, 249-253 (2017).
82. Stylianou, A. & Yova, D. Surface nanoscale imaging of collagen thin films by Atomic Force Microscopy. *Mater Sci Eng C Mater Biol Appl* **33**, 2947-2957 (2013).
83. Yim, E.K. et al. Nanopattern-induced changes in morphology and motility of smooth muscle cells. *Biomaterials* **26**, 5405-5413 (2005).
84. Stylianou, A. & Yova, D. Atomic force microscopy investigation of the interaction of low-level laser irradiation of collagen thin films in correlation with fibroblast response. *Lasers Med Sci* **30**, 2369-2379 (2015).
85. Stylianou, A., Gkretsi, V. & Stylianopoulos, T. Transforming growth factor-beta modulates pancreatic cancer associated fibroblasts cell shape, stiffness and invasion. *Biochimica et biophysica acta* (2018).
86. Hermanowicz, P., Sarna, M., Burda, K. & Gabrys, H. AtomicJ: an open source software for analysis of force curves. *Rev Sci Instrum* **85**, 063703 (2014).
87. Eltzner, B., Wollnik, C., Gottschlich, C., Huckemann, S. & Rehfeldt, F. The filament sensor for near real-time detection of cytoskeletal fiber structures. *PloS one* **10**, e0126346 (2015).
88. Gu, H. et al. Celastrus orbiculatus extract inhibits the migration and invasion of human glioblastoma cells in vitro. *BMC Complement Altern Med* **16**, 387 (2016).
89. Xue, H. et al. MicroRNA-584-3p, a novel tumor suppressor and prognostic marker, reduces the migration and invasion of human glioma cells by targeting hypoxia-induced ROCK1. *Oncotarget* **7**, 4785-4805 (2016).
90. Gong, L. et al. Overexpression of MYC binding protein promotes invasion and migration in gastric cancer. *Oncol Lett* **15**, 5243-5249 (2018).
91. Wang, K., Jin, W., Song, Y. & Fei, X. LncRNA RP11-436H11.5, functioning as a competitive endogenous RNA, upregulates BCL-W expression by sponging miR-335-5p and promotes proliferation and invasion in renal cell carcinoma. *Molecular cancer* **16**, 166 (2017).
92. Chen, L. et al. Expression and function of miR-27b in human glioma. *Oncology reports* **26**, 1617-1621 (2011).
93. Wen, M. et al. Cytokine-like 1 is involved in the growth and metastasis of neuroblastoma cells. *Int J Oncol* **41**, 1419-1424 (2012).
94. Gao, S. et al. Overexpression of RASD1 inhibits glioma cell migration/invasion and inactivates the AKT/mTOR signaling pathway. *Scientific reports* **7**, 3202 (2017).
95. Del Duca, D., Werbowetski, T. & Del Maestro, R.F. Spheroid preparation from hanging drops: characterization of a model of brain tumor invasion. *Journal of neuro-oncology* **67**, 295-303 (2004).
96. Foty, R. A simple hanging drop cell culture protocol for generation of 3D spheroids. *J Vis Exp* (2011).
97. Kelm, J.M., Timmins, N.E., Brown, C.J., Fussenegger, M. & Nielsen, L.K. Method for generation of homogeneous multicellular tumor spheroids applicable to a wide variety of cell types. *Biotechnol Bioeng* **83**, 173-180 (2003).

98. Binnemars-Postma, K., Bansal, R., Storm, G. & Prakash, J. Targeting the Stat6 pathway in tumor-associated macrophages reduces tumor growth and metastatic niche formation in breast cancer. *FASEB journal : official publication of the Federation of American Societies for Experimental Biology* **32**, 969-978 (2018).
99. Nappo, G. et al. The immunosuppressive cytokine interleukin-4 increases the clonogenic potential of prostate stem-like cells by activation of STAT6 signalling. *Oncogenesis* **6**, e342 (2017).
100. da Silva, R., Uno, M., Marie, S.K. & Oba-Shinjo, S.M. LOX expression and functional analysis in astrocytomas and impact of IDH1 mutation. *PloS one* **10**, e0119781 (2015).
101. Wang, J. et al. Involvement of microRNA-1297, a new regulator of HMGA1, in the regulation of glioma cell growth in vivo and in vitro. *Am J Transl Res* **8**, 2149-2158 (2016).
102. Kalli, M., Papageorgis, P., Gkretsi, V. & Stylianopoulos, T. Solid Stress Facilitates Fibroblasts Activation to Promote Pancreatic Cancer Cell Migration. *Annals of biomedical engineering* **46**, 657-669 (2018).
103. Debinski, W. & Gibo, D.M. Fos-related antigen 1 modulates malignant features of glioma cells. *Mol Cancer Res* **3**, 237-249 (2005).
104. Dixit, V.D. et al. Ghrelin and the growth hormone secretagogue receptor constitute a novel autocrine pathway in astrocytoma motility. *The Journal of biological chemistry* **281**, 16681-16690 (2006).
105. Vereb, G., Jr. et al. Depletion of intracellular calcium stores facilitates the influx of extracellular calcium in platelet derived growth factor stimulated A172 glioblastoma cells. *Cytometry* **24**, 64-73 (1996).
106. Hotulainen, P. & Lappalainen, P. Stress fibers are generated by two distinct actin assembly mechanisms in motile cells. *The Journal of cell biology* **173**, 383-394 (2006).
107. Radmacher, M. Measuring the elastic properties of living cells by the atomic force microscope. *Methods in cell biology* **68**, 67-90 (2002).
108. Lekka, M. Discrimination Between Normal and Cancerous Cells Using AFM. *Bionanoscience* **6**, 65-80 (2016).
109. Morgia, G. et al. Matrix metalloproteinases as diagnostic (MMP-13) and prognostic (MMP-2, MMP-9) markers of prostate cancer. *Urol Res* **33**, 44-50 (2005).
110. Zhang, B. et al. Tumor-derived matrix metalloproteinase-13 (MMP-13) correlates with poor prognoses of invasive breast cancer. *BMC cancer* **8**, 83 (2008).
111. Merk, B.C., Owens, J.L., Lopes, M.B., Silva, C.M. & Hussaini, I.M. STAT6 expression in glioblastoma promotes invasive growth. *BMC cancer* **11**, 184 (2011).
112. Lee, S.Y. et al. Characterization of a Novel Anti-Cancer Compound for Astrocytomas. *PloS one* **9**, e108166 (2014).
113. Lian, S. et al. Artesunate attenuates glioma proliferation, migration and invasion by affecting cellular mechanical properties. *Oncology reports* **36**, 984-990 (2016).
114. Xu, W. et al. Cell stiffness is a biomarker of the metastatic potential of ovarian cancer cells. *PloS one* **7**, e46609 (2012).
115. Stylianou, A. & Stylianopoulos, T. Atomic Force Microscopy Probing of Cancer Cells and Tumor Microenvironment Components. *BioNanoScience* **6**, 33-46 (2016).
116. Li, Q.S., Lee, G.Y., Ong, C.N. & Lim, C.T. AFM indentation study of breast cancer cells. *Biochemical and biophysical research communications* **374**, 609-613 (2008).
117. Wang, N. et al. miR-135b inhibits tumour metastasis in prostate cancer by targeting STAT6. *Oncol Lett* **11**, 543-550 (2016).

118. Zhang, Y., Tu, Y., Gkretsi, V. & Wu, C. Migfilin interacts with vasodilator-stimulated phosphoprotein (VASP) and regulates VASP localization to cell-matrix adhesions and migration. *The Journal of biological chemistry* **281**, 12397-12407 (2006).
119. Belot, N. et al. Molecular characterization of cell substratum attachments in human glial tumors relates to prognostic features. *Glia* **36**, 375-390 (2001).
120. Bokel, C. & Brown, N.H. Integrins in development: moving on, responding to, and sticking to the extracellular matrix. *Developmental cell* **3**, 311-321 (2002).
121. Hoffmann, M. & Schwarz, U.S. A kinetic model for RNA-interference of focal adhesions. *Bmc Systems Biology* **7** (2013).
122. Gkretsi, V. & Stylianopoulos, T. Cell Adhesion and Matrix Stiffness: Coordinating Cancer Cell Invasion and Metastasis. *Frontiers in oncology* **8**, 145 (2018).
123. Izdebska, M., Zielinska, W., Grzanka, D. & Gagat, M. The Role of Actin Dynamics and Actin-Binding Proteins Expression in Epithelial-to-Mesenchymal Transition and Its Association with Cancer Progression and Evaluation of Possible Therapeutic Targets. *BioMed research international* **2018**, 4578373 (2018).
124. Dougherty, G.W., Chopp, T., Qi, S. & Cutler, M.L. The Ras suppressor Rsu-1 binds to the LIM 5 domain of the adaptor protein PINCH1 and participates in adhesion-related functions. *Experimental cell research* **306**, 168-179 (2005).
125. Zhang, Y. et al. Assembly of the PINCH-ILK-CH-ILKBP complex precedes and is essential for localization of each component to cell-matrix adhesion sites. *Journal of cell science* **115**, 4777-4786 (2002).
126. Wu, C. The PINCH-ILK-parvin complexes: assembly, functions and regulation. *Biochimica et biophysica acta* **1692**, 55-62 (2004).
127. Qin, J. & Wu, C. ILK: a pseudokinase in the center stage of cell-matrix adhesion and signaling. *Current opinion in cell biology* **24**, 607-613 (2012).
128. Nobes, C.D. & Hall, A. Rho, rac, and cdc42 GTPases regulate the assembly of multimolecular focal complexes associated with actin stress fibers, lamellipodia, and filopodia. *Cell* **81**, 53-62 (1995).
129. Bar-Sagi, D. & Hall, A. Ras and Rho GTPases: a family reunion. *Cell* **103**, 227-238 (2000).
130. Fortin Ensign, S.P., Mathews, I.T., Symons, M.H., Berens, M.E. & Tran, N.L. Implications of Rho GTPase Signaling in Glioma Cell Invasion and Tumor Progression. *Frontiers in oncology* **3**, 241 (2013).
131. Patel, B.B. et al. APC +/- alters colonic fibroblast proteome in FAP. *Oncotarget* **2**, 197-208 (2011).
132. Louca, M. et al. Ras suppressor-1 (RSU-1) promotes cell invasion in aggressive glioma cells and inhibits it in non-aggressive cells through STAT6 phospho-regulation. *Scientific reports* **9**, 7782 (2019).
133. Roth, P. et al. GDF-15 contributes to proliferation and immune escape of malignant gliomas. *Clinical cancer research : an official journal of the American Association for Cancer Research* **16**, 3851-3859 (2010).
134. Hromas, R. et al. PLAB, a novel placental bone morphogenetic protein. *Biochimica et biophysica acta* **1354**, 40-44 (1997).
135. Li, P.X. et al. Placental transforming growth factor-beta is a downstream mediator of the growth arrest and apoptotic response of tumor cells to DNA damage and p53 overexpression. *The Journal of biological chemistry* **275**, 20127-20135 (2000).
136. Paralkar, V.M. et al. Cloning and characterization of a novel member of the transforming growth factor-beta/bone morphogenetic protein family. *The Journal of biological chemistry* **273**, 13760-13767 (1998).

137. Baek, S.J., Kim, K.S., Nixon, J.B., Wilson, L.C. & Eling, T.E. Cyclooxygenase inhibitors regulate the expression of a TGF-beta superfamily member that has proapoptotic and antitumorigenic activities. *Molecular pharmacology* **59**, 901-908 (2001).
138. Segerer, S.E. et al. MIC-1 (a multifunctional modulator of dendritic cell phenotype and function) is produced by decidual stromal cells and trophoblasts. *Human reproduction* **27**, 200-209 (2012).
139. Kalli, M. et al. Solid stress-induced migration is mediated by GDF15 through Akt pathway activation in pancreatic cancer cells. *Scientific reports* **9**, 978 (2019).
140. Sasahara, A. et al. An autocrine/paracrine circuit of growth differentiation factor (GDF) 15 has a role for maintenance of breast cancer stem-like cells. *Oncotarget* **8**, 24869-24881 (2017).
141. Senapati, S. et al. Overexpression of macrophage inhibitory cytokine-1 induces metastasis of human prostate cancer cells through the FAK-RhoA signaling pathway. *Oncogene* **29**, 1293-1302 (2010).
142. Codo, P. et al. Control of glioma cell migration and invasiveness by GDF-15. *Oncotarget* **7**, 7732-7746 (2016).
143. Yoshioka, H., Kamitani, H., Watanabe, T. & Eling, T.E. Nonsteroidal anti-inflammatory drug-activated gene (NAG-1/GDF15) expression is increased by the histone deacetylase inhibitor trichostatin A. *The Journal of biological chemistry* **283**, 33129-33137 (2008).
144. Kadowaki, M. et al. DNA methylation-mediated silencing of nonsteroidal anti-inflammatory drug-activated gene (NAG-1/GDF15) in glioma cell lines. *International journal of cancer* **130**, 267-277 (2012).
145. Strelau, J. et al. Expression and putative functions of GDF-15, a member of the TGF-beta superfamily, in human glioma and glioblastoma cell lines. *Cancer letters* **270**, 30-39 (2008).
146. Zimmers, T.A. et al. Effect of in vivo loss of GDF-15 on hepatocellular carcinogenesis. *Journal of cancer research and clinical oncology* **134**, 753-759 (2008).
147. Ulu, A. & Frost, J.A. Regulation of RhoA activation and cell motility by c-Jun N-terminal kinases and Net1. *Small GTPases*, 1-7 (2018).
148. Law, M.E. et al. Molecular cytogenetic analysis of chromosomes 1 and 19 in glioma cell lines. *Cancer genetics and cytogenetics* **160**, 1-14 (2005).
149. Kim, T.A. et al. Genomic organization, chromosomal localization and regulation of expression of the neuronal nuclear matrix protein NRP/B in human brain tumors. *Gene* **255**, 105-116 (2000).
150. Ridley, A.J. Rho GTPase signalling in cell migration. *Current opinion in cell biology* **36**, 103-112 (2015).
151. Ivaska, J. & Heino, J. Adhesion receptors and cell invasion: mechanisms of integrin-guided degradation of extracellular matrix. *Cellular and molecular life sciences : CMLS* **57**, 16-24 (2000).
152. Bellail, A.C., Hunter, S.B., Brat, D.J., Tan, C. & Van Meir, E.G. Microregional extracellular matrix heterogeneity in brain modulates glioma cell invasion. *The international journal of biochemistry & cell biology* **36**, 1046-1069 (2004).
153. Kai, F., Drain, A.P. & Weaver, V.M. The Extracellular Matrix Modulates the Metastatic Journey. *Developmental cell* **49**, 332-346 (2019).
154. Agrez, M., Chen, A., Cone, R.I., Pytela, R. & Sheppard, D. The alpha v beta 6 integrin promotes proliferation of colon carcinoma cells through a unique region of the beta 6 cytoplasmic domain. *The Journal of cell biology* **127**, 547-556 (1994).
155. Cruet-Hennequart, S. et al. alpha(v) integrins regulate cell proliferation through integrin-linked kinase (ILK) in ovarian cancer cells. *Oncogene* **22**, 1688-1702 (2003).

156. Chin, Y.T. et al. Tetrac and NDAT Induce Anti-proliferation via Integrin alphavbeta3 in Colorectal Cancers With Different K-RAS Status. *Frontiers in endocrinology* **10**, 130 (2019).
157. Li, R., Shi, Y., Zhao, S., Shi, T. & Zhang, G. NF-kappaB signaling and integrin-beta1 inhibition attenuates osteosarcoma metastasis via increased cell apoptosis. *International journal of biological macromolecules* **123**, 1035-1043 (2019).
158. Horton, E.R. et al. Definition of a consensus integrin adhesome and its dynamics during adhesion complex assembly and disassembly. *Nature cell biology* **17**, 1577 (2015).
159. Gkretsi, V. et al. Loss of integrin linked kinase from mouse hepatocytes in vitro and in vivo results in apoptosis and hepatitis. *Hepatology* **45**, 1025-1034 (2007).
160. Liang, F., Zhang, S., Wang, B., Qiu, J. & Wang, Y. Overexpression of integrin-linked kinase (ILK) promotes glioma cell invasion and migration and down-regulates E-cadherin via the NF-kappaB pathway. *Journal of molecular histology* **45**, 141-151 (2014).
161. Zheng, C.C. et al. Significance of integrin-linked kinase (ILK) in tumorigenesis and its potential implication as a biomarker and therapeutic target for human cancer. *American journal of cancer research* **9**, 186-197 (2019).
162. Wang, S.C. et al. DOC-2/hDab-2 inhibits ILK activity and induces anoikis in breast cancer cells through an Akt-independent pathway. *Oncogene* **20**, 6960-6964 (2001).
163. Bravou, V., Klironomos, G., Papadaki, E., Taraviras, S. & Varakis, J. ILK over-expression in human colon cancer progression correlates with activation of beta-catenin, down-regulation of E-cadherin and activation of the Akt-FKHR pathway. *The Journal of pathology* **208**, 91-99 (2006).
164. Wang, M. et al. Down-regulated miR-625 suppresses invasion and metastasis of gastric cancer by targeting ILK. *FEBS letters* **586**, 2382-2388 (2012).
165. Zheng, K., Wang, G., Li, C., Shan, X. & Liu, H. Knockdown of ILK inhibits glioma development via upregulation of E-cadherin and downregulation of cyclin D1. *Oncology reports* **34**, 272-278 (2015).
166. Hall, A. & Nobes, C.D. Rho GTPases: molecular switches that control the organization and dynamics of the actin cytoskeleton. *Philosophical transactions of the Royal Society of London. Series B, Biological sciences* **355**, 965-970 (2000).
167. Worthylake, R.A., Lemoine, S., Watson, J.M. & Burridge, K. RhoA is required for monocyte tail retraction during transendothelial migration. *The Journal of cell biology* **154**, 147-160 (2001).
168. Zervas, C.G., Gregory, S.L. & Brown, N.H. Drosophila integrin-linked kinase is required at sites of integrin adhesion to link the cytoskeleton to the plasma membrane. *The Journal of cell biology* **152**, 1007-1018 (2001).
169. Sakai, T. et al. Integrin-linked kinase (ILK) is required for polarizing the epiblast, cell adhesion, and controlling actin accumulation. *Genes & development* **17**, 926-940 (2003).
170. Etienne-Manneville, S. In vitro assay of primary astrocyte migration as a tool to study Rho GTPase function in cell polarization. *Methods in enzymology* **406**, 565-578 (2006).
171. Deng, L. et al. Rho-kinase inhibitor, fasudil, suppresses glioblastoma cell line progression in vitro and in vivo. *Cancer biology & therapy* **9**, 875-884 (2010).
172. Rath, N. et al. ROCK signaling promotes collagen remodeling to facilitate invasive pancreatic ductal adenocarcinoma tumor cell growth. *EMBO molecular medicine* **9**, 198-218 (2017).
173. Li, D. et al. Targeting the NRF-2/RHOA/ROCK signaling pathway with a novel aziridonin, YD0514, to suppress breast cancer progression and lung metastasis. *Cancer letters* **424**, 97-108 (2018).

174. Zhang, H. et al. High Expression Levels of Fascin-1 Protein in Human Gliomas and its Clinical Relevance. *Open medicine* **13**, 544-550 (2018).
175. Jayo, A., Parsons, M. & Adams, J.C. A novel Rho-dependent pathway that drives interaction of fascin-1 with p-Lin-11/Isl-1/Mec-3 kinase (LIMK) 1/2 to promote fascin-1/actin binding and filopodia stability. *BMC biology* **10**, 72 (2012).
176. Vignjevic, D. et al. Fascin, a novel target of beta-catenin-TCF signaling, is expressed at the invasive front of human colon cancer. *Cancer research* **67**, 6844-6853 (2007).
177. Hashimoto, Y., Skacel, M. & Adams, J.C. Roles of fascin in human carcinoma motility and signaling: prospects for a novel biomarker? *The international journal of biochemistry & cell biology* **37**, 1787-1804 (2005).
178. Grothey, A. et al. C-erbB-2/ HER-2 upregulates fascin, an actin-bundling protein associated with cell motility, in human breast cancer cell lines. *Oncogene* **19**, 4864-4875 (2000).
179. Louca, M., Gkretsi, V. & Stylianopoulos, T. Coordinated Expression of Ras Suppressor 1 (RSU-1) and Growth Differentiation Factor 15 (GDF15) Affects Glioma Cell Invasion. *Cancers* **11** (2019).
180. Roufas, C. et al. The Expression and Prognostic Impact of Immune Cytolytic Activity-Related Markers in Human Malignancies: A Comprehensive Meta-analysis. *Frontiers in oncology* **8**, 27 (2018).
181. Yizhak, K. et al. RNA sequence analysis reveals macroscopic somatic clonal expansion across normal tissues. *Science* **364** (2019).
182. Dayal, N. et al. Potently inhibiting cancer cell migration with novel 3H-pyrazolo[4,3-f]quinoline boronic acid ROCK inhibitors. *European journal of medicinal chemistry* **180**, 449-456 (2019).
183. Peraud, A. et al. Expression of fascin, an actin-bundling protein, in astrocytomas of varying grades. *Brain tumor pathology* **20**, 53-58 (2003).
184. Roma, A.A. & Prayson, R.A. Fascin expression in 90 patients with glioblastoma multiforme. *Annals of diagnostic pathology* **9**, 307-311 (2005).
185. Senger, D., Cairncross, J.G. & Forsyth, P.A. Long-term survivors of glioblastoma: statistical aberration or important unrecognized molecular subtype? *Cancer journal* **9**, 214-221 (2003).
186. Parsons, M. & Adams, J.C. Rac regulates the interaction of fascin with protein kinase C in cell migration. *Journal of cell science* **121**, 2805-2813 (2008).
187. Tsai, W.C. et al. Association of cortactin and fascin-1 expression in gastric adenocarcinoma: correlation with clinicopathological parameters. *The journal of histochemistry and cytochemistry : official journal of the Histochemistry Society* **55**, 955-962 (2007).
188. Hayashi, Y., Osanai, M. & Lee, G.H. Fascin-1 expression correlates with repression of E-cadherin expression in hepatocellular carcinoma cells and augments their invasiveness in combination with matrix metalloproteinases. *Cancer science* **102**, 1228-1235 (2011).
189. Fan, Y. et al. Leptin signaling enhances cell invasion and promotes the metastasis of human pancreatic cancer via increasing MMP-13 production. *Oncotarget* **6**, 16120-16134 (2015).
190. Zhang, R. et al. Golgi Membrane Protein 1 (GOLM1) Promotes Growth and Metastasis of Breast Cancer Cells via Regulating Matrix Metalloproteinase-13 (MMP13). *Med Sci Monitor* **25**, 847-855 (2019).
191. Kumamoto, K. et al. ING2 is upregulated in colon cancer and increases invasion by enhanced MMP13 expression. *International journal of cancer* **125**, 1306-1315 (2009).

Table 1. Primers used for qPCR

Primer Name	Primer sequence
β-actin	Forward: 5'-CGAGCACAGAGCCTCGCCTTTGCC-3'
	Reverse: 5'-TGTCGACGACGAGCGCGGCGATAT-3'
RSU-1	Forward: 5'- AGGCCACAGAGCAAGGTCTA -3'
	Reverse: 5'- CGTGCAATCTCAAAAGCTCA-3'
MMP13	Forward: 5'-TGGCATTGCTGACATCATGA-3'
	Reverse: 5'-GCCAGAGGGCCCATCAA-3'
PINCH1	Forward: 5'-CCGCTGAGAAGATCGTGAAC-3'
	Reverse: 5'-GGGCAAAGAGCATCTGAAAG -3'
ILK	Forward: 5'-GACATGACTGCCCGAATTAG -3'
	Reverse: 5'-CTGAGCGTCTGTTTGTGTCT-3'
GDF15	Forward: 5'-TCAAGGTCGTGGGACGTGACA-3'
	Reverse: 5'- GCCGTGCGGACGAAGATTCT-3'
RhoA	Forward: 5'-CGGGAGCTAGCCAAGATGAAG-3'
	Reverse: 5'-CCTTGCAGAGCAGCTCTCGTA-3'
ROCK-1	Forward: 5'-ACCTGTAACCCAAGGAGATGT-3'
	Reverse: 5'-CACAATTGGCAGGAAAGTGG-3'
Fascin-1	Forward: 5'-AGCTGCTACTTTGACATCGA-3'
	Reverse: 5'-TCATGAGGAAGAGCTGTGAGT-3'